NASA CR-159401

USER'S MANUAL FOR FRAC3D

Supplement to Report on Stress Analysis for Structures With Surface Cracks

by J. C. Bell, A. T. Hopper, and P A. Hayes

BATTELLE
Columbus Laboratories

prepared for

NATIONAL AERONAUTICS AND SPACE ADMINISTRATION

NASA Lewis Research Center
Contract NAS3-21020
Project Manager, G. T. Smith

1. Report No.	2. Government Accession No	3. Recipient's Catalog No.
NASA CR-159401		

4. Title and Subtitle	5. Report Date
USER'S MANUAL FOR FRAC3D - Supplement to Report on Stress Analysis for Structures with Surface Cracks	August 1978
	6. Performing Organization Code
7. Author(s)	8. Performing Organization Report No
J. C. Bell, A. T. Hopper, P. A. Hayes	
	10 Work Unit No
9. Performing Organization Name and Address	
Battelle Columbus Laboratories 505 King Avenue Columbus, Ohio 43201	11. Contract or Grant No NAS3-21020
	13 Type of Report and Period Covered Contractor Report
12. Sponsoring Agency Name and Address	
National Aeronautics and Space Administration Washington, D. C. 20546	14. Sponsoring Agency Code

15. Supplementary Notes

Project Manager, G. T. Smith, Materials and Structures Division, NASA Lewis Research Center, Cleveland, Ohio 44135

16. Abstract

This manual is designed to explain the intent and broad outline of the computer program FRAC3D, which is designed for use in analyzing stresses in structures (including plates, bars, or blocks) which may contain part-circular surface cracks or embedded circular cracks. Instructions are provided for preparing input, including that for the supporting programs LATTICE and MATSOL as well as for FRAC3D, and the course of a substantial illustrative calculation is shown with both input and output. The formulas underlying the calculations are summarized and related to the subroutines in which they are used. Many issues of strategy in using this program for analysing stresses around surface cracks are elucidated by applications of it that are discussed in the report to which this manual is a supplement (NASA CR 159400).

17. Key Words (Suggested by Author(s))	18. Distribution Statement
surface cracks, fracture analysis, calculation of stresses, circular cracks, surface loads, coordinated stress analyses, stress intensity factors, back effects, integrals involving Bessel functions	Unclassified - unlimited

19. Security Classif. (of this report)	20. Security Classif (of this page)	21. No. of Pages	22. Price*
Unclassified	Unclassified	123	$5.25

*For sale by the National Technical Information Service, Springfield, Virginia 22161

TABLE OF CONTENTS

TABLE OF CONTENTS
(Continued)

LIST OF TABLES

LIST OF FIGURES

LIST OF SYMBOLS

Symbols Used in Formulas

a = radius of crack

A = depth of penetration on surface crack

a,b,c = subscripts or superscripts denoting front, back or crack systems

a_1, b_1, c_1 = functions of ρ and ζ shown by Equations (24) in Appendix A

C = half length of surface crack

$c_{i,\ell}, c'_{i,\ell'}, c''_{i,\ell''}$ = coordinated notation for front, back and crack loads (See p A36)

C_1, C_2, C_3 = constants defining lattice lines with y constant (See p 17)

D_1, D_2, D_3 = constants defining lattice lines with x constant (See p 17)

E = Young's modulus

E_1, E_2, E'_1, E'_2 = constants ($= \pm 1$) identifying branches of arctangents (See p A31)

$F^{rr}_{m,k,i}(\rho,\zeta)$, etc = nonangular factors of crack load influences on stresses (See p A9)

$F^{u}_{m,k,i}(\rho,\zeta)$, etc = nonangular factors of crack load influences on displacements (p A8)

$H^j_i(\alpha,\beta,z)$ = functions connecting surface load effects and stresses (See Eqs (39).)

$\mathcal{H}^j_i(\alpha,\beta,z)$ = functions connecting surface load effects and displacements (~Eqs (40))

$I^{n'}_{M,N}(\rho,\zeta)$ = crack function integrals (See Appendix A, Equation (1).)

$J_M(\rho\xi), J_{N+\frac{1}{2}}(\xi)$ = Bessel functions of the first kind

k = index related to radial variations in crack function series

k_1, k_2, k_3 = stress intensity factors (without factor $\sqrt{\pi}$. See p A9.)

$k_{1\infty} = 2\sigma_o\sqrt{a/\pi} = k_1$ for deeply embedded crack under uniform normal load σ_o

K_I, K_{II}, K_{III} = stress intensity factors (being $\sqrt{\pi}$ times k_1, k_2 or k_3)

$K_{I\infty} = 2\sigma_o\sqrt{a/\pi} = K_I$ for deeply embedded crack under uniform normal load σ_o

$K^j_i(\alpha,\beta,z)$ = influence functions for surface loads affecting stress (See p A23.)

$\mathcal{K}^j_i(\alpha,\beta,z)$ = influence functions for surface loads on displacements (See p A23.)

$K^{a,j,n}_{a,i,\ell}$, etc. = coordinated load influence affecting stress (See pp A35, A39.)

$\mathcal{K}^{a,j,n}_{a,i,\ell}$, etc. = coordinated load influence affecting displacement (See pp A35, A40.)

$\ell_{x,\ell}, \ell_{x,u}$ = lower and upper x-lengths of pyramidal surface load (See p A22.)

$\ell_{y,\ell}, \ell_{y,u}$ = lower and upper y-lengths of pyramidal surface load (See p A22.)

L, L' = number of pyramid points on front (or back) face of plate

L'' = number of pairs m,k for each type of crack constant (See p A38.)

m = index related to angular variations in crack function series

$M_{b,a}$, etc. = matrix converting stresses from second system to first (p A33ff)

$\mathcal{M}_{b,a}$, etc. = matrix transforming displacements from second system to first

n_m, n_k = numbers of m's and k's used for one kind of crack constants

p_m = peak value for pyramidal normal surface load ($\sim -\sigma_z$)

$P_N(x)$ = Legendre polynomial of order N

r, θ, ζ = cylindrical coordinates associated with crack (See Figures 1, A2.)

r_c = radial offset of crack circle center from front face (Fig. 1, A2)

$R(x,\rho,\zeta)$ = function used in quadrature of crack function integrals (See Eq(20).)

s_m, t_m = peak value for pyramidal tangential surface load ($\sim \tau_{zx}$ or τ_{yz})

$\mathrm{sgn}(X)$ = constant ($= \pm 1$) determined by sign of X (See p A31.)

T = thickness of plate or bar (also called z_t)

u, v, w = displacement components in coordinate directions for system in use

u^j = displacement components for lone system in use (See Equations (37).)

$u^{a,j,n}$ = displacement in system a by component j at point n (See pp A35, A36.)

$U_{m,k,i}(\rho,\zeta)$ = auxiliary functions defined by Equations (3)

$V_{m,k,i}(\rho,\zeta)$ = auxiliary functions defined by Equations (3)

x, y, z = rectangular coordinates associated with face of body (Fig. 1, A2)

x', y', z' = rectangular coordinates associated with back face (See Figure A2.)

$x^{(i)}, y^{(i)}, z^{(i)}$ = rectangular coordinates associated with $i^{\underline{th}}$ face (See Figure 1.)

x_c, y_c = values of x and y at base corner point for pyramidal surface load

x_ℓ, x_m, x_u = values of x_c at lower, middle or upper corners of pyramidal base

y_ℓ, y_m, y_u = values of y_c at lower, middle or upper corners of pyramidal base

z_t = thickness of plate or bar (also called T)

z = distance from front face in rectangular system (distinguish from ζ)

ζ = distance from crack plane in cylindrical system (distinguish from z)

$\alpha'_{m,k}$ = constants for normal crack loads symmetric around $\theta = 0$ (See p A8.)

$\beta'_{m,k}, \gamma'_{m,k}$ = constants for tangential crack loads symmetric around $\theta = 0$

$\hat{\alpha}'_{m,k}$ = constants for normal crack loads antisymmetric around $\theta = 0$

$\hat{\beta}'_{m,k}, \hat{\gamma}'_{m,k}$ = constants for tangential crack loads antisymmetric around $\theta = 0$

$\alpha''_m, \beta''_m, \gamma''_m$ = sums of $\alpha'_{m,k}, \beta'_{m,k}, \gamma'_{m,k}$ given by Equations (12), (15)

$\hat{\alpha}''_m, \hat{\beta}''_m, \hat{\gamma}''_m$ = sums of $\hat{\alpha}'_{m,k}, \hat{\beta}'_{m,k}, \hat{\gamma}'_{m,k}$ given by Equations (12), (15)

α (or β) = x (or y) distance of loaded surface point from stressed point

α_c (or β_c) = α (or β) when loaded point is at x_c, y_c. (May use c → ℓ, m or u.)

$\epsilon = \zeta/|\zeta|$ (or +1 if $\zeta = 0$)

$\zeta = \zeta/a$

θ = cylindrical coordinate polar angle, $\theta = 0$ at crack root (Figure 1)

$\theta_1, \theta_2, \theta_3$ = angles used in surface load analysis, given by Equations (38)

μ = shear modulus = $E/[2(1+\nu)]$

ν = Poisson's ratio

ρ = r/a , if used in crack theory

$\rho = \sqrt{\alpha^2 + \beta^2 + \gamma^2}$, if used in surface load theory

$\sigma_x, \sigma_y, \sigma_z$ = normal stress components in rectangular system

$\sigma_r, \sigma_\theta, \sigma_\zeta$ = normal stress components in cylindrical system

σ_o = uniform normal load on crack

σ^j = stress components for lone system in use (See Equation (37).)

$\sigma^{a,j,n}$ = stress component j in system a at point n (See pp A35, A36.)

$\tau_{yz}, \tau_{zx}, \tau_{xy}$ = shearing stress components in rectangular system

$\tau_{\theta\zeta}, \tau_{\zeta r}, \tau_{r\theta}$ = shearing stress components in cylindrical system

ω = inclination of ζ-axis with respect to front face (See Figure 1.)

$\binom{N}{r}$ = number of combinations of N things taken r at once (also denoted ${}_N C_r$)

$(\alpha)_n$ = Pochhammer notation (See p A16.)

$\left[\frac{N}{2}\right]$ = quantity defined by Equation 22

$[\ldots]^*$ = operator defined by Equation 35

$[\sigma^a], [K^a_a]$, etc. = full vectors or matrices (See pp A32 or A36.)

$\{\sigma^{a,j,n}\}$, etc. = edited vectors (See p A41.)

$\{K^{a,j,n}_{a,i,\ell}\}$, etc. = edited matrices (See p A41.)

Coding Symbols for Input to LATTICE and FRAC3D

A0, A1, A2, etc. = constants for optional generation of crack conditions (See pp 23,24.)

AXS(I,J), etc. = elements of arrays specifying symmetries (See pp 19,20,26.)

IFACE(I) = numbers specifying body faces used in analysis (See pp 21,26.)

IN(L,J) = indices of lattice points for $J^{\underline{th}}$ pyramid (from LATTICE. See p 27.)

IX1S,IX2S,etc. = admissible coded values for JXS, JYS, JZS (See pp 19, 25.)
JXS, JYS, JZS = parameters allowing description of symmetries (See pp 19, 25.)
MODE = parameter specifying mode of operation of FRAC3D (See pp 17,25.)
MFLAG = parameter controlling printout from FRAC3D (See pp 17, 25.)
MAXL(I) = number of pyramid points on I^{th} face (from LATTICE. See p 27.)
MAXS(I) = number of stress points to be read for I^{th} face. (See p 27.)
NL(I) = number of lattice points on I^{th} face (from LATTICE. See p 27.)
NALFI,NALFJ,etc.= counts for lengths of crack series from FRAC3D (See pp 21, 26.)
NU = Poisson's ratio (See pp 21, 26.)
RHO(I) = radial cylindrical coordinate for I^{th} result point (See p 30.)
RSUBC = radial offset of crack circle center from front ($= r_c$. See pp 22,27,28.)
SIGMA(I.J) = prescribed boundary stress of I^{th} kind at J^{th} point (See pp 28,29.)
THETA(I) = angular cylindrical coordinate for I^{th} result point (See p 30.)
TITLE1,TITLE2 = labels chosen by user (See pp 19, 25.)
W = inclination of z-axis to the xy-plane ($= \omega$. See pp 22, 27.)
XL(J),YL(J) = local coordinates of J^{th} lattice point (from LATTICE. See p 27.)
XLO,YLO,XU,YU = x and y limits of region to be analysed (See pp 21, 22, 26.)
XSA(I),YSA(I),ZSA(I)= coordinates of stress points or result points (See pp 28, 30.)
XEQ,YEQ,ZEQ = parameters specifying translational equilibrium (See pp 22, 29.)
XROT,YROT,ZROT = parameters specifying rotational equilibrium (See pp 22, 29.)
ZETA(I) = axial cylindrical coordinate for I^{th} result point (See p 30.)
ZSUBT = thickness of plate ($= z_t$. See pp 21, 22, 26.)

Coding Symbols for Input to Editing Version of MATSOL*

IR1,IR2,... = terminal row counts for weighted blocks of equations (See p 31.)
LE(I) = column count for I^{th} load constant to be deleted (See p 32.)
LZ = number of load constants being deleted (See p 32.)
MSR = number of boundary condition equations from body faces (See p 32.)
NAUX = number of equilibrium equations to be enforced (See p 32.)
WT1,WT2,... = extra weight factors for separate blocks of equations (See p 31.)

---

* Arrays in MATSOL itself which may need dimensional adjustments are identified and discussed on pp 31,32.

USER'S MANUAL FOR PROGRAM FRAC3D
SUPPLEMENT TO REPORT ON
STRESS ANALYSIS FOR STRUCTURES WITH SURFACE CRACKS

by

J. C. Bell, A. T. Hopper, and P. A. Hayes

SUMMARY

This manual is designed to explain the intent and broad outline of the computer program FRAC3D, which is designed for use in analyzing stresses in structures (including plates, bars, or blocks) which may contain part-circular surface cracks or embedded circular cracks. Instructions are provided for preparing input, including that for the supporting programs LATTICE and MATSOL as well as for FRAC3D, and the course of a substantial illustrative calculation is shown with both input and output. The formulas underlying the calculations are summarized and related to the subroutines in which they are used. Many issues of strategy in using this program for analysing stresses around surface cracks are elucidated by applications of it that are discussed in the report to which this manual is a supplement (NASA CR 159400).

INTRODUCTION

This manual describes the capabilities of the computer program FRAC3D which is based on the theory developed in [1]*. The analysis capability consists of solving for the three-dimensional stress state in a three-dimensional region which may or may not contain a flaw. The types of flaws analyzable by the program include completely buried circular flaws or part-circular surface flaws. The manual begins with a description of the allowable geometric configurations. This section is followed by a brief synopsis of the various analytical forms which describe the stresses and

---

* Numbers in brackets refer to entries in the list of references.

displacements and of the procedure of developing the needed input data and their various formats. A representative stress analysis is used as a comprehensive illustration, with discussion of the strategy, the input and several forms of output. One appendix summarizes the formulas underlying the program, and another appendix lists its component parts, including a brief description of each and references to the formulas each employs.

The program described here is operational on Battelle's Columbus Laboratories' CDC Cyber 73 computer system. Typical computer times on this system are ten to twenty minutes for a substantial three-dimensional analysis, with considerable variation possible according to the extent of detail employed in the analysis. Many illustrative results are included in the report which this manual accompanies [2].

RANGE OF APPLICABILITY OF THE PROGRAM

Geometries Considered

The geometries analyzable with the computer code FRAC3D range from a circular flaw in three-space to a tilted, part-through crack in a right-parallelepiped as shown in Figure 1.* Shown there is a six-faced solid, all edges meeting at right angles, with a tilted circular surface flaw cutting the top surface. Each face is numbered and has associated with it a local rectangular coordinate system. The crack is described by the angle ω and the directed distance labelled r_c. The program uses the crack radius a as the reference (unit) length. The tilt angle, ω, can be in the range $-\frac{\pi}{2} < \omega \leq \frac{\pi}{2}$, but must be less than $\frac{\pi}{2}$ for the crack to cut the top surface. The quantity r_c is the distance between the crack center and the $(x^{(1)}, y^{(1)}, z^{(1)})$ origin, with sign being positive if the center is outside the body or negative if it is inside.

---

* The crack also can be omitted, so that the program can be used for analyzing stresses in a half-space, quarter-space, slab or block subjected to a wide variety of boundary conditions.

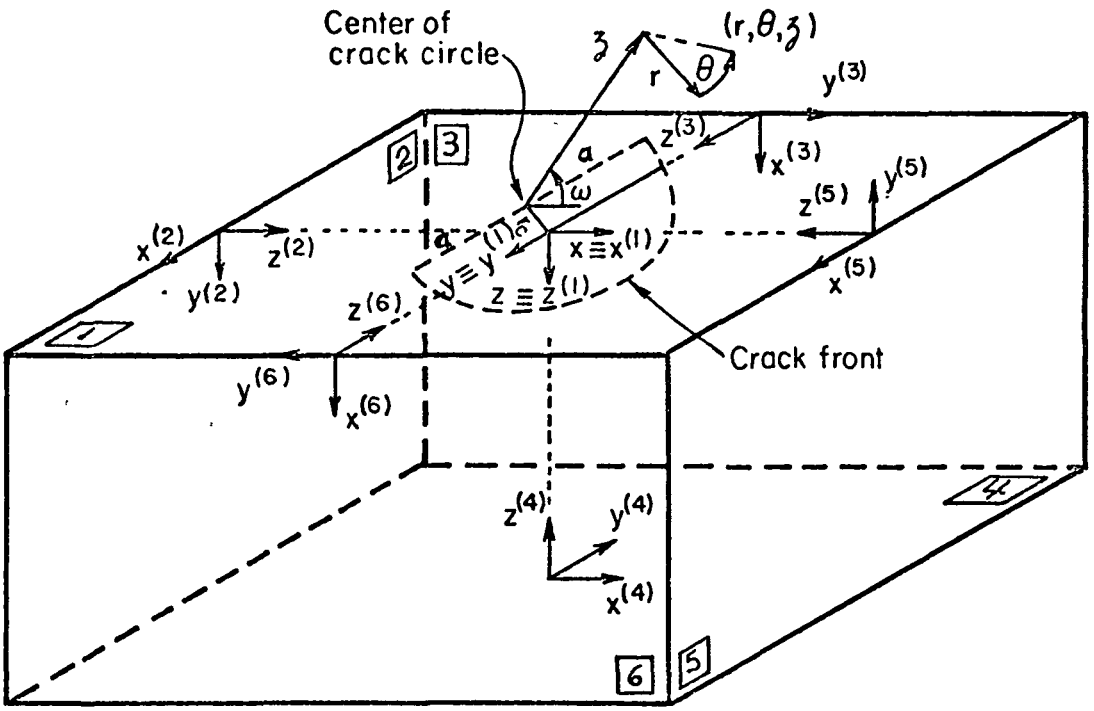

FIGURE 1. COORDINATE SYSTEMS ASSOCIATED WITH A RECTANGULAR BLOCK WITH A CIRCULAR CRACK

The local rectangular coordinate systems shown in Figure 1 and the numbering scheme which identifies them are fixed conventions within the program. The cylindrical system associated with the crack arbitrarily has been assigned the identification number 7. Global coordinates (x,y,z) are taken to coincide with those of the system labelled 1, and the geometry of a region to be analyzed is defined relative to this system. Ignoring the crack for the moment, the six faces are defined by the planes listed in the following table.

TABLE 1. PLANES DEFINING ANALYZABLE REGIONS

Face No.	Plane	Local Coordinate System
1	$z = 0$	$x^{(1)}, y^{(1)}, z^{(1)}$
2	$x = x_\ell$	$x^{(2)}, y^{(2)}, z^{(2)}$
3	$y = y_\ell$	$x^{(3)}, y^{(3)}, z^{(3)}$
4	$z = z_t$	$x^{(4)}, y^{(4)}, z^{(4)}$
5	$x = x_u$	$x^{(5)}, y^{(5)}, z^{(5)}$
6	$y = y_u$	$x^{(6)}, y^{(6)}, z^{(6)}$

The user can include or exclude any meaningful combination of the seven numbered coordinate systems to describe various regions to be analyzed. Thus a half space with a crack can be described by choosing only Face 1 and the crack system. Similarly, a finite thickness slab can be described by choosing either face pairs 1 and 4, or 2 and 5, or 3 and 6, in addition to the crack system. A slab with a crack along an edge might be described by Faces 1, 3, and 6 in addition to the crack, and so forth.

Loads Considered

The analyses underlying FRAC3D express both stresses and displacements in the body in terms of the influence of certain constants which define loads acting either on the crack or on any of the six faces. If all the load constants are known initially, they can be used directly in the

"RESULT" mode of operation of the program to find stress and displacement components anywhere in the body. If the load constants are not known, but instead a definite set of their implied boundary tractions (and/or displacements) is known, then it is necessary first to use the program in another mode ("SOLVE") to find all the load constants. This is the more common way in which the program has been used.

In considering stresses associated with cracks, it is customary to take the defining boundary tractions to be the stresses which would be transmitted across the plane of the crack if no crack were present, but which are not transmitted when the crack is there. Such tractions ordinarily have a fairly limited range of influence, and they fully determine the stress intensity factors along the crack front. The stresses and displacements they imply can be added to those which would arise in the absence of the crack in order to get a full description of the stresses and displacements in the body. For some situations, it may be desirable to use the program in a preliminary calculation to find the stress patterns that would exist in the crack location if no crack were there. The program allows evaluation of such stresses under a wide variety of loadings.

ANALYTICAL FORMS AND OPERATIONS APPEARING IN THE PROGRAM

The intent of this section is only to present typical analytical forms of stresses and displacements and to describe in broad terms how information flows in a calculation, so that the user can understand the various input and output quantities. Derivations and further discussion are given in References 1, 3, and 4.

Stresses and displacements arise from surface loads applied to the crack or to any of the six plane surfaces bounding the body. Load constants associated with the crack or with any other single surface are used to define those surface loads, but the load constants, for any one surface, are not alone in implying tractions on that surface, since loads applied anywhere may imply stresses everywhere. A primary goal is to coordinate the choice of all the load constants in a way to provide good satisfaction

of overall boundary conditions, and to this end, generalized expressions are used for stresses from loads on any one surface.

Expressions Related to Crack Loads

The expressions for stresses associated with the crack constants are shown by Equations (1) through (6) of Appendix A. For example, the expression for σ_{zz}, the normal stress in the direction perpendicular to the plane of the crack, is

$$\sigma_{zz} = \mu \sum_{m=0}^{\infty} \sum_{k=0}^{\infty} \left\{ \left[\alpha'_{m,k} F^{zz}_{m,k,1} + \beta'_{m,k} F^{zz}_{m,k,2} + \gamma'_{m,k} F^{zz}_{m,k,3} \right] \cos m\theta \right.$$

$$\left. - \left[\hat{\alpha}'_{m,k} F^{zz}_{m,k,1} + \hat{\beta}'_{m,k} F^{zz}_{m,k,2} + \hat{\gamma}'_{m,k} F^{zz}_{m,k,3} \right] \sin m\theta \right\} .$$

Here $\alpha'_{m,k}$, $\beta'_{m,k}$, $\gamma'_{m,k}$, $\hat{\alpha}'_{m,k}$, $\hat{\beta}'_{m,k}$, and $\hat{\gamma}'_{m,k}$ are crack load constants, and μ is the shear modulus. Constants of the first three kinds relate to loads essentially symmetric around $\theta = 0$, while those of the last three kinds refer to conditions antisymmetric around $\theta = 0$ so that they can often be dropped. The constants $\alpha'_{m,k}$ and $\hat{\alpha}'_{m,k}$ refer to normal loads on the crack face, while the other four sets of constants refer to tangential loads on the crack face. Thus, for situations in which only normal loads would be applied to the crack and in which there is symmetry around $\theta = 0$, the only relevant load constants are those denoted as $\alpha'_{m,k}$. The influence functions for all these constants, as they act to produce stresses σ_{zz}, are the trigometric factors $\cos m\theta$ or $\sin m\theta$ multiplied by one of the functions

$$F^{zz}_{m,k,1}(\rho,\zeta) = -\left[I^{1}_{m,m+2k+1} + |\zeta|\, I^{2}_{m,m+2k+1}\right],$$

$$F^{zz}_{m,k,2}(\rho,\zeta) = \frac{\zeta}{2}\, I^{2}_{m,m+2k+2},$$

$$F^{zz}_{m,k,3}(\rho,\zeta) = \begin{cases} \dfrac{\zeta}{2-\nu}\, I^{2}_{m,m} & \text{for } k = 0 \\ \dfrac{\zeta}{2}\, I^{2}_{m,m+2k} & \text{for } k \geq 1 \end{cases}.$$

Here, ν is Poisson's ratio, $\rho = r/a$, $\zeta = z/a$, where a is the crack radius, and

$$I^{n'}_{M,N}(\rho,\zeta) = \int_0^\infty e^{-\xi|\zeta|}\, \xi^{n'-\frac{1}{2}}\, J_M(\rho,\xi)\, J_{N+\frac{1}{2}}(\xi)\, d\zeta .$$

Since integrals of this form perform such an important role in the analysis and special means are needed to evaluate them, several subroutines of the program are devoted to their evaluation. The mathematics involved in this evaluation is discussed in Reference 1. Here it is being observed merely that the stress components (and also displacement components) associated with crack load constants are sums of series of those constants multiplied by influence functions which the program calculates from geometric specifications and from the indices identifying the load constants.

One aspect of treating stresses associated with crack loads is that the user must decide which of all the possible crack constants are to be used, that is which combination of the indices m and k will be admitted. This is not always a simple matter, since the desirable extent of the series depends on the amount of detail needed to provide an adequate fitting of the stress field throughout the body. The program currently is prepared to employ values of m from 0 through 16, and values of k from 0 through 10, but not all of the implied 187 combinations of these indices are necessarily desirable. In particular, if the part of crack circle penetrating the body

is less than a semicircle, if the load is normal, and if there is symmetry around the crack plane and around the plane $\theta = 0$, then it appears desirable to drop all the odd values of m. The remaining even values of m provide series which furnish complete generality for expansions in the half space where $-\frac{\pi}{2} < \theta \leq \frac{\pi}{2}$, and they avoid the ambiguity which would arise from employing also the superfluous odd values of m. Other combinations of indices too may be difficult or unnecessary to use, but it has been found that good results can be obtained for several types of problems using 9 to 45 selected crack constants. Reference 2 describes several informative cases. Some experience may be helpful with problems of a new type before the final choice of crack constants is made.

A property that makes the crack load constants particularly important is that they are the load constants which determine the stress intensity factors along the crack front. In particular, for Mode I loading (that is only normal loads on the crack) in which there is symmetry around $\theta = 0$, the stress intensity is*

$$K_I = \mu\sqrt{\pi a} \sum_{m=0}^{\infty} \alpha''_m \cos m\theta \quad , \qquad \text{where}$$

$$\alpha''_m = \sqrt{\frac{2}{\pi}} \sum_{k=0}^{\infty} (-1)^k \alpha'_{m,k} \quad .$$

The stress intensity calculated by the program MATSOL, which solves the system of equations set up by FRAC3D, is the ratio of this K_I divided by the stress intensity factor $K_{I\infty}$ that would arise in an infinite body with a complete circular crack subjected to a unit normal load. Thus, after computations presuming any load, to get a dimensional value of K_I the computed $K_I/K_{I\infty}$ should be multiplied by $2p_1\sqrt{a/\pi}$ where p_1 is a unit stress.

---

* This formula presumes the definition

$$K_I = \lim_{r \to a} \sqrt{2\pi\ (r-a)}\ \sigma_{\theta}\ (r,\theta,0).$$

If a uniform normal load p_o is used, this implies $K_{I\infty} = \frac{2}{\pi} p_o \sqrt{\pi a}$.

Expressions Related to Surface Loads

The loads associated with any one of the six surfaces are expressed in terms of elemental loads distributed over rectangular areas on that surface, each with intensity that varies in the pyramidal form shown in Figure 2. Elemental loads such as these, chosen with suitable bases and peak values, can be superposed to give efficient and continuous representation to widely varying load patterns. To define such a representation, one must first select the lattice of rectangles used for bases of the pyramidal elements. It should be understood that the lattice need not be regular, but enough lines should be used to provide an adequate number of pyramidal bases, each being a rectangle subdivided into four rectangles, as shown in Figure 2. In a properly drawn lattice, a pyramidal base can be found around any point where two lattice lines cross and extend in both ways beyond the "pyramid" point, and the peak pyramidal load is the value of the elemental load at that point. Three kinds of loads may be applied on any pyramidal base on a surface $z^{(i)} = 0$, namely $p \sim -\sigma_z^{(i)}$, $s \sim \tau_{zx}^{(i)}$, and $t \sim \tau_{yz}^{(i)}$. The three peak values p_m, s_m, and t_m associated with the particular pyramid point become part of the overall set of needed load constants which may be specified or sought as needed to finish defining the surface load. The pyramidal bases are treated as being part of the initially assigned geometry.

The program incorporates formulas for computing stresses and displacements that may be caused anywhere by an elemental load with peak value p_m, s_m, or t_m acting on a particular base, treating the body as a half space bounded by the plane of the base. Thus, for example, the contribution to σ_z from the elemental loads acting on a particular base is

$$\sigma_z = p_m K_1^{zz} + s_m K_2^{zz} + t_m K_3^{zz} .$$

where K_1^{zz}, K_2^{zz}, and K_3^{zz} are influence functions which the program computes from the geometry of the pyramidal base and the location of the point where the stress is to be evaluated. To find the influence function, the program uses weighted sums of certain elementary functions evaluated nine times--

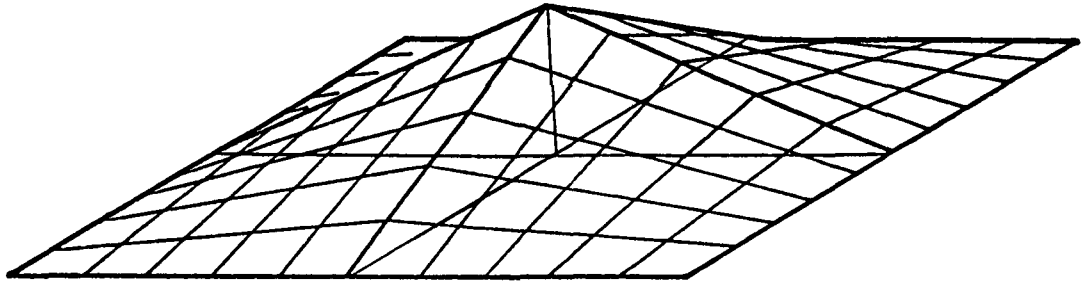

a. Pyramidal Load Element

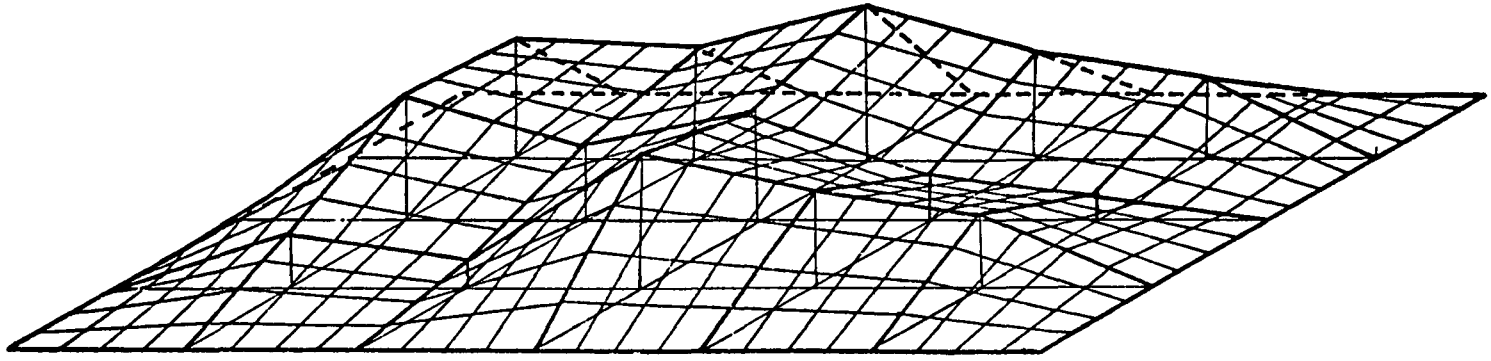

b A Composite Load Pattern Constructed of Pyramidal Elements

FIGURE 2. TYPICAL FORM OF SURFACE LOAD ELEMENTS

each evaluation being based on distances from one of the nine "corner" points (lattice points) in the pyramidal base to the point where the stress is to be evaluated. Thus, for example, if the stress σ_z is to be evaluated at (x,y,z) for a load p applied to the top face, then

$$K_1^{zz}(x,y,x) = -\frac{1}{2\pi}\left[z\rho + \alpha\beta \arctan\frac{\alpha\beta}{z\rho}\right]^* ,$$

where $\alpha = x_c - x$, $\beta = y_c - y$, $\rho = \sqrt{\alpha^2 + \beta^2 + z^2}$, and the asterisk denotes the weighted summation used in combining evaluations for each of the nine pyramidal base corners $(x_c, y_c, 0)$. (Details may be found in Appendix A.) To perform this kind of operation, the computer must be supplied the coordinates of nine corner points of each pyramidal base. To facilitate this process, an auxiliary program called LATTICE has been prepared which computes the information required, and identifies it using index numbers assigned to each lattice point. The information is punched on cards in an arrangement suitable for input to FRAC3D.

The input to the program LATTICE consists of coordinates of end points of each line of the lattice chosen on each of the six plane faces that is used. The process of choosing the lattice design is not rigidly formulated, but for cases involving a crack, the process can be elucidated by preliminary calculations (also from FRAC3D) showing infinite-body stresses needing to be freed when the body is finite. Directions for and illustrations of these matters are furnished later in this manual. Many examples of lattices are furnished in the accompanying report [2].

Assembly of Boundary Conditions and Equilibrium Conditions

The purpose of the program FRAC3D operating in its "SOLVE" mode is to construct a set of linear boundary condition equations which can be solved by a least-squares process to determine an appropriate set of crack and surface load constants. This operation amounts to constructing a matrix of influence functions for unit loads of the kinds represented by the various unknown load constants acting to produce surface tractions of three kinds at

selected surface points. Each column consists of influence functions for a particular load constant and each row shows influence functions for all the constants acting to produce a particular type of traction at a given boundary point. In addition, it is possible to append one or several rows to the matrix expressing overall equilibrium conditions which should be satisfied exactly rather than in the least-square sense.

The order of appearance of the load constants in this system of equations places the surface-load constants for Surface 1 first, then those for Surface 2 (if they are used), and so on through Surface 6, and finally, the crack-load constants. Among the surface constants, the p, s and t for the first pyramid point are placed first, then those for the second pyramid point, and so forth. Among the crack constants, those for m = 0 come first, being ordered by increasing k, then those for m = 1, and so forth. This basic ordering is arranged by the computer through use of the data arranged for FRAC3D by the preliminary program LATTICE. The set of load constants is frequently reduced later when symmetries are accounted or when certain crack constants are withdrawn from consideration, but the ordering of the remaining load constants remains the same as in the basic arrangement.

The ordering of the rows of the matrix depends somewhat on the order in which the user assigns boundary conditions. He is required to assign those for Face 1 first (if any are to be used for it) then those for Face 2, and so on through Face 7 (the crack face). For each assigned point, the computer arranges three equations, namely conditions for $\sigma_z^{(i)}$, $\tau_{yz}^{(i)}$, and $\tau_{zx}^{(i)}$ in that order for a point on an outer surface, or σ_j, $\tau_{\theta j}$, and τ_{jr} on the crack, but the order in which the boundary condition points are assigned for a given face is chosen by the user. This is an option which can facilitate special studies such as of the behavior of influence functions or of convergence of final solutions, though changing the order of points for a given face should not alter the solution for load constants found ultimately by the use of MATSOL.

The program allows the assignment of boundary conditions at points anywhere on any face or on the crack, including the crack front, though boundary conditions at the crack tip may be poorly representative for those on the front face. Crack functions for points off the crack plane are

evaluated in part by a quadrature which loses accuracy significantly for points quite near the crack (say for $|\zeta| << 0.01$ a), but an alternate evaluation procedure called automatically when $\zeta = 0$ is quite accurate and thus permits free assignment of boundary conditions on the crack. (Even for points near but not on the crack plane another special subroutine provides usable values, though a little slowly. Evaluations of crack functions for points near the cylindrical axis of the crack coordinate system is handled by still another special calculation.) The continuity of the surface load functions also allows assignment of boundary condition points anywhere on the plane surfaces, but this is a freedom that should be used judiciously. Separate research into this matter has shown that the proper selection of boundary conditions points can be a vital matter. This matter is discussed later and in the accompanying report [2].

The basic theory of stresses arising from crack loads presumes that the tractions effectively acting at any point on one face of the crack are equal in magnitude, but opposite in direction to those acting at the equivalent point on the other face. Thus, the crack loads should not be expected to produce any net force to upset the overall equilibrium of a body containing all or part of the circular crack. This implies in turn that the surface loads chosen as freeing forces should themselves be in overall equilibrium, but this condition is not implied automatically by the surface load theory. Therefore, the program has in it a procedure for constructing equations which must be satisfied by all the surface load constants being used if the body is to be in equilibrium in each of the three principal directions and if there is to be no net moment about the three principal axes. These equations take into account the size and location of the base over which each elemental load acts, and assign to each element a center of action so that overall moments can be computed. Thus, as many as six exact equations can be appended to the set of boundary conditions, reflecting the need of the body to be in equilibrium in each of six senses. Symmetry may make some of these equations identically zero, and these should be omitted lest they produce a singular matrix. Moreover, a user may simply desire some equilibrium conditions to be unenforced, so the user is simply given the option of satisfying as many of the six equilibrium conditions as he

may desire. For the case of a slab with a particular surface crack situated and loaded symmetrically about both the x and y axes, for example, this means that ordinarily it is appropriate to enforce one equilibrium equation (for the sum of normal loads on the two surfaces), but it may be omitted if the user desires. (It might seem that adequate satisfaction of pointwise boundary conditions on the two surfaces would automatically insure satisfaction of this overall equilibrium condition, but in practical calculations that expectation is often unfulfilled and direct imposition of the equilibrium condition seems beneficial.)

The call for imposition of overall equilibrium conditions of the six possible kinds is inserted on a yes or no basis for each kind of equilibrium, as is explained later.

Allowance for Symmetries

If the shape of the body and the loading pattern are symmetric about any of the planes $x = 0$, $y = 0$, or $z = z_t/2$, or if there is symmetry about any of the lines $x = y = 0$, or $x = z - z_t/2 = 0$, or $y = z - z_t/2 = 0$, then many pairs or even sets of four or eight load constants are predictably equal or equal except for sign. In such cases, it is very desirable to reduce the number of unknowns to be found by combining the influence of all predictably equivalent constants and then solving for only one representative member of each set. To this end, options are provided to make the program allow for symmetries of one or more of the six kinds listed above. In making such an allowance, the program first sorts through the list of load constants to determine which sets of them are predictably equal (except possibly for sign), then selects a representative constant from each set and combines the influence functions for all members of the set into an overall influence function to be multiplied by the representative constant of the set. The mechanism for doing this is a chain of operations which accumulates the necessary information for proper disposition of each load constant and combines the influence functions for related load constants as required. The symmetries in the roles of the constants are recorded in a list of numbers called A(I) in FRAC3D or E(I) in MATSOL. If A(I) = 0, it is implied that the $I^{\underline{th}}$ load constant is one of the chosen representative constants,

so it is not to be displaced. For constants which must vanish because of symmetry (such as τ_{zx} on a plane of antisymmetry at x = 0), the program puts A(I) = I. If A(I) is shown to be some other positive (or negative) number, it is implied that influence functions for the $I^{\underline{th}}$ load constant should be added to (or subtracted from) the influence functions for the load constant with position given by the other number. At the end of the reduction process, the combined influence functions for those constants having their A(I) = 0 are retained, but the columns of influence functions for all other load constants are deleted.

Symmetry which causes predictable equalities between load constants must include symmetry in the boundary conditions applied. Therefore, a further convention employed by the program is that boundary conditions will be prescribed at only one of any set of symmetrically situated points, it being presumed that symmetric boundary conditions are implied at all other points of the set. Since application of a boundary condition at any point of a symmetric set leads to the same reduced equation (that is the same equation connecting the representative load constants), the effect of applying conditions at all points of the set can be had in the least squares solution by employing the equations for tractions at just one point of each set and multiplying them by a weight equal to the square root of the number of points in that symmetry set. The program does that also automatically. Thus, for a slab with a surface crack and symmetry around the planes x = 0 and y = 0, boundary conditions applied on the front face at the origin (where x = y = z = 0) are assigned weight 1, those elsewhere on an axis are assigned weight $\sqrt{2}$, and those on neither axis are assigned weight 2.

The symmetry chain manipulates crack constants and their influence functions as well as surface load constants and their influence functions. Therefore, it offers a convenient approach to editing the solution process in further ways that may be desired. For example, it is possible to use it to delete the crack load constants for odd m, together with their columns of influence functions. This can be accomplished by a strategically situated insertion that A(I) = I for all I related to an odd m.

The means for asserting the kinds of symmetry to be imposed consist of numbers the user supplies showing, in general terms, how tractions of a

given kind in one region are related to those of the same kind in another region where symmetry might exist. Details for doing this are provided later. It may be added that the basic theory of stress analysis requires that along an edge the shear components of stress acting perpendicular to the edge on both the faces must be equal. Since this is a universal requirement, provisions for satisfying it automatically have been included in the program.

Alternative Modes of Operation of FRAC3D

When it is desired to find load constants to satisfy a given set of boundary conditions on the body, then FRAC3D is used to derive a set of boundary conditions by operating it in the "SOLVE" mode as has been described. A modification of this mode is had by adding the instruction "OUTPUT", and when this is done, the computer prints out the influence functions computed for each of the boundary equations. This offers a convenient tool for finding, for example, what stresses would exist on a given plane in an infinite space having a circular crack subjected to a given kind of loading (that is loading of a pattern related to specific crack load constants). If the plane is to be a surface of a finite body, then it is possible to draw a map of the boundary stresses which are to be freed, except as they are modified by interactions between surface and crack loads. Such a map is useful in planning a lattice for the surface load functions.

If the load constants are known, then operation of FRAC3D in its "RESULT" mode makes it possible to compute the resultant stress and displacement components anywhere in the body. This makes it possible to gain much fuller information on the nature of the stress distribution. It also makes it possible to evaluate surface tractions at points other than where the chosen boundary conditions were applied and thus to check the quality of a solution obtained from the SOLVE mode and MATSOL.

INPUT FOR FRAC3D AND ITS AUXILIARY PROGRAMS

Program LATTICE

Because the input for FRAC3D is relatively extensive and sufficiently complex so that human error is easily induced, a great deal of the input data generation has been automated.

The principal function of LATTICE is to generate a set of indices for ordering lattice points on each face of the body and for associating those in each pyramidal base, beginning with minimal input. It begins with a list of lines which the user has decided will be employed in each grid. Each line segment is defined by three constants: the x or y coordinate, and its two bounding extrema. The horizontal lines are denoted as $y = C_1$, $C_2 \leq x \leq C_3$, and the vertical lines are denoted as $x = D_1$, $D_2 \leq y \leq D_3$. The user supplies the C's and D's in local coordinates as input for each face involved in the analysis. From them the program is to find the lattice points, enumerate them, and associate those for each pyramidal base.

Figure 3 shows a typical grid work. Putting all the pyramid points first, the lattice points are enumerated in normal reading order (with increasing x and decreasing y). The figure shows the indices for its case where space allows. The nine points associated with each pyramidal base are also to be taken in the same order, so that for the first pyramidal base in the example the indices are 210, 211, 212, 219, 1, 2, 227, 13, 14. Such orderings are needed in the input to FRAC3D.

The form of the input to LATTICE is described as follows.

Card Type 1 - Mode Card (1 card):

Read MODE, MFLAG
Format (A4,70X,A6)

MODE = SOLVE for matrix generation. Program LATTICE generates input data only for this mode of operation for FRAC3D.

MFLAG = blank if no matrix print-out is desired or OUTPUT if matrix print-out is desired.

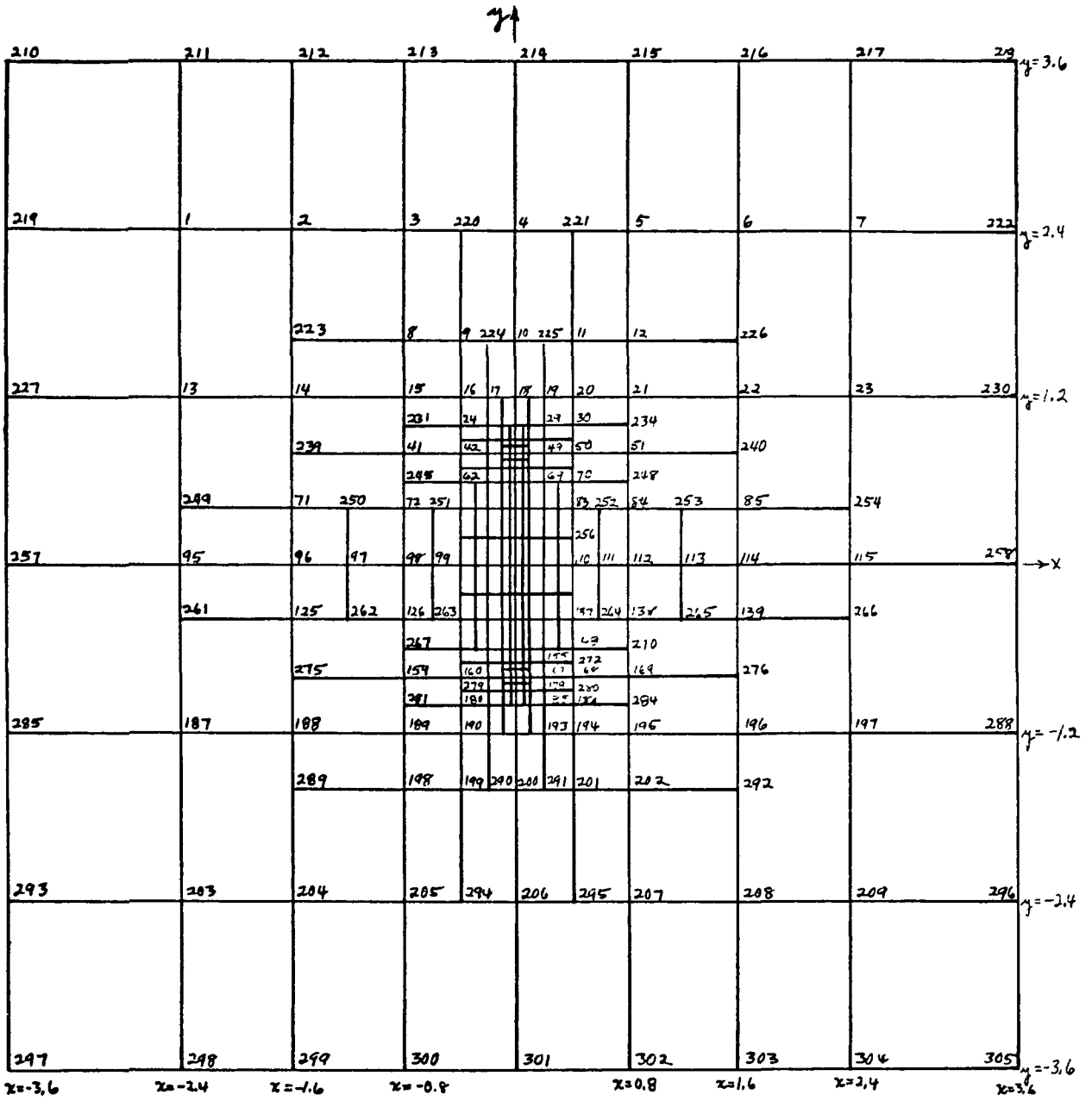

FIGURE 3. ILLUSTRATIVE LATTICE SHOWING INDICES USED BY FRAC3D
(FRONT LATTICE FOR A/2C = 0.25, C = 0.8 a)

Card Type 2 - Title Card (2 cards required):

Read TITLE1, TITLE2
Format 2(8A10)

Each card contains any information the user desires to use to identify the run. This title also appears in subsequent runs of MATSOL and FRAC3D in the RESULT mode of operation.

Card Type 3 - Symmetry Card (1 card):

Read JXS, JYS, JZS
Format (3A4)

JXS = IX1S for symmetry about x = y = 0 line
= IX2S for symmetry about x = 0 plane
JYS = IY1S for symmetry about y = 0, z = $z_t/2$ line
= IY2S for symmetry about y = 0 plane
JZS = IZ1S for symmetry about x = 0, z = $z_t/2$ line
= IZ2S for symmetry about z = $z_t/2$ plane

Card Type 4 - Symmetry Relation Cards (variable number of cards):

Read ((AXS(I,J), J = 1,3), I = 1,3)
Read ((AYS(I,J), J = 1,3), I = 1,3)
Read ((AZS(I,J), J = 1,3), I = 1,3)
Format (9F5.0)

In these arrays, the first index (I) refers to the load component p(I = 1), s(I = 2), or t(I = 3). The second index (J) refers to a pair of faces by the scheme that J = 1 for Faces 1 and 4, J = 2 for Faces 2 and 5, and J = 3 for Faces 3 and 6. The three arrays are used to prescribe desired relationships between the load components (p,s,t) at a point (x,y,z) and the load components (p', s', t') at a symmetrically located point (x', y', z'). A value + 1, for example, implies that p is to be equated to p', while value - 1 implies that p is to be equated to - p'. It is important to keep

in mind that the loads being equated have signs determined according to their respective local systems of coordinates.

As an example, suppose a slab problem is being analyzed and there is symmetry about the x = 0 and y = 0 planes. Across the plane x = 0, it is required that p = p', s = -s', t = t', while across the y = 0 plane, it is required that p = p', s = s', t = - t'. In this case then JXS = IX2S, JYS = IY2S, and JZS is blank. Thus, the first card of Type 4 should contain the instructions

$$\text{AXS} = \begin{array}{c} \\ I \downarrow \end{array} \begin{array}{c} J \longrightarrow \\ \begin{bmatrix} 1 & 0 & 0 \\ -1 & 0 & 0 \\ 1 & 0 & 0 \end{bmatrix} \end{array}$$; on the card it appears 1,0,0, - 1,0,0, 1,0,0.

The second card of Type 4 should state that

$$\text{AYS} = \begin{array}{c} \\ I \downarrow \end{array} \begin{array}{c} J \longrightarrow \\ \begin{bmatrix} 1 & 0 & 0 \\ 1 & 0 & 0 \\ -1 & 0 & 0 \end{bmatrix} \end{array}$$; on the card it appears 1,0,0,1,0,0,-1,0,0

The third card of Type 4, for AZS, should then be omitted.

Each array appears on one input card and there is one card for each type of symmetry claimed. If there is no symmetry of a given type, then the corresponding array card must be omitted.

The information on the cards of Type 4, like that on the preceding card of Type 3 and that on the following cards of Type 5, 6, 8 and 9 is a means for organizing the input to FRAC3D.

Card Type 5 (1 card):

Read NALFI, NALFJ, NBETI, NBETJ, NGAMI, NGAMJ, NAHATI, NAHATJ, NBHATI, NBHATJ, NGHATI, NGHATJ

Format (12I5)

These quantities define the crack series made available for the calculation. The coefficients are:

$\alpha'_{i,j}$, i = 0,1,...,NALFI-1, j = 0,1,...,NALFJ-1 ;

$\beta'_{i,j}$, i = 0,1,...,NBETI-1, j = 0,1,...,NBETJ-1 ;

$\gamma'_{i,j}$, i = 1,2,...,NGAMI-1, j = 0,1,...,NGAMJ-1 ;

$\hat{\alpha}'_{i,j}$, i = 1,2,...,NAHATI-1,j = 0,1,...,NAHATJ-1;

$\hat{\beta}'_{i,j}$, i = 0,1,...,NBHATI-1,j = 0,1,...,NBHATJ-1;

$\hat{\gamma}'_{i,j}$, i - 1,2,...,NGHATI-1,j = 0,1,...,NGHATJ-1.

Card Type 6 (1 card):

Read IFACE(I), I = 1,7

Format (7I5)

This card defines the coordinate systems involved in the calculation. The value of I defines the numbered faces in Figure 1 for I = 1,6 while I = 7 is the crack system. If IFACE(I) = I, then the $I^{\underline{th}}$ system is included in the calculation. If IFACE(I) = 0, then the $I^{\underline{th}}$ system is excluded from further consideration.

Card Type 7 (1 card):

Read XLO, YLO, XU, YU, ZSUBT, NU

Format (6F10.0)

These quantities define the geometry and material properties. The geometry is measured in the first face or (1) system, which is also treated as the global system.

XLO - defines Face 2 (x = XLO plane)
YLO - defines Face 3 (y = YLO plane)
XU - defines Face 5 (x = XU plane)
YU - defines Face 6 (y = YU plane)
ZSUBT - defines Face 4 (z = ZSUBT plane)
NU - Poisson's ratio.

Card Type 8 (1 card):

Read W, RSUBC
Format (2F10.0)

W($\sim\omega$) = inclination of ζ-axis to the xy-plane.
RSUBC = directed distance from crack circle center to the (x,y,z) origin, measured in the plane of the crack. RSUBC carries the sign opposite that of the z-component of the crack center coordinates.

Card Type 9 (1 card):

Read XEQ, YEQ, ZEQ, XROT, YROT, ZROT
Format (8F10.0)

These quantities are either 1. or 0. depending on whether or not force equilibrium conditions in x, y, or z directions or moment equilibrium about the x, y, or z axes are to be imposed.

For each face involved in the problem, the following five cards types must be supplied.

Card Type 10 (1 card):

Read EX, EY, FX, FY
Format (4F10.0)

These values are the local coordinates of the points of intersection of the crack circle and the face being described. If the crack does not intersect the face, a blank card must be supplied. The points can be entered in either order.

Card Type 11 (1 card for each horizontal line segment):

Read C1, C2, C3
Format (3F10.0)

The numbers C1, C2, and C3 are the parameters describing the line segment $y = C1$, $C2 \leq x \leq C3$. The cards must be ordered in increasing values of C1.

Card Type 12 (1 card):

Read 7/8/9 EOF (end of file card)

Card Type 13 (1 card for each vertical line segment)

Read D1, D2, D3
Format (3F10.0)

The numbers D1, D2, and D3 are the parameters describing the line segment $x = D1$, $D2 \leq y \leq D2$. The cards must be ordered in increasing value of D1.

Card Type 14 (1 card):

Read 7/8/9 EOF (end of file card)

→ (Repeat Card Types 10-14 for each face in the problem.)

Card Type 15 (1 card):

Read A0, A1, A2, B0, B1, B2, C0, C1, C2
Format (9F5.0)

These numbers describe the prescribed boundary conditions on the crack surface as follows:

$$\sigma_z = A0 + A1\rho \cos\theta + A2\rho \sin\theta$$
$$\tau_{\theta z} = B0 + B1\rho \cos\theta + B2\rho \sin\theta$$
$$\tau_{zr} = C0 + C1\rho \cos\theta + C2\rho \sin\theta.$$

Card Type 16 (stress points on the crack, 1 card for each value of ρ):

Read ρ, θ_0, $\Delta\theta$ (If no crack EOF 7/8/9 card.)
Format (3F10.0)

Stress points on the crack are generated from this information. Each stress point has coordinates (ρ,θ) where θ successively has the values θ_0, $\theta_0 + \Delta\theta$, $\theta_0 + 2\Delta\theta,\ldots,$ θ_{max}, where θ_{max} is the point of intersection between the circle with the ρ and the top surface having a positive θ.

Note that if automatic generation of crack boundary points and conditions is not desired - as when an irregular array of crack points is to be used - then Card Types 15 and 16 should be replaced by a blank card in order to call for completion of the output from LATTICE.

The punched output from LATTICE provides a nearly complete set of input cards for the "SOLVE" mode of FRAC3D, lacking mainly some of the specifications of the boundary conditions that are to be imposed. It contains first about ten cards containing titles, symmetry information, series structure, forces to be used, and body extent. There follows a count card and a lattice deck for each face to be used, a card showing a count and specifications for the crack, crack boundary condition cards and an equilibrium specification card. Before use in FRAC3D, each count card needs checking of its first field, which should show the number of boundary condition points for its respective face. In addition, LATTICE supplies a card with the coordinates of one pyramid point from each symmetry set for each face (except at the crack tip) to be used in preparing specifications for surface boundary conditions (after adding one near the crack tip). It also supplies a card showing coordinates of the midpoint of each surface rectangle for possible use in a checking operation after load constants have been found.

The next section details the input data needed for FRAC3D and notes how to assign boundary-condition points and to insert counts relating to them.

Program FRAC3D

The program FRAC3D has two modes of operation, both of which are used in analyzing stresses and displacements in a three-dimensional body. One mode of operation ("SOLVE") is used to set up a system of linear equations which are stored or written on tape to be solved by program MATSOL. The second mode of operation ("RESULT") is used to generate stresses and displacements at selected points of the body. Input data will be described for both modes of operation.

Matrix Generation ("SOLVE" Mode)

Card Type 1 (1 card):

Read MODE, MFLAG
Format (A4,70X,A6)

MODE = SOLV - for generating the matrix
= RESULT - for generating stresses and displacements
(See later)

MFLAG = blank - if no matrix print-out is desire
= OUTPUT - if matrix is to be printed out from "SOLVE" mode.

Card Type 2 (2 cards, always):

Read TITLE1, TITLE2
Format (8A10)

Contain descriptions of problem. User supplied for later reference. This information can be carried over from LATTICE.

Card Type 3 (1 card):

Read JXS, JYS, JZS
Format (3A4)

JXS = IX1S for symmetry about x = y = 0 line
= IX2S for symmetry about plane x = 0

JYS = IY1S for symmetry about y = 0, z = $z_t/2$ line
= IY2S for symmetry about plane y = 0
JZS = IZ1S for symmetry about x = 0, z = $z_t/2$ line
= IZ2S for symmetry about plane z = $z_t/2$.

Card Type 4 (1 card for each symmetry claimed):

Read ((AXS(I,J), J = 1,3), I = 1,3)
Read ((AYS(I,J), J = 1,3), I = 1,3)
Read ((AZS(I,J), J = 1,3), I = 1,3)
Format (9F5.0) for each card

This information is normally carried over from LATTICE. A description of its meaning is given for input to LATTICE of Card Type 4.

Card Type 5 (1 card):

Read NALFI, NALFJ, NBETI, NBETJ, NGAMI, NGAMJ, NAHATI, NAHATJ, NBHATI, NBHATJ, NGHATI, NGHATJ
Format (12I5)

These quantities are those described for Card Type 5 of the input to LATTICE.

Card Type 6 (1 card):

Read IFACE(I), I = 1,7
Format (7I5)

These quantities are those described for Card Type 6 of the input to LATTICE.

Card Type 7 (1 card):

Read XLO, YLO, XU, YU, ZSUBT, NU
Format (6F10.0)

These quantities are those described for Card Type 6 of the input to LATTICE.

→ For each value of IFACE(I), I = 1,6 (not 7) which is I (not 0), there is a set of cards to be read in. These are card Types 8 and 9.

Card Type 8 (1 card for each set of cards of Types 8 and 9):

Read MAXS(I), NL(I), MAXL(I)
Format (3I5)

MAXS(I) = number of stress points to be read for Face I.
NL(I) = number of lattice points on the $I^{\underline{th}}$ face.
MAXL(I) = number of pyramid points on Face I.

Note that cards of this type will be provided as output from LATTICE, but the counts MAXS(I) from LATTICE will need correction to account for the number of boundary condition points assigned afresh by the user for FRAC3D.

Card Type 9 (1 card for each lattice point, usually punched by LATTICE):

Read XL(J), YL(J), (IN(L,J), L = 1,9) J = 1, NL(I)
Format (2F10.0, 9I3)

XL(J), YL(J) - coordinates of $J^{\underline{th}}$ lattice point on the $I^{\underline{th}}$ face
IN(L,J) - indices of the lattice points describing the base of the $J^{\underline{th}}$ pyramid.

→ Repeat Card Types 8 and 9 for each face involved in the problem.

Card Type 10 (1 card) (To be omitted if no crack is included.):

Read MAXSI(7), W, RSUBC
Format (I5, 5X, 2F10.0)

MAXSI(7) = number of stress points on the crack.
W(~ω) = inclination of ζ-axis to Face 1.

RSUBC = directed distance from crack circle center to Face 1 origin, measured in the plane of the crack. RSUBC > 0 if center is above first face, negative otherwise.

→ There is a set of cards of Types 11 and 12 for each face in the problem and for the crack.

Card Type 11 (1 card for each face in the problem):

Read TITLE1
Format (8A10)

TITLE1 = stress points for Face I

This card is provided as a spacer between the several sets of stress points.

If the user augments any set of stress points, the additional cards may be placed anywhere within the appropriate set of cards. That is, the stress points are not ordered in any particular fashion.

Card Type 12:

Read XSA(J), YSA(J), SIGMA(1,J), SIGMA(2,J), SIGMA(3,J)
Format (5F10.0)

XSA(J), YSA(J) - stress point coordinates on I^{th} face (not the crack)

SIGMA(1,J) - value of $\sigma_z^{(i)}$ at the stress point

SIGMA(2,J) - value of $\tau_{yz}^{(i)}$ at the stress point

SIGMA(3,J) - value of $\tau_{zx}^{(i)}$ at the stress point

In the case of the crack the coordinates to be shown are ρ and θ for the I^{th} point, and the stress components which can be prescribed are σ_z, $\tau_{\theta z}$, τ_{zr}, respectively.

→ Repeat Card Types 11 and 12 for each system in the problem. Note that boundary conditions on the body faces are usually

applied only at pyramid points (except for one near the crack tip). The coordinates XSA(J) and YSA(J) for them are provided among the punched output from LATTICE.

Card Type 13 (1 card):

Read XEQ, YEQ, ZEQ, XROT, YROT, ZROT
Format (6F10.0)

XEQ = 1. if equation describing force equilibrium in the x direction is to be included in the system of equations. Otherwise, use 0.

YEQ = same, but for equilibrium in the y direction.

ZEQ = same, but for equilibrium in the z direction.

XROT = 1. if the sum of the moments about the x axis are to be equated to zero. Otherwise, use 0.

YROT = same, but for moments about the y axis.

ZROT = same, but for moments about the z axis.

The SOLVE mode of operation results in several actions. The system of equations and certain other needed information is written on TAPE 9 for use in MATSOL, which solves the system of equations. In addition, considerable information is written on TAPE 8 for use in the RESULT mode of operation. Thus, the user must identify two storage units which can be referenced later.

Stress and Displacement Generation ("RESULT" Mode)

The input data required by FRAC3D to generate stresses and displacements is listed below. The program receives a great deal of its input data from TAPE 8 and from TAPE 7 generated by the program MATSOL discussed below.

Card Type 1 (A4):

Read MODE, MFLAG
Format (A4,70X,A6)
MODE = RESULT, MFLAG = blank.

Card Type 2 (2I5):

Read MAXSI(1), MAXSI(7)
MAXSI(1) - number of points in the global system at which stresses and displacements are to be generated.
MAXSI(7) - number of points expressed in the crack system at which stresses and displacements are to be generated.

Card Type 3 (Title card for these points, wording chosen by user).

Card Type 4 (3F10.0) (1 card for each point):

Read XSA(I), YSA(I), ZSA(I)
These are the points, expressed in the global coordinate system, at which results are desired.

Card Type 5 (Title card for these cards).

Card Type 6 (3F10.0) (1 card for each point):

Read RHO(I), THETA(I), ZETA(I)
These are the points, expressed in the cylindrical coordinate system, at which results are desired.

Program MATSOL

Program MATSOL is used after a matrix has been generated by FRAC3D and, together with other needed data, has been stored on TAPE 9. In its

ordinary version, MATSOL receives all of its input from TAPE 9 and uses it in solving for the load constants for all the plane surfaces used and for the crack if it is used. MATSOL prints out the equation residuals, the solution vector, and the distribution of the stress-intensity factors K_I, K_{II}, and K_{III} around the crack, all normalized by division by $K_{I\infty}$ for a unit load. In addition, the solution vector is written on TAPE 7 for use in FRAC3D operated in the RESULT mode.

In its ordinary version, the only special consideration in performing MATSOL is that the dimensions provided in cards 3 and 6 need to be large enough for the arrays A, R, C, D, B, S. All of these but A must have dimension as great as NT, which is the sum of the number of load constants which are allowed (on all the planes around the crack) plus the number of equilibrium conditions. A must then have dimension NT(NT + 1)/2 or more.

A special editing version of MATSOL permits special weighting of blocks of boundary conditions, and allows deletion of chosen load constants. Operation of this version requires data cards of three or four kinds as follow.

Card Type 1 (1 card):

Read WT1, WT2,..., WT8
Format (8FI0.0)

These are weights to apply to equations in 8 blocks defined by Card Type 2.

Card Type 2 (1 card):

Read IR1, IR2,..., IR8
Format (8I4)

These define 8 blocks of rows in the matrix of boundary conditions, having weight WT1 through row IR1, then having weight WT2 through row IR2, then having weight WT3 through row IR3, etc.

Card Type 3 (1 card):

Read NAUX, LZ, MSR
Format (3I4)

NAUX tell how many equilibrium conditions should be enforced. This NAUX usually agrees with the count assigned through FRAC3D, but putting NAUX = 0 allows deletion of equilibrium equations.

LZ tells how many crack constants already admitted in the construction of the matrix by FRAC3D are to be deleted by MATSOL. Use of MSR > 0 permits deletion of shear boundary conditions on the crack by putting MSR = row number of the last boundary condition on a body surface (not the crack).

Card Type 4 (variable number of cards, none if LZ = 0):

Read LE(I) I = 1, LZ
Format (20I4)

This provides the column-count identification of each load constant to be omitted from the calculations by MATSOL. (This is most often applied in editing the crack function series. It requires advance knowledge of order numbers for crack constants.)

See NASA CR 159400 for examples of why and how to edit crack series and sometimes surface load constants).

In the editing version of MATSOL, card 3 should provide dimensions for A, R, C, D, and B as does card 3 for the ordinary MATSOL. In addition the sixth card of the editing version of MATSOL should provide dimension for S to be at least large as NT + LZ, and the seventh card should provide dimension for JE at least as large as LZ and for JS at least as large at NT.

ILLUSTRATIVE CALCULATIONS FOR A SLAB WITH A SURFACE CRACK

In order to illustrate how a stress analysis is performed with FRAC3D, and to show typical numbers that arise, consider a slab with a part-circular surface crack. For the illustration, the crack is taken to be perpendicular to the faces of the slab, passing into the slab to a depth 0.4a where a is the crack radius, and penetrating 0.7 of the thickness of the slab. Poisson's ratio ν is taken to be 0.30. Designating the depth of the crack by A, the surface length of the crack by 2C, and the thickness of the slab by T, the defining parameters thus are A/2C = 0.25 and A/T = 0.7. In particular, also T = 0.57142857a, and C = 0.8a. The crack radius a is taken as the reference length, that is a = 1. The loading is taken to be a uniform normal load applied to the crack surface, that is the crack-induced part of the loading that would arise when the slab is subjected to remote tension perpendicular to the crack.

It is possible to select lattices for the front (cracked) and back surfaces intuitively, but it helps to consider in advance what stresses would arise on similarly situated planes in an infinite body having a circular crack under uniform normal load. The stresses σ_z, τ_{yz}, and τ_{zx} that would arise on those planes under a unit normal load are simply $\sqrt{2/\pi}$ times the influence functions for $\alpha'_{0,0}$ [2,3] in rows of a matrix computable by FRAC3D in its SOLVE OUTPUT mode. This suggests an occasional preliminary, optional calculation using only minimal surface lattices (one pyramidal base on each surface), neglecting symmetries, and using series which need to be long enough only to include functions for $\alpha'_{0,0}$. Points where the influence functions are to be found are treated as boundary-condition points, though no solution for load constants is intended. From computations of this sort, curves of fixed levels of the influence can be interpolated, as shown in Figures 4 and 5*. The stresses σ_z and τ_{zx} are considered there, since they are probably the more influential ones in surface crack stress analysis. Front and back lattices were chosen as also shown in Figures 4 and 5, which hopefully should accommodate the needed freeing stresses on the surfaces,

---

* Figure 4 shows one quadrant of the full lattice shown in Figure 3, there complete with indices. The effective load for Figures 4 and 5 is $\sigma_o = \sqrt{\pi/2}$.

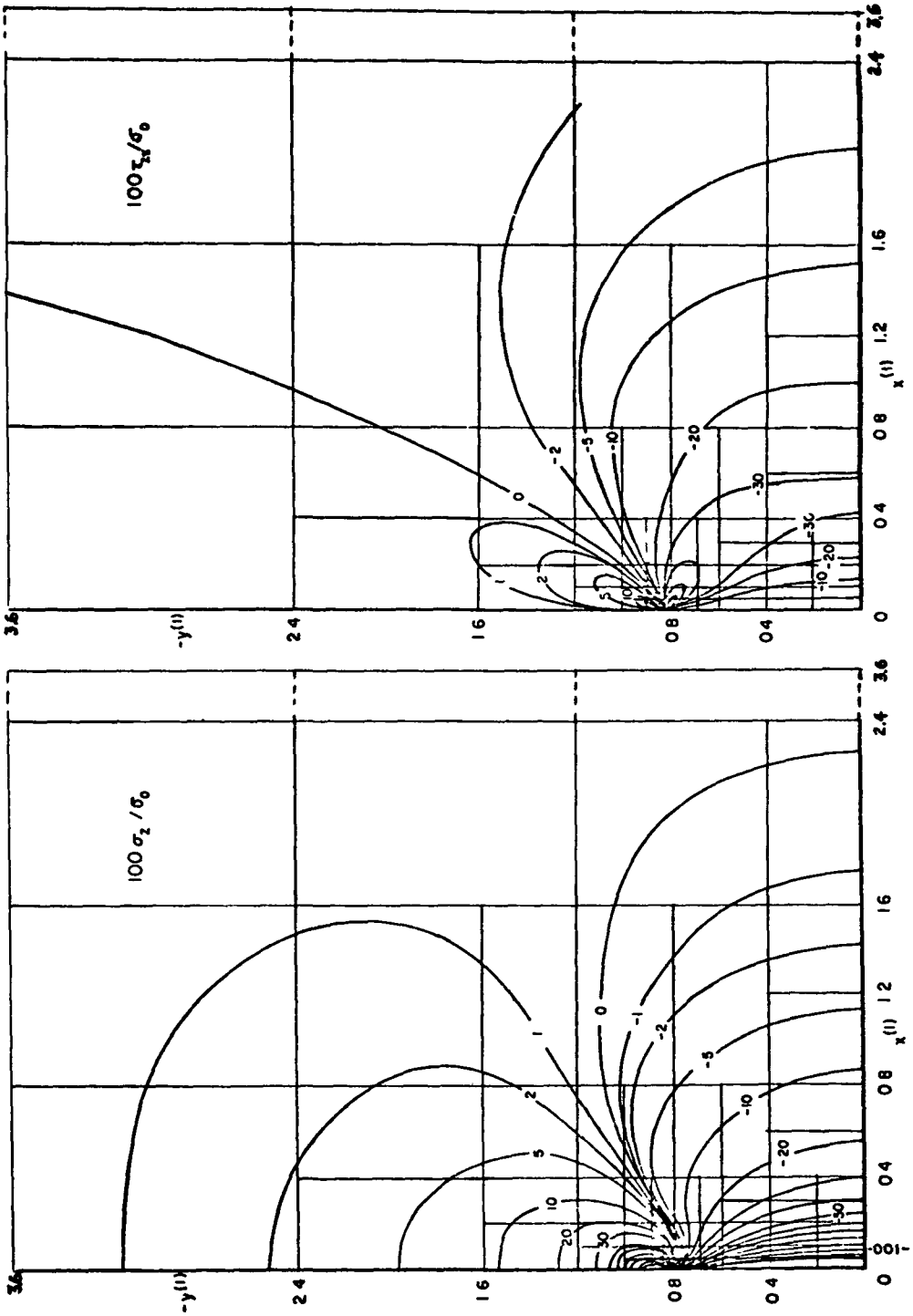

FIGURE 4. RELATION BETWEEN FRONT-SURFACE LATTICE AND INFLUENCE FUNCTIONS FOR $\alpha'_{0,0}$ ON THE CORRESPONDING PLANE IN AN INFINITE BODY (FOR THE CASE A/2C = 0.25)

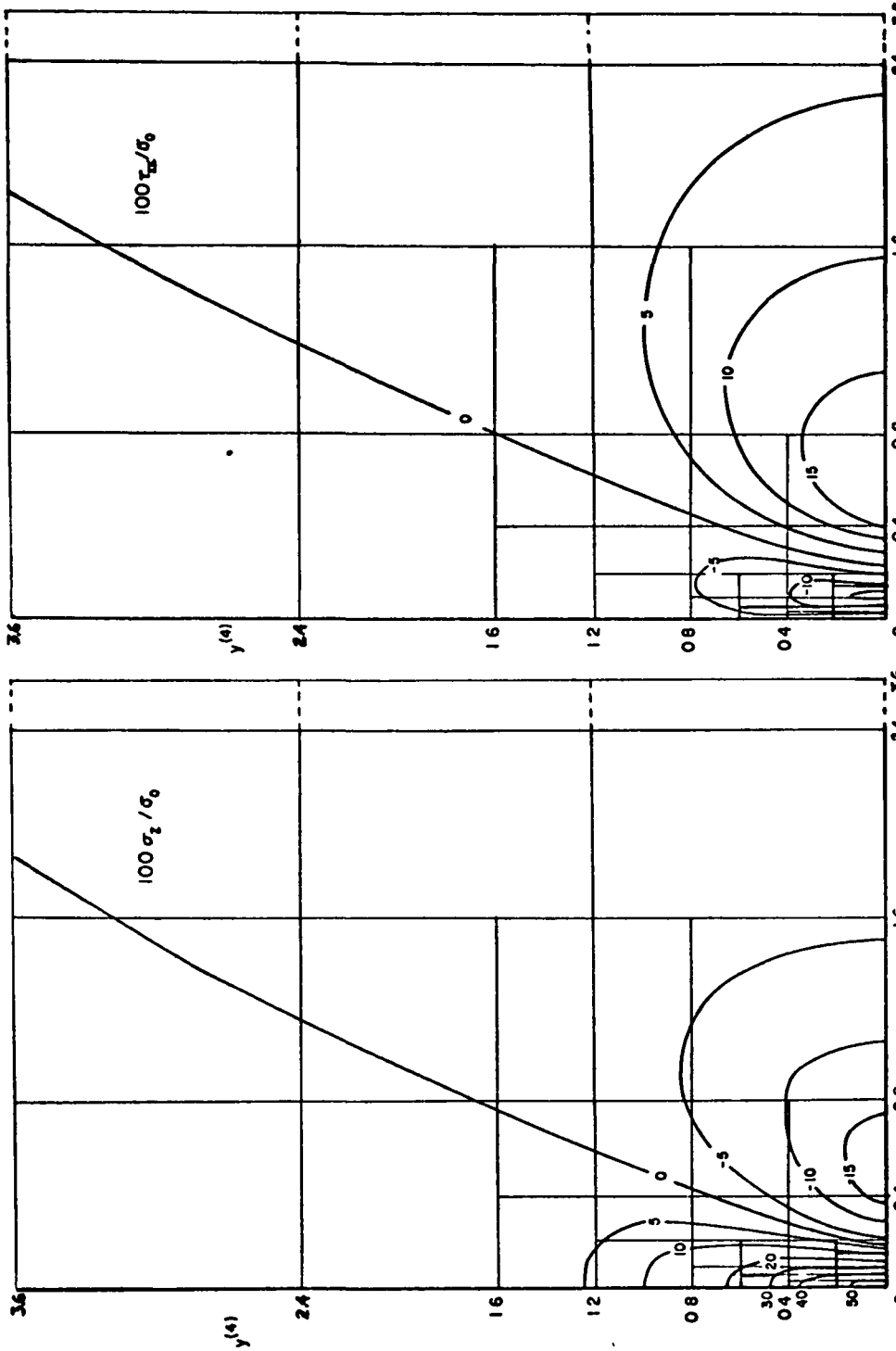

FIGURE 5. RELATION BETWEEN BACK-SURFACE LATTICE AND INFLUENCE FUNCTIONS FOR $\alpha'_{0,0}$ ON THE CORRESPONDING PLANE IN AN INFINITE BODY (FOR THE CASE A/2C = 0.25 AND A/T = 0.7)

though further interactions between surface and crack stress systems are yet to be considered.

In constructing the system of boundary condition equations, the surface loads were to use the lattices of Figures 4 and 5. The line segments for the lattices are shown in the tabulation on pp 37-38. Note that the segments are specified for all four quadrants, not just one quadrant. The crack series were desired with m even, $0 \leq m \leq 16$, and $0 \leq k \leq 16$ m, and these could be provided by putting NALFI = 17 and NALFJ = 9, with m-eveness and trangulation on k to be arranged later. Thus the calculation began by running the program LATTICE with input as follows. (An abbreviated coded form of this input is shown on p 39.)

Card	Data
1	SOLV (in cc 1-4)
2 and 3	(Titles which are shown here at the top of Page 51.)
4	IX 2S (cc 1-4) and IY2S (cc 5-8)
5	bbbl.bbbb.bbbb.bb-l.bbbb.bbbb.bbbl.bbbb.bbbb.
6	bbbl.bbbb.bbbb.bbbl.bbbb.bbbb.bb-l.bbbb.bbbb.
7	bbbl7bbbb9
8	1 (cc5) and 4 (cc20) and 7 (cc35)
9	In 6F10.0: 3.6, -3.6, 3.6, 3.6, 0.57142857, 0.30
10	In 2F10.0: 0.0, 0.6
11	In 8F10.0: 0.0, 0.0, 1.0, 0.0, 0.0, 0.0
12	In 4F10.0: 0.0, -0.8, 0.0, 0.8
13 - 39	(27 cards showing C1, C2, C3 in 3F10.0 for front face)
40	7/8/9 EOF
41 - 63	(23 cards showing D1, D2, D3 in 3F10.0 for front face)
64	7/8/9 EOF
65	blank card (because no crack tips are on back face)
66 - 82	(17 cards showing C1, C2, C3 in 3F10.0 for back face)
83	7/8/9 EOF
84 - 104	(21 cards showing D1,D2, D3 in 3F10.0 for back face)
105	7/8/9 EOF
106	blank card (since crack boundary conditions were to be special).

FACE NO. 1

COORDINATES OF CRACK TIPS = .0000000, -0.8000000 AND .0000000 , 0.8000000

C LINE SEGMENTS (INPUT)

	C1	C2	C3
1	-3.6000000	-3.6000000	3.6000000
2	-2.4000000	-3.6000000	3.6000000
3	-1.6000000	-1.6000000	1.6000000
4	-1.2000000	-3.6000000	3.6000000
5	-1.0000000	-0.8000000	0.8000000
6	-0.9000000	-0.4000000	0.4000000
7	-0.8500000	-0.1000000	0.1000000
8	-0.8000000	-1.6000000	1.6000000
9	-0.7500000	-0.1000000	0.1000000
10	-0.7000000	-0.4000000	0.4000000
11	-0.6000000	-0.8000000	0.8000000
12	-0.4000000	-2.4000000	2.4000000
13	-0.2000000	-0.4000000	0.4000000
14	.0000000	-3.6000000	3.6000000
15	0.2000000	-0.4000000	0.4000000
16	0.4000000	-2.4000000	2.4000000
17	0.6000000	-0.8000000	0.8000000
18	0.7000000	-0.4000000	0.4000000
19	0.7500000	-0.1000000	0.1000000
20	0.8000000	-1.6000000	1.6000000
21	0.8500000	-0.1000000	0.1000000
22	0.9000000	-0.4000000	0.4000000
23	1.0000000	-0.8000000	0.8000000
24	1.2000000	-3.6000000	3.6000000
25	1.6000000	-1.6000000	1.6000000
26	2.4000000	-3.6000000	3.6000000
27	3.6000000	-3.6000000	3.6000000

D LINE SEGMENTS (INPUT)

	D1	D2	D3
1	-3.6000000	-3.6000000	3.6000000
2	-2.4000000	-3.6000000	3.6000000
3	-1.6000000	-3.6000000	3.6000000
4	-1.2000000	-0.4000000	0.4000000
5	-0.8000000	-3.6000000	3.6000000
6	-0.6000000	-0.4000000	0.4000000
7	-0.4000000	-2.4000000	2.4000000
8	-0.3000000	-0.6000000	0.6000000
9	-0.2000000	-1.6000000	1.6000000
10	-0.1000000	-1.2000000	1.2000000
11	-0.0500000	-1.0000000	1.0000000
12	.0000000	-3.6000000	3.6000000
13	0.0500000	-1.0000000	1.0000000
14	0.1000000	-1.2000000	1.2000000
15	0.2000000	-1.6000000	1.6000000
16	0.3000000	-0.6000000	0.6000000
17	0.4000000	-2.4000000	2.4000000
18	0.6000000	-0.4000000	0.4000000
19	0.8000000	-3.6000000	3.6000000
20	1.2000000	-0.4000000	0.4000000
21	1.6000000	-3.6000000	3.6000000
22	2.4000000	-3.6000000	3.6000000
23	3.6000000	-3.6000000	3.6000000

FACE NO. 4

COORDINATES OF CRACK TIPS = *9.0000000, *9.0000000 AND *9.0000000 , *9.0000000

C LINE SEGMENTS (INPUT)

1	-3.6000000	-3.6000000	3.6000000
2	-2.4000000	-3.6000000	3.6000000
3	-1.6000000	-1.6000000	1.6000000
4	-1.2000000	-3.6000000	3.6000000
5	-0.8000000	-1.6000000	1.6000000
6	-0.6000000	-0.2000000	0.2000000
7	-0.4000000	-0.8000000	0.8000000
8	-0.2000000	-0.2000000	0.2000000
9	.0000000	-3.6000000	3.6000000
10	0.2000000	-0.2000000	0.2000000
11	0.4000000	-0.8000000	0.8000000
12	0.6000000	-0.2000000	0.2000000
13	0.8000000	-1.6000000	1.6000000
14	1.2000000	-3.6000000	3.6000000
15	1.6000000	-1.6000000	1.6000000
16	2.4000000	-3.6000000	3.6000000
17	3.6000000	-3.6000000	3.6000000

D LINE SEGMENTS (INPUT)

1	-3.6000000	-3.6000000	3.6000000
2	-2.4000000	-3.6000000	3.6000000
3	-1.6000000	-3.6000000	3.6000000
4	-0.8000000	-3.6000000	3.6000000
5	-0.4000000	-1.6000000	1.6000000
6	-0.2000000	-1.2000000	1.2000000
7	-0.1500000	-0.2000000	0.2000000
8	-0.1000000	-0.8000000	0.8000000
9	-0.0500000	-0.6000000	0.6000000
10	-0.0250000	-0.4000000	0.4000000
11	.0000000	-3.6000000	3.6000000
12	0.0250000	-0.4000000	0.4000000
13	0.0500000	-0.6000000	0.6000000
14	0.1000000	-0.8000000	0.8000000
15	0.1500000	-0.2000000	0.2000000
16	0.2000000	-1.2000000	1.2000000
17	0.4000000	-1.6000000	1.6000000
18	0.8000000	-3.6000000	3.6000000
19	1.6000000	-3.6000000	3.6000000
20	2.4000000	-3.6000000	3.6000000
21	3.6000000	-3.6000000	3.6000000

BATTELLE STANDARD CODING FORM

COMPASS	Location	Operation, Modifiers	Address Field	Comments	IDENT
COBOL	sequence: page / serial	Cont. A	B		IDENT
FORTRAN	C / Statement Number	Cont.	FORTRAN STATEMENT		IDENT

Card	Cols 1–10	Cols 11–20	Cols 21–30	Cols 31–40	Cols 41–50	Cols 51–60	Cols 61–80
1	50LV						
2	PROBLEM I.7A, C=0.8, A/2C=0.25, A/T=0.7, NU=0.30						
3	WITH 17x9 H-EVEN TRIANGULAR SERIES, LATTICES OF 4-21-76, FRAC3D OF 9-30-77						
4	IX2SIY2S						
5	1. .	. -1.	. .	1. .	.		
6	1. .	. 1.	. .	-1. .	.		
7	17						
8	1	4		7			
9	3.6	-3.6	3.6	3.6	0.57142857	0.30	
10	0.0	0.6					
11	0.0	0.0	1.0	0.0	0.0	0.0	
12	0.0	-0.8	0.0	0.8			
13-39	-3.6	-3.6	3.6	(followed by 26 more cards in same format for y-constant lines of front lattice)			
40	(Use an End-of-File Card)						
41-63	-3.6	-3.6	3.6	(followed by 22 more cards in same format for x-constant lines of front lattice)			
64	(Use an End-of-File Card)						
65	(Use a blank card here because no crack tips are on the back face)						
66-82	-3.6	-3.6	3.6	(followed by 16 more cards in same format for y-constant lines of back lattice)			
83	(Use an End-of-File Card)						
84-104	-3.6	-3.6	3.6	(followed by 20 more cards in same format for x-constant lines of back lattice)			
105	(Use an End-of-File Card)						
106	(Use a blank card, since crack boundary conditions are to be key punched but further output - midpoints - is wanted.)						
23							
24							
25							

DATA DESCRIPTION Illustrative input for LATTICE Project No. ________ PREPARED BY ________

DATE ________ PAGE ________ OF ________

The major output from LATTICE is the indices for all the lattice points, and sets of nine indices for all the bases of pyramids. Lists of these indices are printed by LATTICE and again later by FRAC3D as a record of input it received. The list of these indices reported by LATTICE is shown on pp 41 to 47.

The input for FRAC3D came mainly from LATTICE, but that was supplemented by adding five boundary condition points on the front near the crack tip (to be used at option) and also 80 boundary condition points on the crack as shown in Figure 6. Boundary tractions were assigned as needed, these being zero except for the normal load on the crack, which was taken to be unity, so that in effect the normal load on the crack became the reference stress. Thus the following data cards were assembled for running FRAC3D. (An abbreviated coded form of this input is shown on p 48.)

Card	Data
1 - 9	Like cards 1 - 9 of input to LATTICE (Note that in card 9 repunching of ZSUBT restores accuracy dropped by LATTICE.)
10	bbb68bb305bb209 (The 68 was corrected.)
11 - 315	(305 cards from LATTICE for the front face)
316	bbb36bb181bb109
317 - 497	(181 cards from LATTICE for the back face)
498	bbb80, 0.0 (in cc 11-13), 0.6 (in cc 21-23)
499	(Title card: STRESS POINTS FOR FACE 1)
500 - 567	(68 points for boundary conditions on front)
568	(Title card: STRESS POINTS FOR FACE 4)
569 - 604	(36 points for boundary conditions on back)
605	(Title card: STRESS POINTS FOR FACE 7)
606 - 685	(80 cards for boundary conditions on crack)
686	In 6F10.0: 0.0, 0.0, 1.0, 0.0, 0.0, 0.0

It may be observed that symmetry around both the planes x = 0 and y = 0 was specified by Cards 4, 5 and 6. The series specified by Card 7 called for 17 x 9 series with constants $\alpha'_{m,k}$, but this was intended to be reduced by making FRAC3D remove the series terms for which m would be odd

LATTICE POINTS ON FRONT FACE (P1)

FACE NO. 1(OUTPUT) MAXSI= 13 NL1=303 MAXL1=209

Indices for the vertex points in base & pyramid

x	y									
-2.4000000	2.4000000	210	211	212	219	1	2	227	13	14
-1.6000000	2.4000000	211	212	213	1	2	3	13	14	15
-0.8000000	2.4000000	212	213	214	2	3	4	223	8	10
.0000000	2.4000000	213	214	215	3	4	5	8	10	12
0.8000000	2.4000000	214	215	216	4	5	6	10	12	226
1.6000000	2.4000000	215	216	217	5	6	7	21	22	23
2.4000000	2.4000000	216	217	218	6	7	222	22	23	230
-0.8000000	1.6000000	2	3	220	223	8	9	14	15	16
-0.4000000	1.6000000	3	220	4	8	9	10	15	16	18
.0000000	1.6000000	220	4	221	9	10	11	16	18	20
0.4000000	1.6000000	4	221	5	10	11	12	18	20	21
0.8000000	1.6000000	221	5	6	11	12	226	20	21	22
-2.4000000	1.2000000	219	1	2	227	13	14	257	95	96
-1.6000000	1.2000000	1	2	3	13	14	15	249	71	72
-0.8000000	1.2000000	223	8	9	14	15	16	239	41	42
-0.4000000	1.2000000	8	9	224	15	16	17	231	24	25
-0.2000000	1.2000000	9	224	10	16	17	18	24	25	27
.0000000	1.2000000	224	10	225	17	18	19	25	27	29
0.2000000	1.2000000	10	225	11	18	19	20	27	29	30
0.4000000	1.2000000	225	11	12	19	20	21	29	30	234
0.8000000	1.2000000	11	12	226	20	21	22	50	51	240
1.6000000	1.2000000	5	6	7	21	22	23	84	85	254
2.4000000	1.2000000	6	7	222	22	23	230	114	115	258
-0.4000000	1.0000000	15	16	17	231	24	25	41	42	43
-0.2000000	1.0000000	16	17	228	24	25	26	235	31	32
-0.1000000	1.0000000	17	229	18	25	26	27	31	32	34
.0000000	1.0000000	228	18	229	25	27	28	32	34	36
0.1000000	1.0000000	18	229	19	27	28	29	34	36	37
0.2000000	1.0000000	229	19	20	28	29	30	36	37	236
0.4000000	1.0000000	19	20	21	29	30	234	49	50	51
-0.2000000	0.9000000	24	25	26	235	31	32	42	43	44
-0.1000000	0.9000000	25	26	232	31	32	33	43	44	45
-0.0500000	0.9000000	26	232	27	32	33	34	237	38	39
.0000000	0.9000000	232	27	233	33	34	35	38	39	40
0.0500000	0.9000000	27	233	28	34	35	36	39	40	238
0.1000000	0.9000000	233	28	29	35	36	37	47	48	49
0.2000000	0.9000000	28	29	30	36	37	236	48	49	50
-0.0500000	0.8500000	32	33	34	237	38	39	44	45	46
.0000000	0.8500000	33	34	35	38	39	40	45	46	47
0.0500000	0.8500000	34	35	36	39	40	238	46	47	48
-0.8000000	0.8000000	14	15	16	239	41	42	71	72	73
-0.4000000	0.8000000	231	24	25	41	42	43	245	62	63
-0.2000000	0.8000000	235	31	32	42	43	44	243	55	56
-0.1000000	0.8000000	31	32	33	43	44	45	55	56	57
-0.0500000	0.8000000	237	38	39	44	45	46	241	52	53
.0000000	0.8000000	38	39	40	45	46	47	52	53	54
0.0500000	0.8000000	39	40	238	46	47	48	53	54	242
0.1000000	0.8000000	35	36	37	47	48	49	59	60	61
0.2000000	0.8000000	36	37	236	48	49	50	60	61	244
0.4000000	0.8000000	29	30	234	49	50	51	69	70	248
0.8000000	0.8000000	20	21	22	50	51	240	83	84	85
-0.0500000	0.7500000	44	45	46	241	52	53	56	57	58
.0000000	0.7500000	45	46	47	52	53	54	57	58	59
0.0500000	0.7500000	46	47	48	53	54	242	58	59	60
-0.2000000	0.7000000	42	43	44	243	55	56	62	63	64
-0.1000000	0.7000000	43	44	45	55	56	57	63	64	65
-0.0500000	0.7000000	241	52	53	56	57	58	64	65	66
.0000000	0.7000000	52	53	54	57	58	59	65	66	67
0.0500000	0.7000000	53	54	242	58	59	60	66	67	68
0.1000000	0.7000000	47	48	49	59	60	61	67	68	69
0.2000000	0.7000000	48	49	50	60	61	244	68	69	70
-0.4000000	0.6000000	41	42	43	245	62	63	72	73	75
-0.2000000	0.6000000	243	55	56	62	63	64	73	75	76
-0.1000000	0.6000000	55	56	57	63	64	65	75	76	77
-0.0500000	0.6000000	56	57	58	64	65	66	76	77	78
.0000000	0.6000000	57	58	59	65	66	67	77	78	79
0.0500000	0.6000000	58	59	60	66	67	68	78	79	80
0.1000000	0.6000000	59	60	61	67	68	69	79	80	81
0.2000000	0.6000000	60	61	244	68	69	70	80	81	83
0.4000000	0.6000000	49	50	51	69	70	248	81	83	84
-1.6000000	0.4000000	13	14	15	249	71	72	95	96	98
-0.8000000	0.4000000	239	41	42	71	72	73	96	98	100
-0.4000000	0.4000000	245	62	246	72	73	74	98	100	101
-0.3000000	0.4000000	62	246	63	73	74	75	255	86	87
-0.2000000	0.4000000	246	63	64	74	75	76	86	87	88

LATTICE POINTS ON FRONT FACE (P2)

-0.1000000	0.4000000	63	64	65	75	76	77	87	88	89
-0.0500000	0.4000000	64	65	66	76	77	78	88	89	90
.0000000	0.4000000	65	66	67	77	78	79	89	90	91
0.0500000	0.4000000	66	67	68	78	79	80	90	91	92
0.1000000	0.4000000	67	68	69	79	80	81	91	92	93
0.2000000	0.4000000	68	69	247	80	81	82	92	93	94
0.3000000	0.4000000	69	247	70	81	82	83	93	94	256
0.4000000	0.4000000	247	70	248	82	83	84	109	110	112
0.8000000	0.4000000	50	51	240	83	84	85	110	112	114
1.6000000	0.4000000	21	22	23	84	85	254	112	114	115
-0.3000000	0.2000000	73	74	75	255	86	87	100	101	102
-0.2000000	0.2000000	74	75	76	85	87	88	101	102	103
-0.1000000	0.2000000	75	76	77	87	88	89	102	103	104
-0.0500000	0.2000000	76	77	78	88	89	90	103	104	105
.0000000	0.2000000	77	78	79	89	90	91	104	105	106
0.0500000	0.2000000	78	79	80	90	91	92	105	106	107
0.1000000	0.2000000	79	80	81	91	92	93	106	107	108
0.2000000	0.2000000	80	81	82	92	93	94	107	108	109
0.3000000	0.2000000	81	82	83	93	94	256	108	109	110
-2.4000000	-.0000000	227	13	14	257	95	96	285	187	188
-1.6000000	-.0000000	249	71	250	95	96	97	261	125	262
-1.2000000	-.0000000	71	251	72	96	97	98	125	262	126
-0.8000000	-.0000000	250	72	251	97	98	99	262	126	263
-0.6000000	-.0000000	72	251	73	98	99	100	126	263	127
-0.4000000	-.0000000	251	73	74	99	100	101	263	127	128
-0.3000000	-.0000000	255	86	87	100	101	102	259	116	117
-0.2000000	-.0000000	86	87	88	101	102	103	116	117	118
-0.1000000	-.0000000	87	88	89	102	103	104	117	118	119
-0.0500000	-.0000000	88	89	90	103	104	105	118	119	120
.0000000	-.0000000	89	90	91	104	105	106	119	120	121
0.0500000	-.0000000	90	91	92	105	106	107	120	121	122
0.1000000	-.0000000	91	92	93	106	107	108	121	122	123
0.2000000	-.0000000	92	93	94	107	108	109	122	123	124
0.3000000	-.0000000	93	94	256	108	109	110	123	124	260
0.4000000	-.0000000	82	83	252	109	110	111	136	137	264
0.6000000	-.0000000	83	252	84	110	111	112	137	264	138
0.8000000	-.0000000	252	84	253	111	112	113	264	138	265
1.2000000	-.0000000	84	253	85	112	113	114	138	265	139
1.6000000	-.0000000	253	85	254	113	114	115	265	139	266
2.4000000	-.0000000	22	23	230	114	115	258	196	197	268
-0.3000000	-0.2000000	100	101	102	259	116	117	127	128	129
-0.2000000	-0.2000000	101	102	103	116	117	118	128	129	130
-0.1000000	-0.2000000	102	103	104	117	118	119	129	130	131
-0.0500000	-0.2000000	103	104	105	118	119	120	130	131	132
.0000000	-0.2000000	104	105	106	119	120	121	131	132	133
0.0500000	-0.2000000	105	106	107	120	121	122	132	133	134
0.1000000	-0.2000000	106	107	108	121	122	123	133	134	135
0.2000000	-0.2000000	107	108	109	122	123	124	134	135	136
0.3000000	-0.2000000	108	109	110	123	124	260	135	136	137
-1.6000000	-0.4000000	95	96	98	261	125	126	187	188	189
-0.8000000	-0.4000000	96	98	100	125	126	127	275	159	160
-0.4000000	-0.4000000	98	100	101	126	127	128	267	140	268
-0.3000000	-0.4000000	259	116	117	127	128	129	140	268	141
-0.2000000	-0.4000000	116	117	118	128	129	130	268	141	142
-0.1000000	-0.4000000	117	118	119	129	130	131	141	142	143
-0.0500000	-0.4000000	118	119	120	130	131	132	142	143	144
.0000000	-0.4000000	119	120	121	131	132	133	143	144	145
0.0500000	-0.4000000	120	121	122	132	133	134	144	145	146
0.1000000	-0.4000000	121	122	123	133	134	135	145	146	147
0.2000000	-0.4000000	122	123	124	134	135	136	146	147	269
0.3000000	-0.4000000	123	124	260	135	136	137	147	269	148
0.4000000	-0.4000000	109	110	112	136	137	138	269	148	270
0.8000000	-0.4000000	110	112	114	137	138	139	168	169	276
1.5000000	-0.4000000	112	114	115	138	139	266	195	196	197
-0.4000000	-0.6000000	126	127	129	267	140	141	159	160	161
-0.2000000	-0.6000000	127	129	130	140	141	142	271	149	150
-0.1000000	-0.6000000	129	130	131	141	142	143	149	150	151
-0.0500000	-0.6000000	130	131	132	142	143	144	150	151	152
.0000000	-0.6000000	131	132	133	143	144	145	151	152	153
0.0500000	-0.6000000	132	133	134	144	145	146	152	153	154
0.1000000	-0.6000000	133	134	135	145	146	147	153	154	155
0.2000000	-0.6000000	134	135	137	146	147	148	154	155	272
0.4000000	-0.6000000	135	137	138	147	148	270	167	168	169
-0.2000000	-0.7000000	140	141	142	271	149	150	160	161	162
-0.1000000	-0.7000000	141	142	143	149	150	151	161	162	163
-0.0500000	-0.7000000	142	143	144	150	151	152	273	156	157
.0000000	-0.7000000	143	144	145	151	152	153	156	157	158

LATTICE POINTS ON FRONT FACE (P3)

0.0500000	-0.7000000	144	145	146	152	153	154	157	158	274
0.1000000	-0.7000000	145	146	147	153	154	155	165	166	167
0.2000000	-0.7000000	146	147	148	154	155	272	166	167	168
-0.0500000	-0.7500000	150	151	152	273	156	157	162	163	164
.0000000	-0.7500000	151	152	153	156	157	158	163	164	165
0.0500000	-0.7500000	152	153	154	157	158	274	164	165	166
-0.8000000	-0.8000000	125	126	127	275	159	160	188	189	190
-0.4000000	-0.8000000	267	140	141	159	160	161	281	180	181
-0.2000000	-0.8000000	271	149	150	160	161	162	279	173	174
-0.1000000	-0.8000000	149	150	151	161	162	163	173	174	175
-0.0500000	-0.8000000	273	156	157	162	163	164	277	170	171
.0000000	-0.8000000	156	157	158	163	164	165	170	171	172
0.0500000	-0.8000000	157	159	274	164	165	166	171	172	278
0.1000000	-0.8000000	153	154	155	165	166	167	177	178	179
0.2000000	-0.8000000	154	155	272	165	167	168	178	179	280
0.4000000	-0.8000000	147	148	270	167	168	169	185	186	284
0.8000000	-0.8000000	137	139	139	168	169	276	194	195	196
-0.0500000	-0.8500000	162	163	164	277	170	171	174	175	176
.0000000	-0.8500000	163	164	165	170	171	172	175	176	177
0.0500000	-0.8500000	164	165	166	171	172	278	176	177	178
-0.2000000	-0.9000000	160	161	152	279	173	174	180	181	182
-0.1000000	-0.9000000	161	162	153	173	174	175	181	182	282
-0.0500000	-0.9000000	277	170	171	174	175	176	182	282	183
.0000000	-0.9000000	170	171	172	175	176	177	282	183	283
0.0500000	-0.9000000	171	172	278	176	177	178	183	283	184
0.1000000	-0.9000000	165	166	157	177	178	179	283	184	185
0.2000000	-0.9000000	166	167	158	178	179	280	184	185	186
-0.4000000	-1.0000000	159	160	151	281	180	181	189	190	191
-0.2000000	-1.0000000	279	173	174	180	181	182	190	191	286
-0.1000000	-1.0000000	173	174	176	181	182	183	191	286	192
.0000000	-1.0000000	174	176	178	182	183	184	286	192	287
0.1000000	-1.0000000	176	178	179	183	184	185	192	287	193
0.2000000	-1.0000000	178	179	280	184	185	186	287	193	194
0.4000000	-1.0000000	167	168	169	185	186	284	193	194	195
-2.4000000	-1.2000000	257	95	96	285	187	188	293	203	204
-1.6000000	-1.2000000	261	125	126	187	188	189	203	204	205
-0.8000000	-1.2000000	275	159	150	188	189	190	289	198	199
-0.4000000	-1.2000000	281	180	181	189	190	191	198	199	290
-0.2000000	-1.2000000	180	181	183	190	191	192	199	290	200
.0000000	-1.2000000	181	183	185	191	192	193	290	200	291
0.2000000	-1.2000000	183	185	186	192	193	194	200	291	201
0.4000000	-1.2000000	185	186	284	193	194	195	291	201	202
0.8000000	-1.2000000	168	169	276	194	195	196	201	202	292
1.6000000	-1.2000000	138	139	266	195	196	197	207	208	209
2.4000000	-1.2000000	114	115	258	196	197	288	208	209	296
-0.8000000	-1.6000000	188	189	190	289	198	199	204	205	294
-0.4000000	-1.6000000	189	190	192	198	199	200	205	294	206
.0000000	-1.6000000	190	192	194	199	200	201	294	206	295
0.4000000	-1.6000000	192	194	195	200	201	202	206	295	207
0.8000000	-1.6000000	194	195	196	201	202	292	295	207	208
-2.4000000	-2.4000000	285	187	188	293	203	204	297	298	299
-1.6000000	-2.4000000	187	188	189	203	204	205	298	299	300
-0.8000000	-2.4000000	289	198	200	204	205	206	299	300	301
.0000000	-2.4000000	198	200	202	205	206	207	300	301	302
0.8000000	-2.4000000	200	202	292	206	207	208	301	302	303
1.6000000	-2.4000000	195	196	197	207	208	209	302	303	304
2.4000000	-2.4000000	196	197	288	208	209	296	303	304	305
-3.6000000	3.6000000	0	0	0	0	210	0	0	0	0
-2.4000000	3.6000000	0	0	0	0	211	0	0	0	0
-1.6000000	3.6000000	0	0	0	0	212	0	0	0	0
-0.8000000	3.6000000	0	0	0	0	213	0	0	0	0
.0000000	3.6000000	0	0	0	0	214	0	0	0	0
0.8000000	3.6000000	0	0	0	0	215	0	0	0	0
1.6000000	3.6000000	0	0	0	0	216	0	0	0	0
2.4000000	3.6000000	0	0	0	0	217	0	0	0	0
3.6000000	3.6000000	0	0	0	0	218	0	0	0	0
-3.6000000	2.4000000	0	0	0	0	219	0	0	0	0
-0.4000000	2.4000000	0	0	0	0	220	0	0	0	0
0.4000000	2.4000000	0	0	0	0	221	0	0	0	0
3.6000000	2.4000000	0	0	0	0	222	0	0	0	0
-1.6000000	1.6000000	0	0	0	0	223	0	0	0	0
-0.2000000	1.6000000	0	0	0	0	224	0	0	0	0
0.2000000	1.6000000	0	0	0	0	225	0	0	0	0
1.6000000	1.6000000	0	0	0	0	226	0	0	0	0
-3.6000000	1.2000000	0	0	0	0	227	0	0	0	0
-0.1000000	1.2000000	0	0	0	0	228	0	0	0	0
0.1000000	1.2000000	0	0	0	0	229	0	0	0	0

LATTICE POINTS ON FRONT FACE (P4)

3.6000000	1.2000000	0	0	0	0	230	0	0	0	0
-0.8000000	1.0000000	0	0	0	0	231	0	0	0	0
-0.0500000	1.0000000	0	0	0	0	232	0	0	0	0
0.0500000	1.0000000	0	0	0	0	233	0	0	0	0
0.8000000	1.0000000	0	0	0	0	234	0	0	0	0
-0.4000000	0.9000000	0	0	0	0	235	0	0	0	0
0.4000000	0.9000000	0	0	0	0	236	0	0	0	0
-0.1000000	0.8500000	0	0	0	0	237	0	0	0	0
0.1000000	0.8500000	0	0	0	0	238	0	0	0	0
-1.6000000	0.8000000	0	0	0	0	239	0	0	0	0
1.6000000	0.8000000	0	0	0	0	240	0	0	0	0
-0.1000000	0.7500000	0	0	0	0	241	0	0	0	0
0.1000000	0.7500000	0	0	0	0	242	0	0	0	0
-0.4000000	0.7000000	0	0	0	0	243	0	0	0	0
0.4000000	0.7000000	0	0	0	0	244	0	0	0	0
-0.8000000	0.6000000	0	0	0	0	245	0	0	0	0
-0.3000000	0.6000000	0	0	0	0	246	0	0	0	0
0.3000000	0.6000000	0	0	0	0	247	0	0	0	0
0.8000000	0.6000000	0	0	0	0	248	0	0	0	0
-2.4000000	0.4000000	0	0	0	0	249	0	0	0	0
-1.2000000	0.4000000	0	0	0	0	250	0	0	0	0
-0.6000000	0.4000000	0	0	0	0	251	0	0	0	0
0.6000000	0.4000000	0	0	0	0	252	0	0	0	0
1.2000000	0.4000000	0	0	0	0	253	0	0	0	0
2.4000000	0.4000000	0	0	0	0	254	0	0	0	0
-0.4000000	0.2000000	0	0	0	0	255	0	0	0	0
0.4000000	0.2000000	0	0	0	0	256	0	0	0	0
-3.6000000	-.0000000	0	0	0	0	257	0	0	0	0
3.6000000	-.0000000	0	0	0	0	258	0	0	0	0
-0.4000000	-0.2000000	0	0	0	0	259	0	0	0	0
0.4000000	-0.2000000	0	0	0	0	260	0	0	0	0
-2.4000000	-0.4000000	0	0	0	0	261	0	0	0	0
-1.2000000	-0.4000000	0	0	0	0	262	0	0	0	0
-0.6000000	-0.4000000	0	0	0	0	263	0	0	0	0
0.6000000	-0.4000000	0	0	0	0	264	0	0	0	0
1.2000000	-0.4000000	0	0	0	0	265	0	0	0	0
2.4000000	-0.4000000	0	0	0	0	266	0	0	0	0
-0.8000000	-0.6000000	0	0	0	0	267	0	0	0	0
-0.3000000	-0.6000000	0	0	0	0	268	0	0	0	0
0.3000000	-0.6000000	0	0	0	0	269	0	0	0	0
0.8000000	-0.6000000	0	0	0	0	270	0	0	0	0
-0.4000000	-0.7000000	0	0	0	0	271	0	0	0	0
0.4000000	-0.7000000	0	0	0	0	272	0	0	0	0
-0.1000000	-0.7500000	0	0	0	0	273	0	0	0	0
0.1000000	-0.7500000	0	0	0	0	274	0	0	0	0
-1.6000000	-0.8000000	0	0	0	0	275	0	0	0	0
1.6000000	-0.8000000	0	0	0	0	276	0	0	0	0
-0.1000000	-0.8500000	0	0	0	0	277	0	0	0	0
0.1000000	-0.8500000	0	0	0	0	278	0	0	0	0
-0.4000000	-0.9000000	0	0	0	0	279	0	0	0	0
0.4000000	-0.9000000	0	0	0	0	280	0	0	0	0
-0.8000000	-1.0000000	0	0	0	0	281	0	0	0	0
-0.0500000	-1.0000000	0	0	0	0	282	0	0	0	0
0.0500000	-1.0000000	0	0	0	0	283	0	0	0	0
0.8000000	-1.0000000	0	0	0	0	284	0	0	0	0
-3.6000000	-1.2000000	0	0	0	0	285	0	0	0	0
-0.1000000	-1.2000000	0	0	0	0	286	0	0	0	0
0.1000000	-1.2000000	0	0	0	0	287	0	0	0	0
3.6000000	-1.2000000	0	0	0	0	288	0	0	0	0
-1.6000000	-1.6000000	0	0	0	0	289	0	0	0	0
-0.2000000	-1.6000000	0	0	0	0	290	0	0	0	0
0.2000000	-1.6000000	0	0	0	0	291	0	0	0	0
1.6000000	-1.6000000	0	0	0	0	292	0	0	0	0
-3.6000000	-2.4000000	0	0	0	0	293	0	0	0	0
-0.4000000	-2.4000000	0	0	0	0	294	0	0	0	0
0.4000000	-2.4000000	0	0	0	0	295	0	0	0	0
3.6000000	-2.4000000	0	0	0	0	296	0	0	0	0
-3.6000000	-3.6000000	0	0	0	0	297	0	0	0	0
-2.4000000	-3.6000000	0	0	0	0	298	0	0	0	0
-1.6000000	-3.6000000	0	0	0	0	299	0	0	0	0
-0.8000000	-3.6000000	0	0	0	0	300	0	0	0	0
.0000000	-3.6000000	0	0	0	0	301	0	0	0	0
0.8000000	-3.6000000	0	0	0	0	302	0	0	0	0
1.6000000	-3.6000000	0	0	0	0	303	0	0	0	0
2.4000000	-3.6000000	0	0	0	0	304	0	0	0	0
3.6000000	-3.6000000	0	0	0	0	305	0	0	0	0

LATTICE POINTS ON BACK FACE (P1)

FACE NO. 4(OUTPUT) MAXS1= 36 NL1=181 MAXL1=109

Indexes for corner points in base figure each

x'	y'									
-2.4000000	2.4000000	110	111	112	119	1	2	125	11	12
-1.6000000	2.4000000	111	112	113	1	2	3	11	12	13
-0.8000000	2.4000000	112	113	114	2	3	4	121	8	9
.0000000	2.4000000	113	114	115	3	4	5	8	9	10
0.8000000	2.4000000	114	115	116	4	5	6	9	10	124
1.6000000	2.4000000	115	116	117	5	6	7	17	18	19
2.4000000	2.4000000	116	117	118	6	7	120	18	19	128
-0.8000000	1.6000000	2	3	4	121	8	9	12	13	15
.0000000	1.6000000	3	4	5	8	9	10	13	15	17
0.8000000	1.6000000	4	5	6	9	10	124	15	17	18
-2.4000000	1.2000000	119	1	2	125	11	12	145	46	47
-1.6000000	1.2000000	1	2	3	11	12	13	46	47	48
-0.8000000	1.2000000	121	8	122	12	13	14	129	20	21
-0.4000000	1.2000000	8	122	9	13	14	15	20	21	23
.0000000	1.2000000	122	9	123	14	15	16	21	23	25
0.4000000	1.2000000	9	123	10	15	16	17	23	25	26
0.8000000	1.2000000	123	10	124	16	17	18	25	26	132
1.6000000	1.2000000	5	6	7	17	18	19	62	63	64
2.4000000	1.2000000	6	7	120	18	19	128	63	64	146
-0.8000000	0.8000000	12	13	14	129	20	21	47	48	49
-0.4000000	0.8000000	13	14	126	20	21	22	137	30	31
-0.2000000	0.8000000	14	126	15	21	22	23	30	31	34
.0000000	0.8000000	126	15	127	22	23	24	133	28	136
0.2000000	0.8000000	15	127	16	23	24	25	34	37	38
0.4000000	0.8000000	127	16	17	24	25	26	37	38	140
0.8000000	0.8000000	16	17	18	25	26	132	61	62	63
-0.1000000	0.6000000	22	130	23	133	27	28	31	32	34
.0000000	0.6000000	130	23	131	27	28	29	32	34	36
0.1000000	0.6000000	23	131	24	28	29	136	34	36	37
-0.4000000	0.4000000	20	21	22	137	30	31	48	49	50
-0.2000000	0.4000000	21	22	130	30	31	32	49	50	52
-0.1000000	0.4000000	133	27	134	31	32	33	141	39	40
-0.0500000	0.4000000	27	134	28	32	33	34	39	40	42
.0000000	0.4000000	134	28	135	33	34	35	40	42	44
0.0500000	0.4000000	28	135	29	34	35	36	42	44	45
0.1000000	0.4000000	135	29	136	35	36	37	44	45	144
0.2000000	0.4000000	131	24	25	36	37	38	58	60	61
0.4000000	0.4000000	24	25	26	37	38	140	60	61	62
-0.1000000	0.2000000	31	32	33	141	39	40	50	52	53
-0.0500000	0.2000000	32	33	138	39	40	41	52	53	54
-0.0250000	0.2000000	33	138	34	40	41	42	53	54	55
.0000000	0.2000000	138	34	139	41	42	43	54	55	56
0.0250000	0.2000000	34	139	35	42	43	44	55	56	57
0.0500000	0.2000000	139	35	36	43	44	45	56	57	58
0.1000000	0.2000000	35	36	37	44	45	144	57	58	60
-2.4000000	-.0000000	125	11	12	145	46	47	163	91	92
-1.6000000	-.0000000	11	12	13	46	47	48	91	92	93
-0.8000000	-.0000000	129	20	21	47	48	49	159	84	85
-0.4000000	-.0000000	137	30	31	48	49	50	151	72	73
-0.2000000	-.0000000	30	31	32	49	50	52	72	73	74
-0.1500000	-.0000000	141	142	39	50	51	52	147	148	65
-0.1000000	-.0000000	142	39	40	51	52	53	148	65	66
-0.0500000	-.0000000	39	40	41	52	53	54	65	66	67
-0.0250000	-.0000000	40	41	42	53	54	55	66	67	68
.0000000	-.0000000	41	42	43	54	55	56	67	68	69
0.0250000	-.0000000	42	43	44	55	56	57	68	69	70
0.0500000	-.0000000	43	44	45	56	57	58	69	70	71
0.1000000	-.0000000	44	45	143	57	58	59	70	71	149
0.1500000	-.0000000	45	143	144	58	59	60	71	149	150
0.2000000	-.0000000	36	37	38	58	60	61	78	79	80
0.4000000	-.0000000	37	38	140	60	61	62	79	80	154
0.8000000	-.0000000	25	26	132	61	62	63	89	90	162
1.6000000	-.0000000	17	19	19	62	63	64	97	98	99
2.4000000	-.0000000	18	19	128	63	64	146	98	99	166
-0.1000000	-0.2000000	50	52	53	147	65	66	73	74	75
-0.0500000	-0.2000000	52	53	54	65	66	67	74	75	152
-0.0250000	-0.2000000	53	54	55	66	67	68	75	152	76
.0000000	-0.2000000	54	55	56	67	68	69	152	76	153
0.0250000	-0.2000000	55	56	57	68	69	70	76	153	77
0.0500000	-0.2000000	56	57	58	69	70	71	153	77	78
0.1000000	-0.2000000	57	58	60	70	71	150	77	78	79
-0.4000000	-0.4000000	48	49	50	151	72	73	84	85	86
-0.2000000	-0.4000000	49	50	52	72	73	74	85	86	160
-0.1000000	-0.4000000	147	65	66	73	74	75	155	81	156
-0.0500000	-0.4000000	65	66	58	74	75	76	81	156	82

LATTICE POINTS ON BACK FACE (P2)

.0000000	-0.4000000	66	68	70	75	76	77	156	82	157
0.0500000	-0.4000000	68	70	71	76	77	78	82	157	83
0.1000000	-0.4000000	70	71	150	77	78	79	157	83	158
0.2000000	-0.4000000	58	60	61	78	79	80	161	88	89
0.4000000	-0.4000000	60	61	62	79	80	154	88	89	90
-0.1000000	-0.6000000	73	74	76	155	81	82	86	160	87
.0000000	-0.6000000	74	76	78	81	82	83	160	87	161
0.1000000	-0.6000000	76	78	79	82	83	158	87	161	88
-0.8000000	-0.8000000	47	48	49	159	84	85	92	93	94
-0.4000000	-0.8000000	151	72	73	84	85	86	93	94	164
-0.2000000	-0.8000000	72	73	76	85	86	87	94	164	95
.0000000	-0.8000000	155	82	158	86	87	88	164	95	165
0.2000000	-0.8000000	76	79	80	87	88	89	95	165	96
0.4000000	-0.8000000	79	80	154	88	89	90	165	96	97
0.8000000	-0.8000000	61	62	63	89	90	162	96	97	98
-2.4000000	-1.2000000	145	46	47	163	91	92	171	103	104
-1.6000000	-1.2000000	46	47	48	91	92	93	103	104	105
-0.8000000	-1.2000000	159	84	85	92	93	94	167	100	168
-0.4000000	-1.2000000	84	85	87	93	94	95	100	168	101
.0000000	-1.2000000	85	87	89	94	95	96	168	101	169
0.4000000	-1.2000000	87	89	90	95	96	97	101	169	102
0.8000000	-1.2000000	89	90	162	96	97	98	169	102	170
1.6000000	-1.2000000	62	63	64	97	98	99	107	108	109
2.4000000	-1.2000000	63	64	146	98	99	166	108	109	172
-0.8000000	-1.6000000	92	93	95	167	100	101	104	105	106
.0000000	-1.6000000	93	95	97	100	101	102	105	106	107
0.8000000	-1.6000000	95	97	98	101	102	170	106	107	108
-2.4000000	-2.4000000	163	91	92	171	103	104	173	174	175
-1.6000000	-2.4000000	91	92	93	103	104	105	174	175	176
-0.8000000	-2.4000000	167	100	101	104	105	106	175	176	177
.0000000	-2.4000000	100	101	102	105	106	107	176	177	178
0.8000000	-2.4000000	101	102	170	106	107	108	177	178	179
1.6000000	-2.4000000	97	98	99	107	108	109	178	179	180
2.4000000	-2.4000000	98	99	166	108	109	172	179	180	181
-3.6000000	3.6000000	0	0	0	0	110	0	0	0	0
-2.4000000	3.6000000	0	0	0	0	111	0	0	0	0
-1.6000000	3.6000000	0	0	0	0	112	0	0	0	0
-0.8000000	3.6000000	0	0	0	0	113	0	0	0	0
.0000000	3.6000000	0	0	0	0	114	0	0	0	0
0.8000000	3.6000000	0	0	0	0	115	0	0	0	0
1.6000000	3.6000000	0	0	0	0	116	0	0	0	0
2.4000000	3.6000000	0	0	0	0	117	0	0	0	0
3.6000000	3.6000000	0	0	0	0	118	0	0	0	0
-3.6000000	2.4000000	0	0	0	0	119	0	0	0	0
3.6000000	2.4000000	0	0	0	0	120	0	0	0	0
-1.6000000	1.6000000	0	0	0	0	121	0	0	0	0
-0.4000000	1.6000000	0	0	0	0	122	0	0	0	0
0.4000000	1.6000000	0	0	0	0	123	0	0	0	0
1.6000000	1.6000000	0	0	0	0	124	0	0	0	0
-3.6000000	1.2000000	0	0	0	0	125	0	0	0	0
-0.2000000	1.2000000	0	0	0	0	126	0	0	0	0
0.2000000	1.2000000	0	0	0	0	127	0	0	0	0
3.6000000	1.2000000	0	0	0	0	128	0	0	0	0
-1.6000000	0.8000000	0	0	0	0	129	0	0	0	0
-0.1000000	0.8000000	0	0	0	0	130	0	0	0	0
0.1000000	0.8000000	0	0	0	0	131	0	0	0	0
1.6000000	0.8000000	0	0	0	0	132	0	0	0	0
-0.2000000	0.6000000	0	0	0	0	133	0	0	0	0
-0.0500000	0.6000000	0	0	0	0	134	0	0	0	0
0.0500000	0.6000000	0	0	0	0	135	0	0	0	0
0.2000000	0.6000000	0	0	0	0	136	0	0	0	0
-0.8000000	0.4000000	0	0	0	0	137	0	0	0	0
-0.0250000	0.4000000	0	0	0	0	138	0	0	0	0
0.0250000	0.4000000	0	0	0	0	139	0	0	0	0
0.8000000	0.4000000	0	0	0	0	140	0	0	0	0
-0.2000000	0.2000000	0	0	0	0	141	0	0	0	0
-0.1500000	0.2000000	0	0	0	0	142	0	0	0	0
0.1500000	0.2000000	0	0	0	0	143	0	0	0	0
0.2000000	0.2000000	0	0	0	0	144	0	0	0	0
-3.6000000	-.0000000	0	0	0	0	145	0	0	0	0
3.6000000	-.0000000	0	0	0	0	146	0	0	0	0
-0.2000000	-0.2000000	0	0	0	0	147	0	0	0	0
-0.1500000	-0.2000000	0	0	0	0	148	0	0	0	0
0.1500000	-0.2000000	0	0	0	0	149	0	0	0	0
0.2000000	-0.2000000	0	0	0	0	150	0	0	0	0
-0.8000000	-0.4000000	0	0	0	0	151	0	0	0	0
-0.0250000	-0.4000000	0	0	0	0	152	0	0	0	0

LATTICE POINTS ON BACK FACE (P3)

0.0250000	-0.4000000	0	0	0	0	153	0	0	0	0
0.8000000	-0.4000000	0	0	0	0	154	0	0	0	0
-0.2000000	-0.6000000	0	0	0	0	155	0	0	0	0
-0.0500000	-0.6000000	0	0	0	0	156	0	0	0	0
0.0500000	-0.6000000	0	0	0	0	157	0	0	0	0
0.2000000	-0.6000000	0	0	0	0	158	0	0	0	0
-1.6000000	-0.8000000	0	0	0	0	159	0	0	0	0
-0.1000000	-0.8000000	0	0	0	0	160	0	0	0	0
0.1000000	-0.8000000	0	0	0	0	161	0	0	0	0
1.6000000	-0.8000000	0	0	0	0	162	0	0	0	0
-3.6000000	-1.2000000	0	0	0	0	163	0	0	0	0
-0.2000000	-1.2000000	0	0	0	0	164	0	0	0	0
0.2000000	-1.2000000	0	0	0	0	165	0	0	0	0
3.6000000	-1.2000000	0	0	0	0	166	0	0	0	0
-1.6000000	-1.6000000	0	0	0	0	167	0	0	0	0
-0.4000000	-1.6000000	0	0	0	0	168	0	0	0	0
0.4000000	-1.6000000	0	0	0	0	169	0	0	0	0
1.6000000	-1.6000000	0	0	0	0	170	0	0	0	0
-3.6000000	-2.4000000	0	0	0	0	171	0	0	0	0
3.6000000	-2.4000000	0	0	0	0	172	0	0	0	0
-3.6000000	-3.6000000	0	0	0	0	173	0	0	0	0
-2.4000000	-3.6000000	0	0	0	0	174	0	0	0	0
-1.6000000	-3.6000000	0	0	0	0	175	0	0	0	0
-0.8000000	-3.6000000	0	0	0	0	176	0	0	0	0
.0000000	-3.6000000	0	0	0	0	177	0	0	0	0
0.8000000	-3.6000000	0	0	0	0	178	0	0	0	0
1.6000000	-3.6000000	0	0	0	0	179	0	0	0	0
2.4000000	-3.6000000	0	0	0	0	180	0	0	0	0
3.6000000	-3.6000000	0	0	0	0	181	0	0	0	0

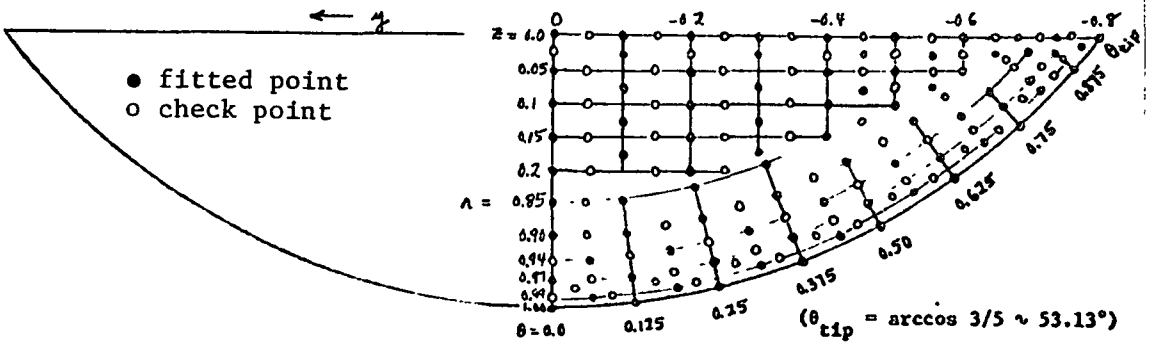

FIGURE 6. BOUNDARY CONDITION POINTS AND CHECK POINTS FOR SURFACE CRACK WITH A/2C = 0.25

BATTELLE STANDARD CODING FORM

COMPASS | COBOL | FORTRAN

Card	Location (sequence page / serial)	C	Statement Number	Cont.	FORTRAN STATEMENT	IDENT
1					SOLV	
2					PROBLEM I=.7A, C=0.8, A/2C=0.25, A/T=0.7, NU=0.30	
3					WITH 17x9 H-EVEN TRIANGULAR SERIES, LATTICES OF 4-21-76, FRAC3D OF 9-30-77	
4					IX25IY25	
5					1. . . -1. . . 1. . .	
6					1. . . . . -1. . .	
7					17 9 (This gives a 17x9 series with constants 1's. The deletion of odd m's and triangulation procedure by inserts to A+4,Z)	
8					1 4 7	
9					3.6 -3.6 3.6 3.6 10.571428570.30	
10					68 305 209	
11-315					-2.400000010 2.400000010210211212219 1 22271314 (plus 304 more cards from LATTICE for front face)	
316					36 181 109	
317-497					-2.400000010 2.400000010111011112119 1 21215112 (plus 180 more cards from LATTICE for back face)	
498					80 0.0 0.6	
499					STRESS POINTS FOR FACE 1	
500-567					0.0 0.81257 (plus 67 more cards specifying boundary condition points on front face)	
568					STRESS POINTS FOR FACE 4	
569-604					0.0 0.0 (plus 35 more cards specifying boundary condition points on back face)	
605					STRESS POINTS FOR FACE 7	
606-685					0.60 0.000 1.0 0.0 0.0	
686					0.0 0.0 1.0 0.0 0.0 0.0	
22						
23						
24						
25						

DATA DESCRIPTION Illustrative input for FRAC3D Project No. PREPARED BY

DATE PAGE OF

or for which m + 2k would be greater than twice the maximum k (that is greater than 16). To accomplish this removal, 18 special cards (as have been provided with FRAC3D) were inserted into the subroutine AXYZ, between the instructions "100 CONTINUE" and"150 CONTINUE". The introduction of the five boundary points at or near the crack tip was made with the understanding that this would offer a choice among possible boundary conditions to be imposed near the tip, the boundary points that were used can be found handwritten as a table given later (Pages 53 to 56). Card 686 called for satisfaction of equilibrium in the z direction among the freeing loads applied to the front and back faces.

The allowance made for symmetry and the deletions of the unwanted crack constants are shown on Pages 50 through 52 as printed by FRAC3D, using the system of notation described earlier. The beginning of this chain shows, for example, that influence functions for the first load constant were added to those of the nineteenth, and those for the second were subtracted from those for the twentieth. The zero entries show which load constants were retained for solution and counting shows that 303 of the possible 1404 were retained. The other standard printed output from FRAC3D consists mainly of a listing of the boundary condition points that were used showing their coordinates used in calling the crack and surface subroutines in the program.

The major output from FRAC3D is the matrix to be solved, but since it is typically large, it is simply placed in a computer storage unit identified as TAPE 9, including the symmetry chain. The input which led to the matrix is stored also in a unit called TAPE 8. The solution for the implied system of equations is obtained then by use of the program MATSOL, which calls for the information in TAPE 9. After the system is solved, MATSOL stores the load constants on a unit called TAPE 7 and it prints output of several types. First, it prints the residual from each of the equations used in the least square process. For the illustrative example, these residuals are shown on Pages 53 through 56, showing fits for σ_z, τ_{yz}, τ_{zx}, or σ'_z, τ'_{yz}, τ'_{zx} or σ_θ, $\tau_{\theta z}$, τ_{zr} at each point indicated for fitting. Note that these residuals are affected by the weights that were applied because of symmetries specified. It may be seen that altogether

SYMMETRY CHAIN (P1)

A(I) ARRAY

19.000	-20.000	21.000	16.000	-17.000	18.000	13.000	-14.000	15.000	0.000
11.000	0.000	0.000	0.000	0.000	0.000	0.000	0.000	0.000	0.000
0.000	34.000	-35.000	36.000	31.000	-32.000	33.000	0.000	29.000	0.000
0.000	0.000	0.000	0.000	0.000	0.000	67.000	-68.000	69.000	64.000
-65.000	66.000	61.000	-62.000	63.000	58.000	-59.000	60.000	55.000	-56.000
57.000	0.000	53.000	0.000	0.000	0.000	0.000	0.000	0.000	0.000
0.000	0.000	0.000	0.000	0.000	0.000	0.000	0.000	0.000	88.000
-89.000	90.000	85.000	-86.000	87.000	82.000	-83.000	84.000	0.000	80.000
0.000	0.000	0.000	0.000	0.000	0.000	0.000	0.000	0.000	0.000
109.000	-110.000	111.000	106.000	-107.000	108.000	103.000	-104.000	105.000	0.000
101.000	0.000	0.000	0.000	0.000	0.000	0.000	0.000	0.000	0.000
0.000	118.000	-119.000	120.000	0.000	116.000	0.000	0.000	0.000	0.000
151.000	-152.000	153.000	148.000	-149.000	150.000	145.000	-146.000	147.000	142.000
-143.000	144.000	139.000	-140.000	141.000	0.000	137.000	0.000	0.000	0.000
0.000	0.000	0.000	0.000	0.000	0.000	0.000	0.000	0.000	0.000
0.000	0.000	0.000	160.000	-161.000	162.000	0.000	158.000	0.000	0.000
0.000	0.000	181.000	-182.000	183.000	178.000	-179.000	180.000	175.000	-176.000
177.000	0.000	173.000	0.000	0.000	0.000	0.000	0.000	0.000	0.000
0.000	0.000	0.000	208.000	-209.000	210.000	205.000	-206.000	207.000	202.000
-203.000	204.000	199.000	-200.000	201.000	0.000	197.000	0.000	0.000	0.000
0.000	0.000	0.000	0.000	0.000	0.000	0.000	0.000	0.000	0.000
253.000	-254.000	255.000	250.000	-251.000	252.000	247.000	-248.000	249.000	244.000
-245.000	246.000	241.000	-242.000	243.000	238.000	-239.000	240.000	235.000	-236.000
237.000	0.000	233.000	0.000	0.000	0.000	0.000	0.000	0.000	0.000
0.000	0.000	0.000	0.000	0.000	0.000	0.000	0.000	0.000	0.000
0.000	0.000	0.000	0.000	0.000	280.000	-281.000	282.000	277.000	-278.000
279.000	274.000	-275.000	276.000	271.000	-272.000	273.000	0.000	269.000	0.000
0.000	0.000	0.000	0.000	0.000	0.000	0.000	0.000	0.000	0.000
0.000	0.000	343.000	-344.000	285.000	340.000	-341.000	288.000	337.000	-338.000
291.000	334.000	-335.000	294.000	331.000	-332.000	297.000	328.000	-329.000	300.000
325.000	-326.000	303.000	322.000	-323.000	306.000	319.000	-320.000	309.000	316.000
-317.000	312.000	0.000	314.000	315.000	0.000	0.000	318.000	0.000	0.000
321.000	0.000	0.000	324.000	0.000	0.000	327.000	0.000	0.000	330.000
0.000	0.000	333.000	0.000	0.000	336.000	0.000	0.000	339.000	0.000
0.000	342.000	0.000	0.000	345.000	260.000	-281.000	-282.000	277.000	-278.000
-279.000	274.000	-275.000	-276.000	271.000	-272.000	-273.000	268.000	359.000	-270.000
271.000	272.000	-273.000	274.000	275.000	-276.000	277.000	278.000	-279.000	280.000
281.000	-282.000	253.000	-254.000	-255.000	256.000	-251.000	-252.000	247.000	-248.000
-249.000	244.000	-245.000	-246.000	241.000	-242.000	-243.000	238.000	-239.000	-240.000
235.000	-236.000	-237.000	232.000	395.000	-234.000	235.000	236.000	-237.000	238.000
239.000	-240.000	241.000	242.000	-243.000	244.000	245.000	-246.000	247.000	248.000
-249.000	250.000	251.000	-252.000	253.000	254.000	-255.000	208.000	-209.000	-210.000
205.000	-206.000	-207.000	202.000	-203.000	-204.000	199.000	-200.000	-201.000	196.000
431.000	-198.000	199.000	200.000	-201.000	202.000	203.000	-204.000	205.000	206.000
-207.000	208.000	209.000	-210.000	181.000	-182.000	-183.000	178.000	-179.000	-180.000
175.000	-176.000	-177.000	172.000	455.000	-174.000	175.000	176.000	-177.000	178.000

SYMMETRY CHAIN (P2)

179.000	-180.000	181.000	182.000	-183.000	160.000	-161.000	-162.000	157.000	470.000
-159.000	160.000	161.000	-162.000	151.000	-152.000	-153.000	148.000	-149.000	-150.000
145.000	-146.000	-147.000	142.000	-143.000	-144.000	139.000	-140.000	-141.000	135.000
491.000	-138.000	139.000	140.000	-141.000	142.000	143.000	-144.000	145.000	146.000
-147.000	148.000	149.000	-150.000	151.000	152.000	-153.000	118.000	-119.000	-120.000
115.000	512.000	-117.000	118.000	119.000	-120.000	109.000	-110.000	-111.000	106.000
-107.000	-108.000	103.000	-104.000	-105.000	100.000	527.000	-102.000	103.000	104.000
-105.000	106.000	107.000	-108.000	109.000	110.000	-111.000	88.000	-89.000	-90.000
85.000	-86.000	-87.000	82.000	-83.000	-84.000	79.000	548.000	-81.000	82.000
83.000	-84.000	85.000	86.000	-87.000	88.000	89.000	-90.000	67.000	-68.000
-69.000	64.000	-65.000	-66.000	61.000	-62.000	-63.000	58.000	-59.000	-60.000
55.000	-56.000	-57.000	52.000	575.000	-54.000	55.000	56.000	-57.000	58.000
59.000	-60.000	61.000	62.000	-63.000	64.000	65.000	-66.000	67.000	68.000
-69.000	34.000	-35.000	-36.000	31.000	-32.000	-33.000	28.000	599.000	-30.000
31.000	32.000	-33.000	34.000	35.000	-36.000	19.000	-20.000	-21.000	16.000
-17.000	-18.000	13.000	-14.000	-15.000	10.000	617.000	-12.000	13.000	14.000
-15.000	16.000	17.000	-18.000	19.000	20.000	-21.000	952.000	-953.000	-954.000
949.000	-950.000	-951.000	946.000	-947.000	-948.000	943.000	638.000	-945.000	946.000
947.000	-948.000	949.000	950.000	-951.000	952.000	953.000	-954.000	931.000	-932.000
-933.000	928.000	653.000	-930.000	931.000	932.000	-933.000	922.000	-923.000	-924.000
919.000	-920.000	-921.000	916.000	-917.000	-918.000	913.000	-914.000	-915.000	910.000
671.000	-912.000	913.000	914.000	-915.000	916.000	917.000	-918.000	919.000	920.000
-921.000	922.000	923.000	-924.000	895.000	-896.000	-897.000	892.000	-893.000	-894.000
889.000	-890.000	-891.000	886.000	695.000	-888.000	889.000	890.000	-891.000	892.000
893.000	-894.000	895.000	896.000	-897.000	874.000	-875.000	-876.000	871.000	710.000
-873.000	874.000	875.000	-876.000	865.000	-866.000	-867.000	862.000	-863.000	-864.000
859.000	-860.000	-861.000	856.000	-857.000	-858.000	853.000	728.000	-855.000	856.000
857.000	-858.000	859.000	860.000	-861.000	862.000	863.000	-864.000	865.000	866.000
-867.000	838.000	-839.000	-840.000	835.000	-836.000	-837.000	832.000	-833.000	-834.000
829.000	752.000	-831.000	832.000	833.000	-834.000	835.000	836.000	-837.000	838.000
839.000	-840.000	817.000	-818.000	765.000	814.000	-815.000	768.000	811.000	-812.000
771.000	818.000	-819.000	774.000	805.000	-806.000	777.000	802.000	-803.000	780.000
799.000	-800.000	783.000	796.000	-797.000	786.000	793.000	-794.000	789.000	0.000
791.000	792.000	0.000	0.000	795.000	0.000	0.000	798.000	0.000	0.000
801.000	0.000	0.000	804.000	0.000	0.000	807.000	0.000	0.000	810.000
0.000	0.000	813.000	0.000	0.000	816.000	0.000	0.000	819.000	838.000
-839.000	840.000	835.000	-836.000	837.000	832.000	-833.000	834.000	0.000	830.000
0.000	0.000	0.000	0.000	0.000	0.000	0.000	0.000	0.000	0.000
865.000	-866.000	867.000	862.000	-863.000	864.000	859.000	-860.000	861.000	856.000
-857.000	858.000	0.000	854.000	0.000	0.000	0.000	0.000	0.000	0.000
0.000	0.000	0.000	0.000	0.000	0.000	0.000	874.000	-875.000	876.000
0.000	872.000	0.000	0.000	0.000	0.000	895.000	-896.000	897.000	892.000
-893.000	894.000	889.000	-891.000	891.000	0.000	887.000	0.000	0.000	0.000
0.000	0.000	0.000	0.000	0.000	0.000	0.000	922.000	-923.000	924.000
919.000	-920.000	921.000	916.000	-917.000	918.000	913.000	-914.000	915.000	0.000
911.000	0.000	0.000	0.000	0.000	0.000	0.000	0.000	0.000	0.000
0.000	0.000	0.000	0.000	931.000	-932.000	933.000	0.000	929.000	0.000
0.000	0.000	0.000	952.000	-953.000	954.000	949.000	-950.000	951.000	946.000

SYMMETRY CHAIN (P3)

-947.000	948.000	0.000	944.000	0.000	0.000	0.000	0.000	0.000	0.000
0.000	0.000	0.000	0.000	0.000	956.000	0.000	958.000	0.000	960.000
0.000	962.000	0.000	964.000	0.000	966.000	0.000	968.000	0.000	970.000
0.000	972.000	973.000	974.000	975.000	976.000	977.000	978.000	979.000	980.000
981.000	982.000	983.000	984.000	985.000	986.000	987.000	988.000	989.000	990.000
991.000	992.000	993.000	994.000	995.000	996.000	997.000	998.000	999.000	0.000
1001.000	1002.000	0.000	1004.000	1005.000	0.000	1007.000	1008.000	0.000	1010.000
1011.000	0.000	1013.000	1014.000	0.000	1016.000	1017.000	0.000	1019.000	1020.000
0.000	1022.000	1023.000	1024.000	1025.000	1026.000	1027.000	1028.000	1029.000	1030.000
1031.000	1032.000	1033.000	1034.000	1035.000	1036.000	1037.000	1038.000	1039.000	1040.000
1041.000	1042.000	1043.000	1044.000	1045.000	1046.000	1047.000	1048.000	1049.000	1050.000
1051.000	1052.000	1053.000	0.000	1055.000	1056.000	0.000	1058.000	1059.000	0.000
1061.000	1062.000	0.000	1064.000	1065.000	0.000	1067.000	1068.000	0.000	1070.000
1071.000	0.000	1073.000	1074.000	1075.000	1076.000	1077.000	1078.000	1079.000	1080.000
1081.000	1082.000	1083.000	1084.000	1085.000	1086.000	1087.000	1088.000	1089.000	1090.000
1091.000	1092.000	1093.000	1094.000	1095.000	1096.000	1097.000	1098.000	1099.000	1100.000
1101.000	1102.000	1103.000	1104.000	1105.000	1106.000	1107.000	0.000	1109.000	1110.000
0.000	1112.000	1113.000	0.000	1115.000	1116.000	0.000	1118.000	1119.000	0.000
1121.000	1122.000	0.000	1124.000	1125.000	1126.000	1127.000	1128.000	1129.000	1130.000
1131.000	1132.000	1133.000	1134.000	1135.000	1136.000	1137.000	1138.000	1139.000	1140.000
1141.000	1142.000	1143.000	1144.000	1145.000	1146.000	1147.000	1148.000	1149.000	1150.000
1151.000	1152.000	1153.000	1154.000	1155.000	1156.000	1157.000	1158.000	1159.000	1160.000
1161.000	0.000	1163.000	1164.000	0.000	1166.000	1167.000	0.000	1169.000	1170.000
0.000	1172.000	1173.000	0.000	1175.000	1176.000	1177.000	1178.000	1179.000	1180.000
1181.000	1182.000	1183.000	1184.000	1185.000	1186.000	1187.000	1188.000	1189.000	1190.000
1191.000	1192.000	1193.000	1194.000	1195.000	1196.000	1197.000	1198.000	1199.000	1200.000
1201.000	1202.000	1203.000	1204.000	1205.000	1206.000	1207.000	1208.000	1209.000	1210.000
1211.000	1212.000	1213.000	1214.000	1215.000	0.000	1217.000	1218.000	0.000	1220.000
1221.000	0.000	1223.000	1224.000	0.000	1226.000	1227.000	1228.000	1229.000	1230.000
1231.000	1232.000	1233.000	1234.000	1235.000	1236.000	1237.000	1238.000	1239.000	1240.000
1241.000	1242.000	1243.000	1244.000	1245.000	1246.000	1247.000	1248.000	1249.000	1250.000
1251.000	1252.000	1253.000	1254.000	1255.000	1256.000	1257.000	1258.000	1259.000	1260.000
1261.000	1262.000	1263.000	1264.000	1265.000	1266.000	1267.000	1268.000	1269.000	0.000
1271.000	1272.000	0.000	1274.000	1275.000	0.000	1277.000	1278.000	1279.000	1280.000
1281.000	1282.000	1283.000	1284.000	1285.000	1286.000	1287.000	1288.000	1289.000	1290.000
1291.000	1292.000	1293.000	1294.000	1295.000	1296.000	1297.000	1298.000	1299.000	1300.000
1301.000	1302.000	1303.000	1304.000	1305.000	1306.000	1307.000	1308.000	1309.000	1310.000
1311.000	1312.000	1313.000	1314.000	1315.000	1316.000	1317.000	1318.000	1319.000	1320.000
1321.000	1322.000	1323.000	0.000	1325.000	1326.000	0.000	1328.000	1329.000	1330.000
1331.000	1332.000	1333.000	1334.000	1335.000	1336.000	1337.000	1338.000	1339.000	1340.000
1341.000	1342.000	1343.000	1344.000	1345.000	1346.000	1347.000	1348.000	1349.000	1350.000
1351.000	1352.000	1353.000	1354.000	1355.000	1356.000	1357.000	1358.000	1359.000	1360.000
1361.000	1362.000	1363.000	1364.000	1365.000	1366.000	1367.000	1368.000	1369.000	1370.000
1371.000	1372.000	1373.000	1374.000	1375.000	1376.000	1377.000	0.000	1379.000	1380.000
1381.000	1382.000	1383.000	1384.000	1385.000	1386.000	1387.000	1388.000	1389.000	1390.000
1391.000	1392.000	1393.000	1394.000	1395.000	1396.000	1397.000	1398.000	1399.000	1400.000
1401.000	1402.000	1403.000	1404.000						

PROBLEM I.7A, C=0.8, A/2C=0.25, A/T=0.7, NU=0.30
WITH 17X9 M-EVEN TRIANGULAR SERIES, LATTICES OF 4-21-76, FRAC3D OF 9-30-77

N = 303 M = 552 NAUX = 1 NO = 40 LZ = 0 MSR = 312

ROW WEIGHTS 0.000, 1.000, 0.000, 1.000, 1.000, 1.000, 1.000, 1.000,

THROUGH ROW 4, 7, 15, 204, 312, 552, 552, 552,

σ_z τ_{yz} τ_{zx}

Row#	EQUATION RESIDUALS	Row#		Row#			Front x	y
1	.10625830E+01	2	.15911566E+00	3	.42215914E-12	not fitted	0.0	0.8125
4	.31866417E+00	5	.19807192E-02	6	.41970855E-12		0.0	0.825
7	.13672444E-02	8	-.84694797E+00	9	-.84552378E+00	not fitted	0.0125	0.8
10	-.24499693E+00	11	-.57623280E+00	12	-.40363386E+00	(weight=0)	0.025	0.8
13	-.16169652E+01	14	-.54385058E+00	15	.79264767E-13		0.0	0.8
16	.33275227E-04	17	-.33433811E-12	18	.11244849E-11		0.0	0.0
19	-.63118068E-03	20	.41464351E-04	21	.15461830E-11			0.2
22	.34479762E-03	23	.95332993E-04	24	.11023219E-11			0.4
25	-.20601857E-02	26	-.12981177E-03	27	.61339925E-12			0.6
28	.38363443E-02	29	.13100984E-03	30	.44359442E-12			0.7
31	-.54481958E-02	32	-.76904115E-03	33	.74396728E-13			0.75
34	-.73406553E-04	35	-.12463852E-02	36	.22705735E-12			0.85
37	-.15813545E-03	38	.57242625E-05	39	.51364156E-12			0.9
40	-.58489694E-03	41	.61280344E-04	42	-.38438232E-12			1.0
43	-.20997785E-02	44	.31667392E-03	45	-.24182493E-12			1.2
46	-.48309532E-02	47	.13646670E-02	48	-.13021960E-11			1.6
49	-.58385203E-02	50	.22990059E-02	51	-.15250516E-11			2.4
52	-.72510341E-03	53	-.13254864E-11	54	-.10438870E-03		0.05	0.0
55	-.85021306E-03	56	.44223469E-04	57	.47300853E-03			0.2
58	-.13907597E-02	59	.24420172E-04	60	-.21562394E-03			0.4
61	-.22754626E-04	62	-.76176973E-04	63	.11140679E-02			0.6
64	-.11898898E-02	65	.66601781E-03	66	-.28500622E-02			0.7
67	.22210805E-02	68	-.95355061E-03	69	.21929140E-02			0.75
70	-.14285504E-02	71	.37210964E-03	72	.53745487E-03			0.8
73	-.28246787E-03	74	.43743004E-04	75	-.13853182E-03			0.85
76	-.23282784E-03	77	.26503372E-04	78	.79168102E-05			0.9
79	-.73712122E-03	80	-.11524277E-11	81	.20955641E-03		0.1	1.0
82	-.98278969E-03	83	.23818614E-04	84	.33954340E-03			0.2
85	-.11569300E-02	86	-.48363171E-04	87	.53724540E-03			0.4
88	-.82241653E-03	89	-.20067014E-04	90	.22243158E-03			0.6
91	-.90412488E-03	92	.12864078E-03	93	.16450819E-03			0.7
94	-.36622204E-03	95	-.27665454E-06	96	.20732403E-03			0.8
97	-.45085035E-03	98	.10232036E-03	99	.13271665E-03			0.9
100	-.81427196E-03	101	.10601081E-03	102	.55270128E-04			1.0
103	-.94842231E-03	104	-.77926779E-12	105	.24700665E-03		1.2	0.0
106	-.13257515E-02	107	.16587284E-04	108	.36395755E-03			0.2
109	-.13016045E-02	110	-.14663157E-04	111	.44225907E-03			0.4
112	-.14286545E-02	113	.31164795E-04	114	.54973323E-03			0.6
115	-.97768932E-03	116	.38729040E-04	117	.49409206E-03			0.7

mean typ

typ

EQUATION RESIDUALS (P2)

118	-.88778387E-03	119	.13145697E-03	120	.35472963E-03	Front (cont) $x=0.2$, $y=$	0.8
121	-.82714655E-03	122	.14111230E-03	123	.22103123E-03		0.9
124	-.11608348E-02	125	.17955613E-03	126	.16317216E-03		1.0
127	-.26992937E-02	128	.47854554E-03	129	.24186841E-03		1.2
130	-.89206988E-03	131	.23187376E-12	132	.25896233E-03	0.3	0.0
133	-.12451536E-02	134	.21396946E-04	135	.37812857E-03		0.2
136	-.12077067E-02	137	.20656875E-04	138	.39769105E-03		0.4
139	-.23833847E-02	140	.81417308E-12	141	.77519690E-03	0.4	0.0
142	-.37787918E-02	143	.14744974E-03	144	.14021219E-02		0.4
145	-.30214907E-02	146	.83805465E-04	147	.11254061E-02		0.6
148	-.29912059E-02	149	.22633709E-03	150	.92838346E-03		0.8
151	-.28275842E-02	152	.36843534E-03	153	.60240157E-03		1.0
154	-.36125191E-02	155	.70547659E-03	156	.52049782E-03		1.2
157	-.59225785E-02	158	.18348287E-02	159	.63617563E-03		1.6
160	-.27764092E-02	161	.26268204E-11	162	.96675109E-03	0.6	0.0
163	-.31746163E-02	164	.39111911E-11	165	.13351525E-02	0.8	0.0
166	-.73860584E-02	167	.54788389E-03	168	.33516716E-02		0.4
169	-.75578971E-02	170	.18974979E-03	171	.29493116E-02		0.8
172	-.73071013E-02	173	.97340264E-03	174	.19245753E-02		1.2
175	-.69817545E-02	176	.19283738E-02	177	.14895900E-02		1.6
178	-.73293539E-02	179	.27146565E-02	180	.71466589E-03		2.4
181	-.30321642E-02	182	.79950251E-11	183	.99736570E-03	1.2	0.0
184	-.41364490E-02	185	.42842573E-11	186	.10827231E-02	1.6	0.0
187	-.80730813E-02	188	.98083466E-03	189	.32897360E-02		0.4
190	-.12855781E-01	191	.15534338E-02	192	.37387385E-02		1.2
193	-.77493547E-02	194	.22867500E-02	195	.15080818E-02		2.4
196	-.70955264E-02	197	.10111657E-10	198	.39527035E-02	2.4	0.0
199	-.85298386E-02	200	.16627616E-02	201	.44149667E-02		1.2
202	-.48741026E-02	203	.14158949E-02	204	.21055808E-02		2.4
205	.18297851E-03	206	-.51025793E-11	207	-.33089375E-12	Back $x'=0.0$, $y'=$	0.0
208	.25266766E-03	209	-.18454290E-05	210	-.16602984E-11		0.2
211	.51154137E-03	212	-.15016695E-04	213	-.64580603E-12		0.4
214	.99516463E-03	215	-.59404681E-04	216	-.50267141E-12	note: $x' = x^{(4)}$	0.6
217	.26989029E-02	218	-.33161786E-03	219	.46849560E-12	$y' = y^{(4)}$	0.8
220	.56050442E-02	221	-.11455201E-02	222	-.81864575E-11		1.2
223	.91485365E-02	224	-.30001741E-02	225	-.66229484E-11		1.6
226	.58908305E-02	227	-.26351460E-02	228	-.76230585E-11		2.4
229	.25700096E-03	230	-.32340158E-11	231	-.31101146E-05	0.025	0.0
232	.35857214E-03	233	-.27159725E-05	234	-.42509195E-05		0.2
235	.37639592E-03	236	-.34553712E-11	237	-.81908514E-05	0.0	0.0
238	.53969847E-03	239	-.47137646E-05	240	-.16702591E-04		0.2
241	.71665147E-03	242	-.20276957E-04	243	-.16891967E-04		0.4
244	.48695002E-03	245	-.32499146E-11	246	-.13392721E-04	0.1	0.0
247	.10666416E-02	248	-.11841377E-04	249	-.69488596E-04		0.2
250	.10416886E-02	251	-.26020582E-04	252	-.51011181E-04		0.4
253	.13831171E-02	254	-.81249257E-04	255	-.64300644E-04		0.6
256	.47463465E-03	257	-.10438564E-10	258	-.18497387E-04	0.15	0.0
259	.25140390E-02	260	.62183738E-11	261	-.22856637E-03	0.2	0.0

EQUATION RESIDUALS (P3)

262	.36833431E-02	263	-.16848226E-03	264	-.36419304E-03	(Back cont) $x=0.2$, $y=0.4$	
265	.45677232E-02	266	-.46461983E-03	267	-.37344245E-03		0.8
268	.45380463E-02	269	-.38009258E-11	270	-.59345224E-03	0.4	0.0
271	.63389514E-02	272	-.16289498E-03	273	-.89137306E-03		0.4
274	.60158601E-02	275	-.45526918E-03	276	-.86550857E-03		0.8
277	.70533362E-02	278	-.12210750E-02	279	-.73553006E-03		1.2
280	.11402465E-01	281	-.19810792E-11	282	-.17083437E-02	0.8	0.0
283	.11305519E-01	284	-.49652327E-03	285	-.21144643E-02		0.8
286	.68672982E-02	287	-.81030774E-03	288	-.12508214E-02		1.2
289	.97552977E-02	290	-.27218787E-02	291	-.14908031E-02		1.6
292	.73306719E-02	293	-.28019476E-02	294	-.50600756E-03		2.4
295	.13413373E-01	296	.72181584E-11	297	-.11743848E-02	1.6	0.0
298	.15115201E-01	299	-.13526612E-02	300	-.16511965E-02		1.2
301	.75892103E-02	302	-.17782176E-02	303	-.66249681E-03		2.4
304	.67221094E-02	305	.85002936E-11	306	-.14427828E-02	2.4	0.0
307	.81007609E-02	308	-.30088048E-03	309	-.18201380E-02		1.2
310	.4642747 E-02	311	-.72254859E-03	312	-.13482873E-02		2.4
313	.18572561E-02	314	-.16383911E-11	315	.11244849E-11	Crack ($y=0.0$ $z=0.0$ (rectangular grid)	0.05
316	.34134479E-03	317	-.11074475E-11	318	.53881138E-12		0.1
319	.21229788E-02	320	-.21175074E-11	321	.45180933E-12		0.15
322	.35078879E-02	323	-.21675268E-11	324	.98660491E-12		1.2
325	.23123620E-02	326	-.13748956E-11	327	.65364414E-12		0.0
328	-.35489341E-02	329	-.21494547E-11	330	.16017619E-11	0.1	0.025
331	.18229937E-02	332	-.19211622E-11	333	.17950276E-11		0.075
334	-.39381863E-02	335	-.15416464E-11	336	.11995411E-11		0.125
337	-.44979215E-03	338	-.23843743E-11	339	.12547951E-11		0.175
340	-.38146932E-02	341	-.24232324E-11	342	.90179449E-12		0.0
343	.45833182E-02	344	-.99612264E-10	345	.30931651E-09	0.2	0.05
346	-.12594748E-02	347	-.23406449E-11	348	.68798572E-12		0.1
349	.15790235E-02	350	-.32242146E-11	351	.62820824E-12		0.15
352	.10882262E-02	353	-.21733804E-11	354	.61788801E-12		0.2
355	-.28952972E-02	356	-.31377267E-11	357	.89250991E-12		0.0
358	-.57398509E-02	359	-.13963317E-11	360	.16974735E-11	0.3	0.025
361	.18506453E-02	362	-.11622082E-11	363	.12348736E-11		0.075
364	-.22223722E-04	365	-.13298968E-11	366	.15424524E-11		0.125
367	.41210690E-02	368	-.89909205E-12	369	.12129439E-11		0.175
370	.51045317E-02	371	-.22513178E-11	372	.87327536E-12		0.0
373	.55418232E-02	374	-.49425401E-11	375	.44834354E-11	0.4	0.1
376	-.28194488E-02	377	-.20223880E-11	378	.73681778E-12		0.2
379	-.64745369E-02	380	-.11296763E-11	381	.12624145E-11		0.3
382	-.81492417E-02	383	-.19828469E-11	384	.90387115E-13		0.025
385	.33696719E-02	386	-.27552636E-11	387	.11536911E-12	0.45	0.075
388	-.29235573E-03	389	-.32831708E-11	390	.46996675E-12		0.0
391	-.80663485E-02	392	-.74410600E-12	393	.13965777E-11	0.5	0.1
394	.50307445E-02	395	-.37523223E-11	396	.10309759E-13		0.2
397	.54270930E-02	398	-.31652675E-11	399	-.49334893E-12		0.025
400	-.78628765E-03	401	-.23716446E-11	402	-.67397195E-13	0.55	0.075
403	.37476764E-02	404	-.31671071E-11	405	-.33198203E-12		

EQUATION RESIDUALS (P4)

406	.66081166E-02	407	-.52793735E-09	408	.59188051E-09	Crack (cont)	$y = 0.6, z = 1.0$	
409	-.60370E62E-02	410	-.3.073577E-11	411	-.61559177E-12			0.1
412	-.64824209E-02	413	-.66422599E-12	414	.15964532E-11		0.65	0.025
415	-.52758148E-02	416	.12663149E-10	417	-.10912496E-10		0.7	0.0
418	.866345 26E-02	419	.76241621E-08	420	-.48320304E-08		0.75	1.0
421	.46504550E-02	422	-.14281558E-11	423	.12214650E-12	(polar grid)	$\rho = 0.85, \theta = 0.0$	
424	-.54129575E-02	425	-.16637572E-11	426	.27025983E-12			0.125
427	-.16711964E-02	428	-.25499210E-11	429	-.53843822E-12			0.25
430	.45619369E-02	431	-.71J06E60E-12	432	.10678613E-11			0.375
433	.58795256E-02	434	-.61704656E-12	435	-.44574475E-12		0.90	0.0
436	-.31346174E-02	437	-.18466411E-11	438	-.13974426E-12			0.125
439	.17114960E-02	440	-.13734270E-11	441	.21245265E-12			0.25
442	.33490E45E-02	443	-.23148242E-11	444	-.43702240E-12			0.375
445	-.54729037E-02	446	-.26922130E-11	447	-.48872783E-13			0.50
448	.50815783E-02	449	-.32460C89E-11	450	-.35487612E-12			0.625
451	-.58541635E-03	452	-.19091312E-11	453	-.36092263E-12		0.94	0.0625
454	-.28259790E-02	455	-.15913042E-11	456	.41185807E-13			0.1875
457	.41935879E-02	458	-.22179310E-11	459	.16695712E-11			0.3125
460	-.62929E00E-02	461	-.64303496E-13	462	-.21409576E-12			0.4375
463	.91130230E-02	464	-.34354954E-11	465	-.47800466E-12			0.5625
466	-.11485255E-01	467	-.35125703E-11	468	-.10428812E-11			0.6875
469	-.30527861E-02	470	-.2898b546E-11	471	-.31098414E-12			0.75
472	.16.34199E-01	473	-.18728652E-11	474	.13283266E-12			0.84
475	.46601C0JE-03	476	-.14917398E-11	477	.92147407E-12		0.97	0.0
478	-.27302223E-02	479	-.17461566E-11	480	.94419184E-12			0.125
481	.41898331E-02	482	-.12365528E-11	483	.96631435E-12			0.25
484	-.47139430E-02	485	-.14464553E-11	486	-.93795741E-12			0.375
487	.14641922E-02	488	-.14647637E-11	489	.49774454E-12			0.5
490	.27191061E-02	491	-.96405490E-12	492	.9.631339E-12			0.625
493	-.52188472E-02	494	-.36812887E-11	495	-.64486399E-12			0.75
496	.29925688E-31	497	-.20574732E-11	498	.23579c90E-12			0.8125
499	-.35239146E-01	500	-.22571239E-11	501	-.67763320E-12			1875
502	.16297884E-02	503	-.13846586E-11	504	.24901879E-12		0.99	0.0625
505	.71221595E-04	506	-.21754762E-11	507	.9E156655E-12			0.1875
508	.29474243E-02	509	-.40706258E-12	510	-.40044077E-12			0.3125
511	-.39798813E-02	512	-.25556877E-11	513	.87727218E-13			0.4375
514	.42747729E-02	515	-.37399794E-11	516	-.45512708E-12			0.5625
517	-.43038696E-02	518	-.29298396E-11	519	.22510448E-12			0.6875
520	-.14054C1JE-01	521	-.1926J686E-11	522	-.3C566C35E-13			0.8125
523	.18256136E-01	524	-.20835329E-11	525	-.64693279E-12			0.90
526	.27781752E-02	527	-.78547619E-12	528	.91479910E-12		1.00	0.0
529	-.39474349E-02	530	-.15708096E-11	531	-.10254882E-11			0.125
532	-.94791358E-04	533	-.36154865E-11	534	-.50078747E-12			0.25
535	.12411253E-02	536	.14048462E-11	537	-.29937737E-12	on crack front		0.375
538	-.16394009E-03	539	-.47489992E-11	540	-.13333596E-12			0.50
541	-.22126441E-02	542	-.35424580E-13	543	.21959448E-11			0.625
544	.66223967E-02	545	-.26497139E-11	546	-.74950454E-12			0.75
547	-.92644173E-03	548	-.19023283E-12	549	.21552005E-11			0.875
550	-.42438667E-02	551	.34204879E-08	552	-.11740705E-07	crack up →		0.92729521

562 equations were used, but where the residuals show E-11, E-12, or E-13, the corresponding equation involved only essentially vanishing influence functions. The many residuals showing E-02 and E-03, being << 1, indicate good fitting at these points. These residuals provide a means for studying the quality of a solution, but they do not tell all that might be desired since satisfaction of boundary conditions is desired everywhere on the front, back and crack surfaces.

In this example, the editing version of MATSOL was used to select boundary conditions to be fitted near the crack tip. The weights of the various rows of the matrix (not of the printout) are shown near the beginning of the printout, and these show that here rows 1 to 4 and 8 to 15 were assigned weight zero, so that rows 5 to 7 provided the boundary conditions used near the crack tip. The occasional large residuals among the non-fitted rows there suggest the difficulty of getting good fitting all around the crack tip.

MATSOL uses the auxiliary information provided by FRAC3D to identify the load constants, and the identified forms are printed as shown on pages 58, 59, 60. Then it uses the crack constants to compute stress-intensity factors for the three standard modes at many points along the crack front as shown on Page 61. In the illustrative example, 40 intervals were used from the crack root to the crack because FRAC3D contained a statement NO = 40 which was carried forward to MATSOL. The highest value of θ, of course, is arccos (r_c/a), which here is arccos 0.6.

In this illustrative calculation, the computer proceeded directly from performance of FRAC3D to performance of MATSOL. Then it returned directly to FRAC3D with data calling for operation in the RESULT mode in order to evaluate stresses at a set of points specified in the global coordinates and a set specified in the crack coordinates. The data provided for the calculation in this latter mode were

Card	Data
1	RESULT (in cc 1-6)
2	bb100bbb71 (counts of points in global and crack systems)
3	(A title card: STRESSES AND DISPLACEMENTS FOR POINTS ON FACE1)

PYRAMIDAL LOADS ON FACE NO. 1

GLOBAL COORDINATES			SURFACE LOADS		
X	Y	Z	P	S	T
0.0000	2.4000	0.0000	.2895966622E-01		-.1991682500E-02
.8000	2.4000	0.0000	.3174594429E-01	-.3430430731E-02	.4436037685E-02
1.6000	2.4000	0.0000	.3314826523E-01	.2811505140E-02	.1068921545E-01
2.4000	2.4000	0.0000	.2297297315E-01	.7575698608E-02	.8169944705E-02
0.0000	1.6000	0.0000	.1295812352E-01		-.3534425344E-01
.4000	1.6000	0.0000	.2984739691E-01	-.2101223136E-01	-.2702559395E-01
.8000	1.6000	0.0000	.3573013877E-01	-.1680780889E-01	.8273621861E-02
0.0000	1.2000	0.0000	-.4044701682E-01		-.9705445475E-01
.2000	1.2000	0.0000	.4100290183E-01	-.4005436618E-01	-.9033786642E-01
.4000	1.2000	0.0000	.5118642388E-01	-.7697936294E-01	-.1079388874E-01
.6000	1.2000	0.0000	.1886642137E-01	-.5537870948E-02	.5681255473E-01
1.6000	1.2000	0.0000	.4784461250E-01	.3002306660E-01	.2882342241E-01
2.4000	1.2000	0.0000	.3936264018E-01	.2372472387E-01	.1072946754E-01
0.0000	1.0000	0.0000	-.7013676791E-02		-.2356199994E+00
.1000	1.0000	0.0000	.7984194974E-01	-.4939455805E-01	-.1700815853E+00
.2000	1.0000	0.0000	.9967668884E-01	-.1057655225E+00	-.2392825416E-01
.4000	1.0000	0.0000	.4879458349E-02	-.5381337172E-01	.1159339817E+00
0.0000	.9000	0.0000	.2263001866E+00		-.4111528774E+00
.0500	.9000	0.0000	.2213805231E+00	-.8280151279E-01	-.2946935338E+00
.1000	.9000	0.0000	.1649831247E+00	-.1080959777E+00	-.1018523983E+00
.2000	.9000	0.0000	.1829374162E-01	-.5740602336E-01	.1206908989E+00
0.0000	.8500	0.0000	.6105355609E+00		-.5753232360E+00
.0500	.8500	0.0000	.3514014784E+00	-.1195863442E+00	-.2214303455E+00
0.0000	.8000	0.0000	.1176170232E+01		-.9007892239E+00
.0500	.8000	0.0000	.3045022622E+00	.1690043988E+00	-.9620483691E-01
.1000	.8000	0.0000	.1393176697E-02	.1322079383E+00	.5308195847E-01
.2000	.8000	0.0000	-.2032250495E+00	.1634684441E+00	.1851259215E+00
.4000	.8000	0.0000	-.2018538923E+00	.1731580465E+00	.2130833865E+00
.6000	.8000	0.0000	-.6222778722E-01	.1326300939E+00	.1254318939E+00
0.0000	.7500	0.0000	-.1870170401E+00		-.4183811023E+00
.0500	.7500	0.0000	.8937298108E-01	.2549983406E+00	-.2995446665E+00
0.0000	.7000	0.0000	-.2124170039E+00		-.3173583812E+00
.0500	.7000	0.0000	-.1408114837E+00	.1078482573E+00	-.3211076700E+00
.1000	.7000	0.0000	-.2473096810E+00	.2638574112E+00	-.1628258788E+00
.2000	.7000	0.0000	-.3845116339E+00	.3351529496E+00	.5820913574E-01
0.0000	.6000	0.0000	-.3826082668E+00		-.2263055667E+00
.0500	.6000	0.0000	-.4050856236E+00	.2023309488E-01	-.2279873078E+00
.1000	.6000	0.0000	-.4242128414E+00	.1518162800E+00	-.1958968216E+00
.2000	.6000	0.0000	-.4769603949E+00	.3352020876E+00	-.5130638249E-01
.4000	.6000	0.0000	-.3832078279E+00	.3655062653E+00	.1205093274E+00
0.0000	.4000	0.0000	-.6076954937E+00		-.1446830815E+00
.0500	.4000	0.0000	-.6446581493E+00	.1188921487E-01	-.1392462940E+00
.1000	.4000	0.0000	-.6460249315E+00	.7741062756E-01	-.1264077636E+00
.2000	.4000	0.0000	-.6185267229E+00	.2479654105E+00	-.6853172122E-01
.3000	.4000	0.0000	-.5632595146E+00	.3630103342E+00	.1933514425E-03
.4000	.4000	0.0000	-.4787541985E+00	.4065313393E+00	.5117017018E-01
.8000	.4000	0.0000	-.1521226855E+00	.2948003001E+00	.8311318891E-01
1.6000	.4000	0.0000	.3485760580E-01	.8965100387E-01	.2177275100E-01
0.0000	.2000	0.0000	-.6937981127E+00		-.8731742635E-01
.0500	.2000	0.0000	-.7326789792E+00	.4701604731E-02	-.7510638306E-01
.1000	.2000	0.0000	-.7554455263E+00	.5462901102E-01	-.5984425157E-01
.2000	.2000	0.0000	-.7376462597E+00	.2161048524E+00	-.2585415960E-01
.3000	.2000	0.0000	-.6597458323E+00	.3515909239E+00	.4930095563E-02
0.0000	0.0000	0.0000	-.7010680854E+00		
.0500	0.0000	0.0000	-.7526716146E+00	-.1200867628E-02	
.1000	0.0000	0.0000	-.7923655203E+00	.4870917870E-01	
.2000	0.0000	0.0000	-.7878267752E+00	.2139171193E+00	
.3000	0.0000	0.0000	-.7026292641E+00	.3550367595E+00	
.4000	0.0000	0.0000	-.5832446191E+00	.4289313628E+00	
.6000	0.0000	0.0000	-.3520727465E+00	.4273396686E+00	
.8000	0.0000	0.0000	-.1859301089E+00	.3474296896E+00	
1.2000	0.0000	0.0000	-.2392740063E-01	.1903805563E+00	
1.6000	0.0000	0.0000	.3088089609E-01	.1012166726E+00	
2.4000	0.0000	0.0000	.4206416706E-01	.3994723845E-01	

PYRAMIDAL LOADS ON FACE NO. 4

GLOBAL COORDINATES				SURFACE LOADS	
X	Y	Z	P	S	T
0.0000	0.0000	.5714	.9189237376E+00		
.0250	0.0000	.5714	.8958690785E+00	.7086900486E-01	
.0500	0.0000	.5714	.8330036205E+00	.1271828554E+00	
.1000	0.0000	.5714	.6504531519E+00	.1727534284E+00	
.1500	0.0000	.5714	.3033350912E+00	.9716966974E-01	
.2000	0.0000	.5714	.3485494529E+00	.1099812895E+00	
.4000	0.0000	.5714	.1193866403E+00	.6575337606E-04	
.8000	0.0000	.5714	.2706535718E-02	-.3294205295E-01	
1.6000	0.0000	.5714	-.3969195411E-01	-.1588841612E-01	
2.4000	0.0000	.5714	-.3258267144E-01	-.1541869527E-01	
0.0000	.2000	.5714	.8423645280E+00		-.9686587753E-01
.0250	.2000	.5714	.8245543901E+00	.6091396692E-01	-.9421983147E-01
.0500	.2000	.5714	.7751778765E+00	.1113132105E+00	-.8692544425E-01
.1000	.2000	.5714	.6246196046E+00	.1604310537E+00	-.6498517543E-01
0.0000	.4000	.5714	.6572374185E+00		-.1593559922E+00
.0500	.4000	.5714	.6218430876E+00	.7734239079E-01	-.1486467139E+00
.1000	.4000	.5714	.5346571412E+00	.1246713196E+00	-.1223293297E+00
.2000	.4000	.5714	.3345095772E+00	.1231269266E+00	-.6419757983E-01
.4000	.4000	.5714	.1205613060E+00	.3650045206E-01	-.6500480069E-02
0.0000	.6000	.5714	.4422209504E+00		-.1747992796E+00
.1000	.6000	.5714	.3404583201E+00	.6375774907E-01	-.1235711559E+00
0.0000	.8000	.5714	.2571038428E+00		-.1484800308E+00
.2000	.8000	.5714	.1865558744E+00	.6590365236E-01	-.9997355687E-01
.4000	.8000	.5714	.9398031100E-01	.5218626278E-01	-.3632509741E-01
.8000	.8000	.5714	.5231969278E-02	.7275979839E-02	.5220235671E-02
0.0000	1.2000	.5714	.6681659392E-01		-.6823703637E-01
.4000	1.2000	.5714	.3370620608E-01	.2699509156E-01	-.3507319190E-01
.8000	1.2000	.5714	-.5813980957E-02	.1397232095E-01	-.5402960738E-02
1.6000	1.2000	.5714	-.4273400299E-01	-.4274353281E-02	.4448178627E-02
2.4000	1.2000	.5714	-.3191845543E-01	-.1210974297E-01	.3714173543E-02
0.0000	1.6000	.5714	.3820306182E-02		-.2784185847E-31
.8000	1.6000	.5714	-.2154130988E-01	.9610670483E-02	-.5345866683E-02
0.0000	2.4000	.5714	-.2270347171E-01		-.6348966475E-03
.8000	2.4000	.5714	-.2641536683E-01	.2347775181E-02	.3397260637E-02
1.6000	2.4000	.5714	-.2843015335E-01	-.1567632784E-02	.6718809277E-02
2.4000	2.4000	.5714	-.1854919960E-01	-.5632689304E-02	.5263241981E-02

SOLUTION VECTOR

M	K	ALPHA
0	0	.113939584E+01
0	1	.142253864E+01
0	2	-.26773.950E+01
0	3	.452082c38E+01
0	4	-.395232942E+01
0	5	.283511196E+01
0	6	-.982311323E+00
0	7	.223291707E+00
0	8	-.26827147CE-01
1	0	0.
1	1	0.
1	2	0.
1	3	0.
1	4	0.
1	5	0.
1	6	0.
1	7	0.
1	8	0.
2	0	.634126578E+00
2	1	-.464216EC1E+01
2	2	.751556159E+01
2	3	-.830152658E+01
2	4	.527388952E+01
2	5	-.217662200E+01
2	6	.407239493E+00
2	7	-.620184771E-01
2	8	0.
3	0	0.
3	1	0.
3	2	0.
3	3	0.
3	4	0.
3	5	0.
3	6	0.
3	7	0.
3	8	0.
4	0	-.181015529E+01
4	1	.593815162E+01
4	2	-.722580866E+01
4	3	.529227477E+01
4	4	-.219014587E+01
4	5	.490538821E+00
4	6	-.539621859E-01
4	7	0.
4	8	0.
5	0	0.
5	1	0.
5	2	0.
5	3	0.
5	4	0.
5	5	0.
5	6	0.
5	7	0.
5	8	0.
6	0	.241936999E+01
6	1	-.534293761E+01
6	2	.481439947E+01
6	3	-.230995303E+01
6	4	.553691285E+00
6	5	-.613825321E-01
6	6	0.
6	7	0.
6	8	0.
7	0	0.
7	1	0.
7	2	0.
7	3	0.
7	4	0.
7	5	0.
7	6	0.
7	7	0.
7	8	0.
8	0	-.226153458E+01
8	1	.353557259E+01
8	2	-.227082046E+01
8	3	.645464403E+00
8	4	-.723257603E-01
8	5	0.
8	6	0.
8	7	0.
8	8	0.
9	0	0.
9	1	0.
9	2	0.
9	3	0.
9	4	0.
9	5	0.
9	6	0.
9	7	0.
9	8	0.
10	0	.156667249E+01
10	1	-.170354867E+01
10	2	.710845105E+00
10	3	-.921046343E-01
10	4	0.
10	5	0.
10	6	0.
10	7	0.
10	8	0.
11	0	0.
11	1	0.
11	2	0.
11	3	0.
11	4	0.
11	5	0.
11	6	0.
11	7	0.
11	8	0.
12	0	-.799799240E+00
12	1	.555988486E+00
12	2	-.116996269E+00
12	3	0.
12	4	0.
12	5	0.
12	6	0.
12	7	0.
12	8	0.
13	0	0.
13	1	0.
13	2	0.
13	3	0.
13	4	0.
13	5	0.
13	6	0.
13	7	0.
13	8	0.
14	0	.27989917EE+00
14	1	-.971949E06E-01
14	2	0.
14	3	0.
14	4	0.
14	5	0.
14	6	0.
14	7	0.
14	8	0.
15	0	0.
15	1	0.
15	2	0.
15	3	0.
15	4	0.
15	5	0.
15	6	0.
15	7	0.
15	8	0.
16	0	-.529737401E-01
16	1	0.
16	2	0.
16	3	0.
16	4	0.
16	5	0.
16	6	0.
16	7	0.
16	8	0.

STRESS INTENSITY FACTORS

THETA	K1	K2	K3
0.	.941229906332O5E+00	0.	0.
.2318238045004OE-01	.941434628398 30E+00	0.	0.
.4636476090058OE-01	.942.2895617.69E+00	0.	0.
.6954714135.121E-01	.9-2957614767 18E+00	0.	0.
.9272952180016 1E-01	.9441416515b489E+00	0.	0.
.1159119022502 0E+00	.9454950 3497786E+00	0.	0.
.1390942827..24E+00	.946942287589 58E+00	0.	0.
.1622766631502 6E+00	.9484330 5646996E+00	0.	0.
.1854590436J032E+00	.9499501 5963831E+00	0.	0.
.2086414240 5036E+00	.9515391 7913229E+0J	0.	0.
.2318238045004OE+00	.9531488 1666276E+00	0.	0.
.2550061849504 4E+00	.9549160 6482845E+00	0.	0.
.2781885654034 8E+00	.9568463 2370769E+00	0.	0.
.3013709458505 2E+00	.9589465 0950336E+00	0.	0.
.3245533263006 6E+00	.9611835 264713E+00	0.	0.
.3477357067506 0E+00	.9634819 1826041E+00	0.	0.
.3709180872006 4E+00	.9657233 628444E+00	0.	0.
.3941004676506 8E+00	.9678086 9956543E+00	0.	0.
.4172828481007 2E+00	.9695911 215332 0E+00	0.	0.
.4404652285507 6E+00	.9709885 3256 3J3E+00	0.	0.
.4636476090008 0E+00	.9719549 4974164E+00	0.	0.
.4868299894508 4E+00	.9724939 9706289E+00	0.	0.
.5100123699J087E+00	.9726486 4458286E+00	0.	0.
.5331947503509 1E+00	.9724766 6041515E+00	0.	0.
.5563771308.95E+00	.9720162 9804275E+00	0.	0.
.5795595112509 9E+00	.9712503 6C08871E+00	0.	0.
.6027418917010 3E+00	.9700789 3534108E+00	0.	0.
.6259242721510 6E+00	.9683108 2137334E+00	0.	0.
.6491066526011 0E+00	.9656802 1225668E+00	0.	0.
.6722890330511 4E+00	.9618884 0732783E+00	0.	0.
.6954714135011 8E+00	.9566604 5079759E+0J	0.	0.
.7186537939512 2E+00	.9497947 8714558E+00	0.	0.
.7418361744012 5E+00	.9411718 9734229E+00	0.	0.
.7650185548512 9E+00	.9306776 4033J00E+00	0.	0.
.7882009353013 3E+00	.9179916 7467599E+00	0.	0.
.8113833157513 7E+00	.9021871 9035158E+00	0.	0.
.8345656962014 1E+00	.8811140 7728936E+00	0.	0.
.8577480766514 4E+00	.8505225 8489993E+00	0.	0.
.8809304571014 8E+00	.8029543 1743315E+00	0.	0.
.9041128375515 2E+00	.7264293 4545943E+00	0.	0.
.9272952180015 6E+00	.6030153 8859915E+00	0.	0.

Card	Data
4 - 403	(100 cards specifying x,y,z in 3F10.0 to be used in finding stresses)
404	(A title card: STRESSES AND DISPLACEMENTS FOR POINTS ON FACE 7)
405-475	(71 cards specifying ρ,θ,z in 3F10.0 to be used in finding stresses)

The output from the calculation in the RESULT mode is shown on pp 63 to 66. It may be noted that points listed as Face 1 are really the midpoints at all the rectangles on Faces 1 and 4, so that they constitute a fairly complete set of check points for the fitting on the plane faces. The columns providing the check are those for σ_z, τ_{yz} and τ_{zx}, and inspection shows that all those entries are a small percent of σ_o except in some small rectangles close to the crack tip. The points listed on Face 7 are the chosen check points on the crack. Here σ_z should be near unity, while $\tau_{\theta z}$ (TAUTZ) and τ_{zr} (misprinted as TAUTR) should be small compared to unity. Inspection shows that these conditions too are well satisfied, so the analysis provided here is taken to be acceptable. The values of W listed for Face 7 provide a map of the crack opening displacement after they are multiplied by $2\mu a/\sigma_o$, where μ is the shear modulus, and σ_o is the applied uniform crack load.*

The illustrative case described here is discussed also in Reference 2, as the accepted analysis for a normally loaded crack with A/2C = 0.25 and A/T = 0. Much of the tabular information here is shown there in graphical form.

---

* The program for getting the other displacement components still needs checking for consistency while combining contributions for surface constants with those from crack constants.

STRESSES AND DISPLACEMENTS FOR POINTS ON FACE 1

XSA	YSA	ZSA	SIGMAX	SIGMAY	SIGMAZ	TAUYZ	TAUZX	TAUXY	U	V	W	TAUOC
.025	.100	0.000	-.9873E+00	-.2191E+00	-.5212E-02	.2666E-02	.7215E-02	-.9099E-02	.4036E+00	.2032E-01	-.7986E+00	.4218E+00
.025	.300	0.000	-.9932E+00	-.2264E+00	-.1678E-01	.1985E-02	.6771E-02	-.2982E-01	.3644E+00	.5927E-01	-.7387E+00	.4205E+00
.025	.500	0.000	-.1005E+01	-.2273E+00	-.3285E-01	-.1031E-01	.1269E-01	-.5964E-01	.2831E+00	.9469E-01	-.6184E+00	.4229E+00
.025	.650	0.000	-.1021E+01	-.1527E+00	-.1139E-01	.8762E-03	.4988E-01	-.1139E+00	.1828E+00	.1193E+00	-.4883E+00	.4611E+00
.025	.725	0.000	-.1031E+01	.3165E-01	-.6817E-01	.6468E-01	.4933E-01	-.2973E+00	.1111E+00	.1329E+00	-.4067E+00	.5686E+00
.025	.775	0.000	-.4953E+00	.1783E+00	.7773E-01	.3422E-01	-.2201E+00	-.8886E+00	.4773E-01	.1449E+00	-.3376E+00	.7976E+00
.025	.825	0.000	.1042E+01	-.4008E-01	.3301E-01	-.1340E+00	.1394E+00	.4475E-01	.2688E-02	.1355E+00	-.2874E+00	.5195E+00
.025	.875	0.000	.5492E+00	.2.87E+00	-.4068E-02	.3841E-01	.2824E-01	.6492E-01	.3486E-02	.1271E+00	-.2643E+00	.2372E+00
.025	.950	0.000	.3807E+00	.1279E+00	-.4273E-01	.1193E-01	-.1163E-01	.7225E-02	.4386E-02	.1193E+00	-.2370E+00	.1746E+00
.050	1.100	0.000	.2446E+00	.2965E-01	-.3886E-01	-.4850E-02	-.1763E-01	-.7796E-02	.7800E-02	.1026E+00	-.1853E+00	.1219E+00
.075	.100	0.000	-.1027E+01	-.1336E+00	-.1135E-01	.8876E-03	.6354E-02	-.2591E-01	.3737E+00	.2351E-01	-.7608E+00	.4533E+00
.075	.300	0.000	-.1.43E+01	-.1352E+00	-.1274E-01	.3652E-03	.6919E-02	-.8698E-01	.3346E+00	.6923E-01	-.7018E+00	.4651E+00
.075	.500	0.000	-.1081E+01	-.1278E+00	-.2673E-01	-.2607E-02	.1107E-01	-.1975E+00	.2511E+00	.1119E+00	-.5834E+00	.5019E+00
.075	.650	0.000	-.9796E+00	-.7594E-01	-.7337E-02	.1923E-01	.1139E-01	-.4458E+00	.1486E+00	.1398E+00	-.4566E+00	.5737E+00
.075	.725	0.000	-.5146E+00	-.1272E+00	-.6442E-02	.5726E-02	-.4352E-01	-.6979E+00	.8091E-01	.1475E+00	-.3814E+00	.6107E+00
.075	.775	0.000	.2579E+00	-.3235E+00	-.2131E-01	-.2933E-01	-.5603E-01	-.6926E+00	.3712E-01	.1414E+00	-.3328E+00	.6155E+00
.075	.825	0.000	.7369E+00	-.1894E+00	.3172E-02	-.5023E-01	.4717E-01	-.1990E+00	.1319E-01	.1294E+00	-.2958E+00	.4354E+00
.075	.875	0.000	.5636E+00	-.2123E-01	.2114E-01	-.8680E-02	.3826E-01	.4420E-01	.1083E-01	.1222E+00	-.2687E+00	.2706E+00
.075	.950	0.000	.3705E+00	.5992E-01	-.5518E-02	.2571E-01	-.5954E-02	.2779E-01	.1209E-01	.1146E+00	-.2373E+00	.1670E+00
.100	1.400	0.000	.1236E+00	-.3823E-01	-.1115E-01	-.5338E-02	-.8428E-02	-.1268E-01	.9481E-02	.7332E-01	-.9717E-01	.7211E-01
.150	.100	0.000	-.1.98E+01	-.5124E-01	-.2365E-01	-.1433E-02	.4862E-02	-.5196E-01	.3255E+00	.2596E-01	-.7008E+00	.5008E+00
.150	.300	0.000	-.1.89E+01	-.5129E-01	-.1387E-01	.8732E-03	.7209E-02	-.1724E+00	.2857E+00	.7628E-01	-.6447E+00	.5179E+00
.150	.500	0.000	-.9967E+00	-.6592E-01	-.1237E-01	.1596E-01	-.3681E-03	-.3676E+00	.2017E+00	.1199E+00	-.5353E+00	.5445E+00
.150	.650	0.000	-.5902E+00	-.1142E+00	-.2173E-01	.8554E-02	-.3085E-01	-.5928E+00	.1086E+00	.1389E+00	-.4255E+00	.5450E+00
.150	.750	0.000	-.4929E-01	-.2701E+00	-.5153E-01	-.3391E-01	-.5030E-01	-.5567E+00	.4935E-01	.1320E+00	-.3486E+00	.4770E+00
.150	.850	0.000	.5148E+00	-.1772E+00	-.3372E-02	-.5712E-01	.3489E-01	-.1815E+00	.2198E-01	.1151E+00	-.2855E+00	.3337E+00
.150	.950	0.000	.3833E+00	-.5142E-01	.2589E-01	.1756E-02	.2532E-01	-.1704E-01	.2144E-01	.1050E+00	-.2367E+00	.1907E+00
.150	1.100	0.000	.2128E+00	-.7658E-02	.3612E-02	.2423E-01	-.1103E-01	-.1152E-01	.2031E-01	.9425E-01	-.1806E+00	.1053E+00
.200	2.000	0.000	.3351E-01	-.4521E-01	-.5807E-03	-.1748E-02	-.1721E-02	-.7385E-02	.6200E-02	.3017E-01	.4076E-02	.3286E-01
.250	.100	0.000	-.1.74E+01	.2939E-01	-.1805E-01	-.2556E-02	-.7228E-02	-.7778E-01	.2598E+00	.2561E-01	-.6210E+00	.5114E+00
.250	.300	0.000	-.9946E+00	.1997E-01	-.8994E-02	-.6657E-03	-.2965E-02	-.2473E+00	.2219E+00	.7388E-01	-.5719E+00	.5130E+00
.250	.500	0.000	-.726E+00	-.1468E-01	-.1417E-01	.8455E-02	-.1986E-01	-.4274E+00	.1485E+00	.1103E+00	-.4805E+00	.4845E+00
.300	.650	0.000	-.2373E+00	-.1116E+00	-.3467E-01	-.2824E-01	-.3604E-01	-.4652E+00	.7315E-01	.1073E+00	-.3770E+00	.3907E+00
.300	.750	0.000	.4202E-01	-.1863E+00	-.3692E-01	-.3598E-01	-.2589E-01	-.3887E+00	.4718E-01	.9917E-01	-.3229E+00	.3331E+00
.300	.850	0.000	.2169E+00	-.1495E+00	-.2032E-01	-.4956E-01	.1313E-02	-.2440E+00	.3581E-01	.9029E-01	-.2713E+00	.2532E+00
.300	.950	0.000	.2456E+00	-.1409E+00	-.2678E-03	-.3828E-01	.2069E-01	-.1233E+00	.3410E-01	.8522E-01	-.2245E+00	.1921E+00
.300	1.100	0.000	.1966E+00	-.7502E-01	.2315E-01	.1302E-01	.2816E-01	-.4418E-01	.3156E-01	.7824E-01	-.1691E+00	.1206E+00
.300	1.400	0.000	.9.97E-01	-.5479E-01	-.7703E-02	.125.E-01	-.5998E-02	-.2910E-01	.2345E-01	.6268E-01	-.8533E-01	.6601E-01
.350	.100	0.000	-.9956E+00	.7607E-01	-.1699E-01	-.2449E-02	-.9689E-02	-.8506E-01	.2006E+00	.2275E-01	-.5441E+00	.4712E+00
.350	.300	0.000	-.8316E+00	.5264E-01	-.1151E-01	-.1032E-02	-.6204E-02	-.2625E+00	.1685E+00	.6369E-01	-.5038E+00	.4561E+00
.350	.500	0.000	-.5952E+00	-.6708E-02	-.1395E-01	.2023E-02	-.2140E-01	-.4066E+00	.1113E+00	.9992E-01	-.4300E+00	.4201E+00
.400	3.000	0.000	.6309E-02	-.6113E-02	-.1680E-03	-.3301E-02	.3782E-04	-.1674E-02	.1724E-02	-.1082E-02	.3358E-01	.5905E-02
.500	.200	0.000	-.099.E+0	.9410E-01	-.9.71E-02	-.1024E-01	-.2963E-01	-.1518E+00	.1258E+00	.3321E-01	-.4274E+00	.3741E+00
.600	.500	0.000	-.3395E+00	.1829E-01	.1380E-01	-.2025E-01	-.1971E-01	-.2683E+00	.6243E-01	.5080E-01	-.3100E+00	.2768E+00
.600	.700	0.000	-.1331E+00	-.7539E-01	.5723E-02	-.2200E-01	-.8641E-02	-.2562E+00	.4358E-01	.5127E-01	-.2503E+00	.2177E+00
.600	.900	0.000	.1219E-01	-.8035E-01	-.3336E-02	-.1918E-01	.4413E-02	-.1812E+00	.3779E-01	.4847E-01	-.1849E+00	.1542E+00
.600	1.100	0.000	.5250E-01	-.9744E-01	-.7985E-02	-.1628E-01	.9577E-02	-.1063E+00	.3738E-01	.4870E-01	-.1249E+00	.1076E+00
.600	1.400	0.000	.4.22E-01	-.8218E-01	-.2497E-02	.6287E-02	.8660E-02	-.4843E-01	.2946E-01	.4191E-01	-.5808E-01	.6487E-01
.600	2.000	0.000	.1184E-01	-.4923E-01	-.1962E-02	.2054E-02	-.1516E-02	-.1888E-01	.1330E-01	.2053E-01	.1723E-01	.3041E-01
.700	.200	0.000	-.5342E+00	.7339E-01	.6424E-03	-.8039E-02	-.2096E-01	-.1154E+00	.7096E-01	.1889E-01	-.3103E+00	.2874E+00

STRESSES AND DISPLACEMENTS FOR POINTS ON FACE 1 (P2)

1.000	.200	0.000	-.3333E+00	.4348E-01	.2384E-01	.2549E-03	.6268E-02	-.7015E-01	.2544E-01	.5183E-02	-.1793E+00	.1825E+00
1.200	.600	0.000	-.1495E+00	.8053E-02	.2883E-01	.4701E-02	.1649E-01	-.8471E-01	.1119E-01	.5415E-02	-.8724E-01	.1064E+00
1.200	1.000	0.000	-.6666E-01	-.2692E-01	.7766E-02	.1943E-02	.1912E-02	-.7905E-01	.1864E-01	.9061E-02	-.3808E-01	.7138E-01
1.200	1.400	0.000	-.3381E-01	-.5337E-01	-.1706E-02	-.1947E-02	-.1411E-02	-.6134E-01	.1879E-01	.1098E-01	.6938E-02	.5446E-01
1.200	2.000	0.000	-.1663E-01	-.4594E-01	-.1942E-03	.1399E-02	.3251E-02	-.2245E-01	.8498E-02	.4437E-02	.4316E-01	.2650E-01
1.200	3.000	0.000	.1765E-03	-.6039E-02	-.1153E-03	-.2999E-02	.2854E-03	-.2737E-02	.1680E-02	-.5191E-02	.3860E-01	.4387E-02
1.400	.200	0.000	-.1822E+00	.2250E-01	.1414E-01	.1834E-02	.1114E-01	-.3084E-01	.5168E-02	.2957E-03	-.6089E-01	.9831E-01
2.000	.200	0.000	-.1159E+00	.4551E-02	.3826E-02	.9667E-03	.9762E-02	-.9746E-02	-.9084E-02	-.2961E-03	.2752E-01	.5312E-01
2.000	.800	0.000	-.7796E-01	-.1289E-01	.1825E-02	.4114E-04	.4715E-02	-.3099E-01	-.5731E-02	-.8817E-03	.4021E-01	.4307E-01
2.000	1.800	0.000	-.2316E-01	-.2608E-01	.2148E-03	.1910E-02	.5005E-02	-.1871E-01	-.5424E-02	-.5396E-02	.5817E-01	.1977E-01
2.000	3.000	0.000	-.1139E-02	-.2866E-02	-.2569E-03	-.2337E-02	.3505E-03	-.3189E-03	-.2174E-02	-.7055E-02	.3704E-01	.2228E-02
3.000	.600	0.000	-.1739E-01	.4533E-02	.5827E-03	-.2476E-03	-.4219E-02	-.7237E-02	-.9549E-02	-.5039E-03	.3711E-01	.1174E-01
3.000	1.800	0.000	.3566E-03	-.4423E-02	.3070E-03	-.3433E-03	-.2896E-02	-.6409E-02	-.7764E-02	-.3062E-02	.3665E-01	.6170E-02
3.000	3.000	0.000	.5161E-02	.1333E-04	.5435E-03	-.1574E-02	-.1382E-02	.8534E-03	-.2962E-02	-.3203E-02	.2187E-01	.2959E-02
.013	.100	.571	-.9497E+00	-.7702E+00	.2316E-01	.2826E-02	.2056E-02	.8236E-02	-.8212E-02	-.3388E-01	-.7136E+00	.4228E+00
.013	.300	.571	-.8310E+00	-.6178E+00	.1419E-01	.6842E-02	.1176E-02	.1919E-01	-.7280E-02	-.9354E-01	-.6533E+00	.3593E+00
.025	.500	.571	-.6133E+00	-.3619E+00	.9647E-02	.9582E-02	.2230E-02	.4023E-01	-.1145E-01	-.1309E+00	-.5459E+00	.2581E+00
.038	.100	.571	-.8479E+00	-.7322E+00	.1979E-01	.2237E-02	.5307E-02	.2318E-01	-.2386E-01	-.3334E-01	-.7065E+00	.3852E+00
.038	.300	.571	-.7647E+00	-.6355E+00	.1393E-01	.6193E-02	.2357E-02	.5315E-01	-.2132E-01	-.9231E-01	-.6479E+00	.3372E+00
.050	.700	.571	-.3764E+00	-.1337E+00	.7872E-02	.1151E-01	.5224E-02	.6274E-01	-.1614E-01	-.1399E+00	-.4182E+00	.1697E+00
.075	.100	.571	-.5792E+00	-.6272E+00	.1510E-01	.1067E-02	.1393E-01	.3765E-01	-.4311E-01	-.3169E-01	-.6848E+00	.2940E+00
.075	.300	.571	-.5731E+00	-.5290E+00	.1416E-01	.4453E-02	.8408E-02	.9144E-01	-.3947E-01	-.8848E-01	-.6313E+00	.2774E+00
.075	.500	.571	-.4978E+00	-.3325E+00	.9834E-02	.8305E-02	.3856E-02	.1044E+00	-.3246E-01	-.1261E+00	-.5335E+00	.2281E+00
.100	1.000	.571	-.1596E+00	.8119E-01	-.9614E-02	.6152E-02	.2691E-02	.6357E-01	-.1784E-01	-.1166E+00	-.2506E+00	.1122E+00
.125	.100	.571	-.2134E+00	-.4778E+00	-.2525E-02	-.2135E-02	.1034E-01	.4101E-01	-.5912E-01	-.2867E-01	-.6438E+00	.1962E+00
.150	.300	.571	-.1691E+00	-.3735E+00	-.4528E-03	-.3225E-02	.1592E-01	.1099E+00	-.6154E-01	-.7676E-01	-.5794E+00	.1775E+00
.150	.500	.571	-.2269E+00	-.2556E+00	.9301E-02	.6984E-02	.1331E-01	.1530E+00	-.5462E-01	-.1124E+00	-.4983E+00	.1727E+00
.150	.700	.571	-.2166E+00	-.9373E-01	.9662E-02	.1142E-01	.9088E-02	.1421E+00	-.4281E-01	-.1265E+00	-.3938E+00	.1489E+00
.175	.100	.571	.2408E-01	-.3507E+00	-.4145E-02	-.4628E-02	.4135E-02	.3527E-01	-.6593E-01	-.2541E-01	-.5981E+00	.1729E+00
.200	1.400	.571	-.3032E-01	.1106E+00	.3982E-02	.3198E-02	.4249E-02	.4439E-01	-.1469E-01	-.7259E-01	-.1003E+00	.7022E-01
.300	.200	.571	.1751E+00	-.1866E+00	-.2819E-01	-.9688E-02	-.1483E-01	.3745E-01	-.6731E-01	-.3573E-01	-.4825E+00	.1518E+00
.300	.600	.571	.5426E-01	-.1118E+00	-.2129E-02	-.3598E-04	.1265E-01	.1309E+00	-.6555E-01	-.9044E-01	-.3745E+00	.1276E+00
.300	1.000	.571	-.2626E-01	.4543E-01	-.2547E-02	.3870E-02	.2852E-02	.1149E+00	-.4263E-01	-.9488E-01	-.2175E+00	.9854E-01
.400	2.000	.571	.7918E-02	.6682E-01	.4567E-03	.1482E-02	.2189E-02	.2291E-01	-.9076E-02	-.2795E-01	.7330E-02	.3515E-01
.400	3.000	.571	.4646E-02	.1786E-01	.6293E-03	-.3525E-02	.2076E-04	.5080E-02	-.1586E-02	.4540E-03	.3293E-01	.8926E-02
.600	.200	.571	.1173E+00	-.4502E-01	-.1528E-01	-.8173E-02	-.1813E-01	-.6926E-02	-.5330E-01	-.1619E-01	.3007E+00	.7262E-01
.600	.600	.571	.1221E+00	-.4839E-01	-.9290E-02	-.1251E-01	-.5674E-02	.3195E-01	-.6021E-01	-.4599E-01	-.2421E+00	.7825E-01
.600	1.000	.571	.7636E-01	-.5555E-04	-.2412E-02	-.4239E-02	.1632E-02	.7151E-01	-.4996E-01	-.5894E-01	-.1491E+00	.6951E-01
.600	1.400	.571	.3619E-01	-.5109E-01	.2408E-02	.4514E-03	.3159E-02	.5990E-01	-.3036E-01	-.4961E-01	-.6175E-01	.5304E-01
1.200	.400	.571	.3167E-01	.7819E-02	.4191E-02	-.5653E-02	-.4028E-02	-.1828E-01	-.3654E-01	-.1026E-01	-.8279E-01	.2008E-01
1.200	1.000	.571	.6151E-01	-.7822E-03	.1253E-02	-.1717E-02	-.1275E-02	.1125E-02	-.3375E-01	-.2152E-01	-.3196E-01	.2896E-01
1.200	1.400	.571	.9851E-01	.1588E-01	-.4388E-03	-.1468E-02	.5216E-03	.1753E-01	-.2433E-01	-.2061E-01	.6591E-02	.2871E-01
1.200	2.000	.571	.3876E-01	.2734E-01	-.9513E-03	-.2273E-03	.9525E-03	.1731E-01	-.1083E-01	-.9076E-02	.4185E-01	.2189E-01
1.200	3.000	.571	.1285E-01	.6305E-02	.9329E-03	-.3599E-02	.9932E-05	.5677E-02	-.1319E-02	.4618E-02	.3799E-01	.7340E-02
2.000	.600	.571	.2344E-01	.1812E-01	.3161E-02	-.3794E-03	.8722E-04	-.9754E-02	-.7384E-02	-.3799E-02	.3535E-01	.1171E-01
2.000	1.800	.571	.3208E-01	.1214E-01	.8557E-03	-.1496E-03	.6383E-03	-.3573E-02	.7434E-03	.5012E-03	.5707E-01	.1325E-01
2.000	3.000	.571	.1226E-01	-.1943E-02	.1380E-02	-.2989E-02	-.1335E-03	-.2272E-02	.3053E-02	.6879E-02	.3638E-01	.6797E-02
3.000	.600	.571	-.1321E-01	.7516E-02	.3885E-02	-.5693E-04	-.7093E-02	-.5600E-02	.1066E-01	.1321E-03	.3598E-01	.1167E-01
3.000	1.800	.571	-.3157E-02	.2392E-02	.2920E-02	-.6098E-03	-.4448E-02	-.9941E-02	.3108E-02	.3579E-01	.9320E-02
3.000	3.000	.571	.7612E-03	-.4041E-02	.1987E-02	-.1679E-02	-.1697E-02	-.7246E-02	.5846E-02	.5005E-02	.2152E-01	.6747E-02

STRESSES AND DISPLACEMENTS FOR POINTS ON FACE 7

RHO	THETA	ZETA	SIGMAR	SIGMAT	SIGMAZ	TAUTZ	TAUTR	TAURT	U	V	W	TAUOC
.625	0.000	0.000	-.8433E-02	-.3297E+00	-.9941E+00	-.1218E-11	.1210E-11	.7068E-11	-.8175E+00	-.2946E-12	.4038E+00	.4105E+00
.602	.083	0.000	-.3676E-02	-.2792E+00	-.1001E+01	-.1819E-11	.1274E-11	-.2152E-01	-.8187E+00	.7740E-01	.4207E+00	.4206E+00
.652	.077	0.000	-.3451E-01	-.3824E+00	-.1001E+01	-.1930E-11	.6137E-12	-.1618E-01	-.8060E+00	.6719E-01	.3849E+00	.4000E+00
.702	.071	0.000	-.1103E+00	-.4782E+00	-.9991E+00	-.7750E-12	.9219E-12	-.9820E-02	-.7936E+00	.5870E-01	.3498E+00	.3647E+00
.752	.067	0.000	-.2113E+00	-.5674E+00	-.9981E+00	-.1312E-11	-.7688E-13	-.3244E-02	-.7832E+00	.5162E-01	.3147E+00	.3217E+00
.802	.062	0.000	-.3211E+00	-.6494E+00	-.9999E+00	-.1235E-11	.2364E-12	.2326E-02	-.7753E+00	.4569E-01	.2781E+00	.2772E+00
.618	.245	0.000	-.1962E-01	-.2653E+00	-.1001E+01	-.7752E-12	.9046E-12	-.6301E-01	-.7768E+00	.2222E+00	.4113E+00	.4202E+00
.667	.227	0.000	-.4214E-01	-.3812E+00	-.1003E+01	-.1377E-11	.2110E-12	-.5046E-01	-.7700E+00	.1934E+00	.3757E+00	.4000E+00
.716	.211	0.000	-.1143E+00	-.4859E+00	-.1001E+01	-.1046E-11	.4920E-12	-.3098E-01	-.7623E+00	.1693E+00	.3409E+00	.3645E+00
.765	.197	0.000	-.2133E+00	-.5812E+00	-.1002E+01	-.8206E-12	.6690E-12	-.1136E-01	-.7555E+00	.1491E+00	.3059E+00	.3223E+00
.814	.185	0.000	-.3213E+00	-.6665E+00	-.1005E+01	-.2346E-11	.2217E-12	.5282E-02	-.7505E+00	.1322E+00	.2692E+00	.2793E+00
.656	.310	0.000	-.2798E-01	-.3154E+00	-.9966E+00	-.1527E-11	.8283E-12	-.7425E-01	-.7417E+00	.2663E+00	.3851E+00	.4104E+00
.650	.395	0.000	-.5.11E-01	-.2494E+00	-.1002E+01	-.1461E-11	.1431E-11	-.9636E-01	-.7003E+00	.3400E+00	.3921E+00	.4173E+00
.696	.367	0.000	-.5674E-01	-.3777E+00	-.1003E+01	-.1728E-11	.6133E-12	-.7645E-01	-.7038E+00	.2972E+00	.3569E+00	.3965E+00
.743	.343	0.000	-.1266E+00	-.4941E+00	-.9969E+00	-.1121E-11	.7435E-12	-.4833E-01	-.7041E+00	.2612E+00	.3225E+00	.3611E+00
.791	.322	0.000	-.2124E+00	-.5958E+00	-.9961E+00	-.1467E-11	.7036E-12	-.1846E-01	-.7038E+00	.2309E+00	.2875E+00	.3203E+00
.838	.303	0.000	-.3122E+00	-.6821E+00	-.9971E+00	-.1167E-11	.2988E-12	.7602E-02	-.7040E+00	.2053E+00	.2503E+00	.2800E+00
.695	.528	0.000	-.8219E-01	-.2224E+00	-.1003E+01	-.1264E-11	.1030E-11	-.1203E+00	-.6019E+00	.4212E+00	.3629E+00	.4169E+00
.738	.494	0.000	-.8196E-01	-.3781E+00	-.1003E+01	-.1576E-11	.1035E-11	-.1149E+00	-.6170E+00	.3700E+00	.3285E+00	.3931E+00
.783	.464	0.000	-.1404E+00	-.5202E+00	-.1002E+01	-.6259E-12	.9955E-12	-.6614E-01	-.6267E+00	.3265E+00	.2946E+00	.3568E+00
.828	.437	0.000	-.2256E+00	-.6335E+00	-.1002E+01	-.9297E-12	.9403E-12	-.2555E-01	-.6340E+00	.2899E+00	.2595E+00	.3179E+00
.742	.569	0.000	-.7941E-01	-.2918E+00	-.9969E+00	-.1276E-11	.4685E-12	-.1318E+00	-.5596E+00	.4194E+00	.3272E+00	.4064E+00
.750	.644	0.000	-.1185E+00	-.1871E+00	-.1003E+01	-.1109E-11	.1238E-11	-.1385E+00	-.4920E+00	.4636E+00	.3228E+00	.4174E+00
.791	.606	0.000	-.1.56E+00	-.3891E+00	-.9995E+00	-.1511E-11	.7371E-12	-.1209E+00	-.5186E+00	.4081E+00	.2890E+00	.3858E+00
.832	.571	0.000	-.1066E+00	-.5592E+00	-.1001E+01	-.2507E-11	-.1889E-12	-.7345E-01	-.5377E+00	.3615E+00	.2555E+00	.3462E+00
.800	.675	0.000	-.1234E+00	-.2884E+00	-.9980E+00	-.9994E-12	.8673E-12	-.1414E+00	-.4529E+00	.4412E+00	.2811E+00	.3975E+00
.840	.638	0.000	-.1514E+00	-.4971E+00	-.9955E+00	-.2173E-11	-.8034E-13	-.9813E-01	-.4800E+00	.3900E+00	.2479E+00	.3556E+00
.814	.742	0.000	-.1568E+00	-.1711E+00	-.1005E+01	-.8436E-12	.1023E-11	-.1526E+00	-.3796E+00	.4685E+00	.2698E+00	.4154E+00
.851	.702	0.000	-.1526E+00	-.4266E+00	-.9987E+00	-.4156E-12	.8339E-12	-.1260E+00	-.4163E+00	.4127E+00	.2365E+00	.3678E+00
.866	.765	0.000	-.1569E+00	-.3126E+00	-.1005E+01	-.6721E-12	.8956E-12	-.1499E+00	-.3467E+00	.4293E+00	.2207E+00	.3884E+00
.885	.825	0.000	-.1647E+00	-.1192E+00	-.1006E+01	-.7869E-12	.8374E-12	-.1409E+00	-.2688E+00	.4401E+00	.1993E+00	.4235E+00
.941	.879	0.000	-.1019E+00	-.5654E-01	-.1016E+01	-.2153E-12	.1426E-11	-.8673E-01	-.1862E+00	.3990E+00	.1298E+00	.4475E+00
.980	.912	0.000	-.5598E+00	-.3207E+00	-.1226E+01	-.1698E-11	-.7996E-12	.2639E+00	-.1182E+00	.3550E+00	.6557E-01	.4394E+00
.850	.063	0.000	-.4219E+00	-.7199E+00	-.9983E+00	-.1135E-11	.6712E-12	.6511E-02	-.7703E+00	.4330E-01	.2394E+00	.2354E+00
.900	.063	0.000	-.5195E+00	-.7875E+00	-.9971E+00	-.1469E-11	.8416E-12	.9455E-02	-.7673E+00	.4088E-01	.1934E+00	.1956E+00
.900	.188	0.000	-.4869E+00	-.7864E+00	-.1003E+01	-.7389E-12	.8673E-12	.2587E-01	-.7415E+00	.1208E+00	.1941E+00	.2127E+00
.900	.313	0.000	-.417.E+00	-.7685E+00	-.9953E+00	-.1211E-11	.6090E-12	.3159E-01	-.6917E+00	.1955E+00	.1947E+00	.2393E+00
.900	.438	0.000	-.3465E+00	-.7591E+00	-.1003E+01	-.1113E-11	.6799E-12	.1773E-01	-.6207E+00	.2623E+00	.1955E+00	.2713E+00
.900	.563	0.000	-.2761E+00	-.7201E+00	-.9989E+00	-.1634E-11	.2913E-12	-.1222E-01	-.5310E+00	.3194E+00	.1949E+00	.2978E+00
.900	.688	0.000	-.2244E+00	-.6306E+00	-.1001E+01	-.1159E-11	.3093E-12	-.6461E-01	-.4220E+00	.3682E+00	.1919E+00	.3216E+00
.920	.813	0.000	-.1616E+00	-.4076E+00	-.9927E+00	-.6003E-12	.9501E-12	-.1081E+00	-.2825E+00	.3948E+00	.1622E+00	.3530E+00
.940	0.000	0.000	-.5972E+00	-.8436E+00	-.9985E+00	-.6732E-12	-.6531E-12	.5396E-11	-.7705E+00	.1472E-11	.1483E+00	.1651E+00
.940	.125	0.000	-.5801E+00	-.8434E+00	-.1003E+01	-.2.72E-11	.2853E-13	.2151E-01	-.7570E+00	.7741E-01	.1487E+00	.1751E+00
.940	.250	0.000	-.5212E+00	-.8252E+00	-.9980E+00	-.1357E-11	-.2660E-12	.3911E-01	-.7173E+00	.1513E+00	.1494E+00	.1997E+00
.940	.375	0.000	-.4478E+00	-.8159E+00	-.1001E+01	-.2734E-11	-.1013E-11	.4184E-01	-.6544E+00	.2182E+00	.1504E+00	.2325E+00
.940	.500	0.000	-.3705E+00	-.8016E+00	-.1001E+01	-.2822E-11	-.4663E-12	.2833E-01	-.5719E+00	.2752E+00	.1508E+00	.2639E+00
.940	.625	0.000	-.3124E+00	-.7691E+00	-.9967E+00	-.1548E-11	.3382E-12	.2217E-02	-.4720E+00	.3214E+00	.1495E+00	.2846E+00
.940	.813	0.000	-.2111E+00	-.5316E+00	-.9776E+00	-.2219E-11	-.6092E-12	-.6893E-01	-.2801E+00	.3745E+00	.1390E+00	.3193E+00
.970	.063	0.000	-.6396E+00	-.8767E+00	-.1001E+01	-.2501E-11	.5055E-12	.1104E-01	-.7681E+00	.3743E-01	.1040E+00	.1505E+00
.970	.188	0.000	-.5996E+00	-.8673E+00	-.1000E+01	-.2304E-11	.8520E-12	.3336E-01	-.7403E+00	.1106E+00	.1046E+00	.1690E+00

STRESSES AND DISPLACEMENTS FOR POINTS ON FACE 7 (P2)

.970	.313	0.000	-.5293E+00	-.8577E+00	-.9982E+00	-.2291E-11	.2280E-12	.4770E-01	-.6870E+00	.1786E+00	.1054E+00	.1996E+00
.970	.438	0.000	-.4545E+00	-.8454E+00	-.1005E+01	-.8379E-12	.1879E-12	.4801E-01	-.6122E+00	.2378E+00	.1063E+00	.2346E+00
.970	.563	0.000	-.3786E+00	-.8238E+00	-.9927E+00	-.1886E-11	.9656E-13	.3495E-01	-.5196E+00	.2859E+00	.1061E+00	.2605E+00
.970	.688	0.000	-.3561E+00	-.8161E+00	-.1015E+01	-.1685E-11	-.9181E-13	.1775E-01	-.4102E+00	.3220E+00	.1046E+00	.2745E+00
.970	.844	0.000	-.2640E+00	-.8421E+00	-.9819E+00	-.9476E-12	.3203E-12	-.1161E-01	-.2367E+00	.3525E+00	.9434E-01	.2931E+00
.980	.031	0.000	-.6545E+00	-.8938E+00	-.9989E+00	-.9747E-12	.4227E-12	.5416E-02	-.7712E+00	.1848E-01	.8458E-01	.1439E+00
.980	.156	0.000	-.6259E+00	-.8826E+00	-.1011E+01	-.1511E-11	.1196E-11	.2796E-01	-.7501E+00	.9135E-01	.8504E-01	.1581E+00
.980	.261	0.000	-.5606E+00	-.8632E+00	-.9963E+00	-.1877E-11	.4034E-12	.4607E-01	-.7024E+00	.1601E+00	.8570E-01	.1863E+00
.980	.406	0.000	-.4674E+00	-.8566E+00	-.1004E+01	-.5043E-12	-.6054E-12	.5155E-01	-.6319E+00	.2209E+00	.8659E-01	.2215E+00
.980	.531	0.000	-.4091E+00	-.8454E+00	-.9958E+00	-.1567E-11	-.3427E-12	.4415E-01	-.5431E+00	.2708E+00	.8671E-01	.2508E+00
.980	.656	0.000	-.3752E+00	-.8333E+00	-.1004E+01	-.6408E-12	.1082E-11	.2879E-01	-.4379E+00	.3086E+00	.8594E-01	.2665E+00
.980	.781	0.000	-.3538E+00	-.7983E+00	-.9963E+00	-.2143E-11	-.3785E-12	.3548E-01	-.3121E+00	.3340E+00	.8188E-01	.2702E+00
.980	.875	0.000	-.2546E+00	-.6641E+00	-.1012E+01	-.1759E-11	-.2634E-12	.1538E-01	-.1910E+00	.3471E+00	.7311E-01	.3096E+00
.990	0.000	0.000	-.6662E+00	-.9025E+00	-.9974E+00	-.1163E-11	.4866E-12	.2855E-11	-.7727E+00	.1432E-11	.5956E-01	.1393E+00
.990	.094	0.000	-.6571E+00	-.9022E+00	-.1006E+01	-.1184E-11	.1476E-11	.1603E-01	-.7647E+00	.5443E-01	.5973E-01	.1446E+00
.990	.219	0.000	-.6092E+00	-.8335E+00	-.9986E+00	-.9494E-12	.8464E-13	.3826E-01	-.7295E+00	.1247E+00	.6018E-01	.1662E+00
.990	.344	0.000	-.5366E+00	-.8674E+00	-.9996E+00	-.7254E-12	-.1164E-12	.5126E-01	-.6693E+00	.1892E+00	.6081E-01	.1991E+00
.990	.469	0.000	-.4597E+00	-.8589E+00	-.1002E+01	-.3213E-11	-.5371E-12	.5288E-01	-.5865E+00	.2437E+00	.6132E-01	.2334E+00
.990	.594	0.000	-.4015E+00	-.8468E+00	-.9981E+00	-.3386E-11	-.6980E-12	.4111E-01	-.4911E+00	.2866E+00	.6114E-01	.2554E+00
.990	.719	0.000	-.3843E+00	-.8411E+00	-.1002E+01	-.1878E-11	-.1260E-12	.4065E-01	-.3770E+00	.3167E+00	.5986E-01	.2637E+00
.990	.844	0.000	-.3836E+00	-.8180E+00	-.1015E+01	-.1544E-11	-.7400E-12	.7172E-01	-.2350E+00	.3338E+00	.5456E-01	.2702E+00

COMMENTS ON USE OF FRAC3D

The report to which this manual is a supplement discusses several aspects of the accuracy of the program FRAC3D. It is observed there that the formulas underlying the program seem dependable, as do the parts of the program that have been used for finding load constants, stress intensity factors, and crack opening displacements for plates or bars with cracks perpendicular to the front face and loaded normally or obliquely. The program needs checking where it combined displacements from crack and surface loads. It may be possible that some errors persist in still unused parts, such as those relating to obliquity of the crack, but the program probably must be used in new kinds of calculations in order to reveal any such errors.

The time consumed by a calculation depends greatly on the amount of detail put into the calculation. It is possible, however, to estimate the central processor time required by considering LATTICE, FRAC3D, and MATSOL separately. The part done by LATTICE usually is brief. Thus, using the CDC Cyber 73 at Battelle's Columbus Laboratories, a run of LATTICE to get the latticework shown in the above illustrative example would require about 23 CP seconds. The time used by FRAC3D varies roughly in proportion to the product of the total number of lattice points (for both faces) times the number of boundary condition points used. In the illustrative example, there were 486 lattice points (that is 305 + 181), and there were 175 boundary condition points (that is 68 for the front, 36 for the back and 71 for the crack), and the time used by FRAC3D in assembling the matrix was 700 CP seconds. The time required by MATSOL varies roughly as the cube of the number of unknown load constants. In the illustrative example there were 303 load constants, and solving for them required 455 CP seconds. It may be added that there are probably several improvements which could speed these calculations substantially, but they have not been pursued yet because the main thrust of the investigation has been related to getting dependability in the results rather than speed.

Attainment of dependability in results computed by FRAC3D is closely tied to the way the user designs the calculations to be made. Some of the elements of good design are built into the illustrative example provided here, such as deletion of odd values of m when treating a crack that is less than semicircular, and putting emphasis on the latticework on the front face. (Even when back surface effects were being sought, the design of front-face latticework seemed more critical than that for the back face.) The many cases discussed in the accompanying report [2] illustrate more principles of good design for the calculations and also show the importance of extensive checking of non-fitted boundary conditions, since unchecked results can easily be poor. It is not to be thought that this situation reflects any unique weakness of FRAC3D; it is quite likely that parallel problems exist in most calculations in which solutions of two basic kinds (e.g. crack and surface analyses) are merged by fitting at discrete points. Problems of this sort probably characterize the current state of the art in fracture analysis.

REFERENCES

[1] Bell, J. C., "Analytical Methods for Improved Fracture Analysis", Technical Report AFFDL-TR-75-67, prepared for Air Force Flight Dynamics Laboratory, August 30, 1975. (Contract No. F33615-72-C-1739)

[2] Bell, J. C., "Stress Analysis for Structures with Surface Cracks", NASA CR159400, Report to NASA-Lewis Research Center, from Battelle's Columbus Laboratories under Contract No. NAS3-21020, 1978.

[3] Bell, J. C., "Stresses from Variously Loaded Circular Cracks", Journal of the Structural Division of the ASCE., Vol. 103, No. St 2, pp 355-376.

[4] Bell, J. C., "Stress from Arbitrary Loads on a Circular Crack", International Journal of Fracture, Vol. 15, No. 1, February 1979.

[5] Muki, R., "Asymmetric Problems of the Theory of Elasticity for a Semi-Infinite Solid and a Thick Plate", Progress in Solid Mechanics, Vol. I, edited by I. N. Sneddon and R. Hill, North Holland Publishers, Amsterdam, 1960. (Interscience Publishers, Inc., New York).

APPENDIX A

THEORETICAL BACKGROUND OF FRAC3D

Overall Plan for Analysis

The purpose for Program FRAC3D is to analyse three-dimensional stress fields around a crack with a circular front situated in a body which may have up to six plane faces. The crack may be wholly or only partly within the body, so that surface cracks may be treated, and much flexibility is to be allowed in the orientation of the crack and in the kind of loads applied to it and to the faces of the body.

The analysis is based on a merger of one for stresses around are arbitrarily loaded circular crack in an infinite body, and on one for stresses due to arbitrarily distributed loads on the surface of a half space. Analyses of these two kinds, described in terms of arbitrary load constants, are to be merged by choosing load constants so that appropriate boundary conditions are satisfied on the relevant crack and body surfaces. The merger is to be accomplished by the boundary point least squares technique. Thus one goal in using FRAC3D is to assemble equations for imposing boundary conditions at chosen points sampling all the appropriate surfaces. The least squares solution of these equations is to be performed by the auxiliary program MATSOL, which solves for the load constants and uses them at once to compute stress intensity factors. The evaluation of stress components at any point closely resembles the construction of the boundary condition equations, so it is to be accomplished by returning to FRAC3D after MATSOL has evaluated the appropriate load constants.

A discussion of the principle equations used in these calculations follows. Fuller explanation of their derivations are given in References 1 and 4.

Stresses Around a Loaded Circular Crack in an Infinite Body

Since it is planned that the stresses in a cracked, finite body will be analyzed by merger of separate analyses of stresses from crack loads and from body-surface loads, one may begin by considering a crack in an infinite body. A form of crack which is particularly desirable for study is the circular crack, which is genuinely three-dimensional and for which much analysis is possible because of the abundance of mathematical theory relating to geometries that are basically circular. Therefore, this research began by considering stresses around a circular (penny-shaped) crack in an infinite body. The loads to be applied to it in the analysis are those which the body would transmit there if there were no crack, but which can not be transmitted across the crack, so that they are in effect the crack's addition to the loads on the body. In consideration of the eventual merger with effects from fairly arbitrary effects from body-surface loads, it is desirable to consider crack loads which are as general as possible. Therefore, the crack loads to be considered here embrace all that can be transmitted across a circular, plane section of a body, namely arbitrary distributions of normal loads and tangential loads in two directions.

A beginning for the present analysis was found in Muki's treatment [5] of stresses in a half space subjected to normal and tangential forces arbitrarily distributed over a circular section of its surface. Proceeding from this foundation, two half spaces were considered, being joined continuously everywhere except over a circular section of their interface, and with equal distributions of three load components applied to each half space on that circular section. Since Muki's analysis was performed by expressing the load distributions by Fourier series and manipulating conditions implied for each term by use of Hankel transformations, this new analysis soon required the solution of many systems of integral equations with Bessel functions inside the integrals. Fortunately it was found possible to solve these systems analytically, as is shown References 1 and 4. The final formulas found for the stresses and displacements are reasonably compact, though they do make free use of integrals of a seemingly formidable type. The discussion that follows first shows the stress and displacement formulas, and then it shows means to make those integrals efficiently calculable.

Formulas for Stresses Associated with the Crack

The analysis outlined above showed that all the stresses and displacements around an arbitrarily loaded circular crack in an infinite body can be expressed as simple combinations of integrals of the form

$$I^{n'}_{M,N}(\rho,\zeta) = \int_0^\infty e^{-\xi|\zeta|}\xi^{n'-1/2}J_M(\rho\xi)J_{N+1/2}(\xi)d\xi \quad . \tag{1}$$

Here cylindrical coordinates (r,θ,z) are used, the crack lies in the region where $r \leq a$ and $z = 0$, and $\rho = r/a$, $\zeta = z/a$. In order to organize the expressions that have been found for the stresses and displacements around the circular crack for computing, it is desirable to introduce several sets of auxiliary functions. In doing this, allowance for the appearance of negative as well as positive values of the axial coordinate ζ is made through use of the notation

$$\epsilon = \zeta/|\zeta| \tag{2}$$

Letting ν be Poisson's ratio, the first set of auxiliary functions is

$$\left.\begin{aligned}
U_{m,k,1}(\rho,\zeta) &= -\frac{1}{2}\left[(1-2\nu)I^0_{m+1,m+2k+1} - |\zeta|I^1_{m+1,m+2k+1}\right] \text{ for } k \geq 0 \ , \\
U_{m,k,2}(\rho,\zeta) &= \frac{\epsilon}{2}\left[(2-\nu)I^0_{m+1,m+2k+2} - \frac{|\zeta|}{2}I^1_{m+1,m+2k+2}\right] \text{ for } k \geq 0 \ , \\
U_{m,k,3}(\rho,\zeta) &= \begin{cases} -\frac{\zeta}{2(2-\nu)}I^1_{m+1,m} & \text{for } k = 0 \\ -\frac{\epsilon}{2}\left[\nu I^0_{m+1,m+2k} + \frac{|\zeta|}{2}I^1_{m+1,m+2k}\right] & \text{for } k \geq 1 \end{cases} ; \\
V_{m,k,1}(\rho,\zeta) &= -\frac{1}{2}\left[(1-2\nu)I^0_{m-1,m+2k+1} - |\zeta|I^1_{m-1,m+2k+1}\right] \quad \text{for } k \geq 0 \ , \\
V_{m,k,2}(\rho,\zeta) &= -\frac{\epsilon}{2}\left[\nu I^0_{m-1,m+2k+2} + \frac{|\zeta|}{2}I^1_{m-1,m+2k+2}\right] \quad \text{for } k \geq 0, \\
V_{m,k,3}(\rho,\zeta) &= \begin{cases} \frac{\epsilon}{2-\nu}\left[2(1-\nu)I^0_{m-1,m} - \frac{|\zeta|}{2}I^1_{m-1,m}\right] & \text{for } k = 0 \\ \frac{\epsilon}{2}\left[(2-\nu)I^0_{m-1,m+2k} - \frac{|\zeta|}{2}I^1_{m-1,m+2k}\right] & \text{for } k \geq 1 \end{cases} .
\end{aligned}\right\} \tag{3}$$

Then the following functions appear in the expressions for the displacements.

$$
\left.
\begin{aligned}
F^{u}_{m,k,1}(\rho,\zeta) &= \tfrac{1}{2}\,[U_{m,k,1}-V_{m,k,1}] && \text{for } k \geq 0\ ,\\
F^{u}_{m,k,2}(\rho,\zeta) &= \tfrac{1}{2}\,[U_{m,k,2}-V_{m,k,2}] && \text{for } k \geq 0\ ,\\
F^{u}_{m,k,3}(\rho,\zeta) &= \tfrac{1}{2}\,[U_{m,k,3}-V_{m,k,3}] && \text{for } k \geq 0\ ,\\
F^{v}_{m,k,1}(\rho,\zeta) &= \tfrac{1}{2}\,[U_{m,k,1}+V_{m,k,1}] && \text{for } k \geq 0\ ,\\
F^{v}_{m,k,2}(\rho,\zeta) &= \tfrac{1}{2}\,[U_{m,k,2}+V_{m,k,2}] && \text{for } k \geq 0\ ,\\
F^{v}_{m,k,3}(\rho,\zeta) &= \tfrac{1}{2}\,[U_{m,k,3}+V_{m,k,3}] && \text{for } k \geq 0\ ,\\
F^{w}_{m,k,1}(\rho,\zeta) &= \tfrac{\epsilon}{2}\left[2(1-\nu)I^{o}_{m,m+2k+1}+|\zeta|I^{1}_{m,m+2k+1}\right] && \text{for } k \geq 0\ ,\\
F^{w}_{m,k,2}(\rho,\zeta) &= -\tfrac{1}{4}\left[(1-2\nu)I^{o}_{m,m+2k+2}+|\zeta|I^{1}_{m,m+2k+2}\right] && \text{for } k \geq 0\ ,\\
F^{w}_{m,k,3}(\rho,\zeta) &= \begin{cases} -\dfrac{1}{2(2-\nu)}\left[(1-2\nu)I^{o}_{m,m}+|\zeta|I^{1}_{m,m}\right] & \text{for } k = 0 \\ -\tfrac{1}{4}\left[(1-2\nu)I^{o}_{m,m+2k}+|\zeta|I^{1}_{m,m+2k}\right] & \text{for } k \geq 1 \end{cases} .
\end{aligned}
\right\} \quad (4)
$$

The following functions appear in the expressions for stresses.

$$
\left.
\begin{aligned}
F^{rr}_{m,k,1}(\rho,\zeta) &= -[I^1_{m,m+2k+1}-|\zeta| I^2_{m,m+2k+1}]-\frac{m+1}{\rho}U_{m,k,1}-\frac{m-1}{\rho}V_{m,k,1} && \text{for } k \geq 0\ ,\\
F^{rr}_{m,k,2}(\rho,\zeta) &= \epsilon[I^1_{m,m+2k+2}-\frac{|\zeta|}{2}I^2_{m,m+2k+2}]-\frac{m+1}{\rho}U_{m,k,2}-\frac{m-1}{\rho}V_{m,k,2} && \text{for } k \geq 0\ ,\\
F^{rr}_{m,k,3}(\rho,\zeta) &= \begin{cases}\frac{2\epsilon}{2-\nu}[I^1_{m,m}-\frac{|\zeta|}{2}I^2_{m,m}]-\frac{m+1}{\rho}U_{m,o,3}-\frac{m-1}{\rho}V_{m,o,3} & \text{for } k=0\\ \epsilon[I^1_{m,m+2k}-\frac{|\zeta|}{2}I^2_{m,m+2k}]-\frac{m+1}{\rho}U_{m,k,3}-\frac{m-1}{\rho}V_{m,k,3} & \text{for } k\geq 1\end{cases};\\
F^{\theta\theta}_{m,k,1}(\rho,\zeta) &= -2\nu I^1_{m,m+2k+1}+\frac{m+1}{\rho}U_{m,k,1}+\frac{m-1}{\rho}V_{m,k,1} && \text{for } k \geq 0\ ,\\
F^{\theta\theta}_{m,k,2}(\rho,\zeta) &= \epsilon\nu I^1_{m,m+2k+2}+\frac{m+1}{\rho}U_{m,k,2}+\frac{m-1}{\rho}V_{m,k,2} && \text{for } k \geq 0\ ,\\
F^{\theta\theta}_{m,k,3}(\rho,\zeta) &= \begin{cases}\frac{2\epsilon\nu}{2-\nu}I^1_{m,m}+\frac{m+1}{\rho}U_{m,o,3}+\frac{m-1}{\rho}V_{m,o,3} & \text{for } k=0\\ \epsilon\nu I^1_{m,m+2k}+\frac{m+1}{\rho}U_{m,k,3}+\frac{m-1}{\rho}V_{m,k,3} & \text{for } k\geq 1\end{cases};\\
F^{zz}_{m,k,1}(\rho,\zeta) &= -[I^1_{m,m+2k+1}+|\zeta| I^2_{m,m+2k+1}] && \text{for } k \geq 0\ ,\\
F^{zz}_{m,k,2}(\rho,\zeta) &= \frac{\zeta}{2}I^2_{m,m+2k+2} && \text{for } k \geq 0\ ,\\
F^{zz}_{m,k,3}(\rho,\zeta) &= \begin{cases}\frac{\zeta}{2-\nu}I^2_{m,m} & \text{for } k=0\\ \frac{\zeta}{2}I^2_{m,m+2k} & \text{for } k\geq 1\end{cases};\\
F^{\theta z}_{m,k,1}(\rho,\zeta) &= -\frac{\zeta}{2}[I^2_{m+1,m+2k+1}+I^2_{m-1,m+2k+1}] && \text{for } k \geq 0\ ,\\
F^{\theta z}_{m,k,2}(\rho,\zeta) &= -\frac{1}{2}[I^1_{m+1,m+2k+2}-\frac{|\zeta|}{2}(I^2_{m+1,m+2k+2}+I^2_{m-1,m+2k+2})] && \text{for } k \geq 0\ ,\\
F^{\theta z}_{m,k,3}(\rho,\zeta) &= \begin{cases}-\frac{1}{2-\nu}[I^1_{m-1,m}-\frac{|\zeta|}{2}(I^2_{m+1,m}+I^2_{m-1,m})]-\frac{\nu}{2(2-\nu)}(I^1_{m+1,m}-I^1_{m-1,m}) & \text{for } k=0\\ -\frac{1}{2}[I^1_{m-1,m+2k}-\frac{|\zeta|}{2}(I^2_{m+1,m+2k}+I^2_{m-1,m+2k})] & \text{for } k\geq 1\end{cases};\\
F^{zr}_{m,k,1}(\rho,\zeta) &= -\frac{\zeta}{2}[I^2_{m+1,m+2k+1}-I^2_{m-1,m+2k+1}] && \text{for } k \geq 0,\\
F^{zr}_{m,k,2}(\rho,\zeta) &= -\frac{1}{2}[I^1_{m+1,m+2k+2}-\frac{|\zeta|}{2}(I^2_{m+1,m+2k+2}-I^2_{m-1,m+2k+2})] && \text{for } k > 0\ ,\\
F^{zr}_{m,k,3}(\rho,\zeta) &= \begin{cases}\frac{1}{2-\nu}[I^1_{m-1,m}+\frac{|\zeta|}{2}(I^2_{m+1,m}-I^2_{m-1,m})]-\frac{\nu}{2(2-\nu)}(I^1_{m+1,m}+I^1_{m-1,m}) & \text{for } k=0\\ \frac{1}{2}[I^1_{m-1,m+2k}+\frac{|\zeta|}{2}(I^2_{m+1,m+2k}-I^2_{m-1,m+2k})] & \text{for } k\geq 1\end{cases};\\
F^{r\theta}_{m,k,1}(\rho,\zeta) &= -\frac{m+1}{\rho}U_{m,k,1}+\frac{m-1}{\rho}V_{m,k,1} && \text{for } k \geq 0\ ,\\
F^{r\theta}_{m,k,2}(\rho,\zeta) &= \frac{\epsilon}{2}I^1_{m,m+2k+2}-\frac{m+1}{\rho}U_{m,k,2}+\frac{m-1}{\rho}V_{m,k,2} && \text{for } k \geq 0\ ,\\
F^{r\theta}_{m,k,3}(\rho,\zeta) &= \begin{cases}-\frac{\epsilon(1-\nu)}{2-\nu}I^1_{m,m}-\frac{m+1}{\rho}U_{m,o,3}+\frac{m-1}{\rho}V_{m,o,3} & \text{for } k=0\\ -\frac{\epsilon}{2}I^1_{m,m+2k}-\frac{m+1}{\rho}U_{m,k,3}+\frac{m-1}{\rho}V_{m,k,3} & \text{for } k\geq 1\end{cases}.
\end{aligned}
\right\} \qquad (5)
$$

Using the above functions of ρ and ζ, and letting a be the crack radius and μ the shear modulus*, the expressions for displacements and stresses given in the cited report, after extension to include antisymmetric as well as symmetric loads, become:

$$
\left.
\begin{aligned}
u &= a\sum_{m=0}^{\infty}\sum_{k=0}^{\infty}\left\{\left[\alpha'_{m,k}F^{u}_{m,k,1}+\beta'_{m,k}F^{u}_{m,k,2}+\gamma'_{m,k}F^{u}_{m,k,3}\right]\cos m\theta\right. \\
&\quad \left.-\left[\hat{\alpha}'_{m,k}F^{u}_{m,k,1}+\hat{\beta}'_{m,k}F^{u}_{m,k,2}+\hat{\gamma}'_{m,k}F^{u}_{m,k,3}\right]\sin m\theta\right\} , \\
v &= a\sum_{m=0}^{\infty}\sum_{k=0}^{\infty}\left\{\left[\alpha'_{m,k}F^{v}_{m,k,1}+\beta'_{m,k}F^{v}_{m,k,2}+\gamma'_{m,k}F^{v}_{m,k,3}\right]\sin m\theta\right. \\
&\quad \left.+\left[\hat{\alpha}'_{m,k}F^{v}_{m,k,1}+\hat{\beta}'_{m,k}F^{v}_{m,k,2}+\hat{\gamma}'_{m,k}F^{v}_{m,k,3}\right]\cos m\theta\right\} , \\
w &= a\sum_{m=0}^{\infty}\sum_{k=0}^{\infty}\left\{\left[\alpha'_{m,k}F^{w}_{m,k,1}+\beta'_{m,k}F^{w}_{m,k,2}+\gamma'_{m,k}F^{w}_{m,k,3}\right]\cos m\theta\right. \\
&\quad \left.-\left[\hat{\alpha}'_{m,k}F^{w}_{m,k,1}+\hat{\beta}'_{m,k}F^{w}_{m,k,2}+\hat{\gamma}'_{m,k}F^{w}_{m,k,3}\right]\sin m\theta\right\} ; \\
\sigma_r &= \mu\sum_{m=0}^{\infty}\sum_{k=0}^{\infty}\left\{\left[\alpha'_{m,k}F^{rr}_{m,k,1}+\beta'_{m,k}F^{rr}_{m,k,2}+\gamma'_{m,k}F^{rr}_{m,k,3}\right]\cos m\theta\right. \\
&\quad \left.-\left[\hat{\alpha}'_{m,k}F^{rr}_{m,k,1}+\hat{\beta}'_{m,k}F^{rr}_{m,k,2}+\hat{\gamma}'_{m,k}F^{rr}_{m,k,3}\right]\sin m\theta\right\} , \\
\sigma_\theta &= \mu\sum_{m=0}^{\infty}\sum_{k=0}^{\infty}\left\{\left[\alpha'_{m,k}F^{\theta\theta}_{m,k,1}+\beta'_{m,k}F^{\theta\theta}_{m,k,2}+\gamma'_{m,k}F^{\theta\theta}_{m,k,3}\right]\cos m\theta\right. \\
&\quad \left.-\left[\hat{\alpha}'_{m,k}F^{\theta\theta}_{m,k,1}+\hat{\beta}'_{m,k}F^{\theta\theta}_{m,k,2}+\hat{\gamma}'_{m,k}F^{\theta\theta}_{m,k,3}\right]\sin m\theta\right\} , \\
\sigma_z &= \mu\sum_{m=0}^{\infty}\sum_{k=0}^{\infty}\left\{\left[\alpha'_{m,k}F^{zz}_{m,k,1}+\beta'_{m,k}F^{zz}_{m,k,2}+\gamma'_{m,k}F^{zz}_{m,k,3}\right]\cos m\theta\right. \\
&\quad \left.-\left[\hat{\alpha}'_{m,k}F^{zz}_{m,k,1}+\hat{\beta}'_{m,k}F^{zz}_{m,k,2}+\hat{\gamma}'_{m,k}F^{zz}_{m,k,3}\right]\sin m\theta\right\} , \\
\tau_{\theta z} &= \mu\sum_{m=0}^{\infty'}\sum_{k=0}^{\infty}\left\{\left[\alpha'_{m,k}F^{\theta z}_{m,k,1}+\beta'_{m,k}F^{\theta z}_{m,k,2}+\gamma'_{m,k}F^{\theta z}_{m,k,3}\right]\sin m\theta\right. \\
&\quad \left.+\left[\hat{\alpha}'_{m,k}F^{\theta z}_{m,k,1}+\hat{\beta}'_{m,k}F^{\theta z}_{m,k,2}+\hat{\gamma}'_{m,k}F^{\theta z}_{m,k,3}\right]\cos m\theta\right\} , \\
\tau_{zr} &= \mu\sum_{m=0}^{\infty}\sum_{k=0}^{\infty}\left\{\left[\alpha'_{m,k}F^{zr}_{m,k,1}+\beta'_{m,k}F^{zr}_{m,k,2}+\gamma'_{m,k}F^{zr}_{m,k,3}\right]\cos m\theta\right. \\
&\quad \left.-\left[\hat{\alpha}'_{m,k}F^{zr}_{m,k,1}+\hat{\beta}'_{m,k}F^{zr}_{m,k,2}+\hat{\gamma}'_{m,k}F^{zr}_{m,k,3}\right]\sin m\theta\right\} , \\
\tau_{r\theta} &= \mu\sum_{m=0}^{\infty}\sum_{k=0}^{\infty}\left\{\left[\alpha'_{m,k}F^{r\theta}_{m,k,1}+\beta'_{m,k}F^{r\theta}_{m,k,2}+\gamma'_{m,k}F^{r\theta}_{m,k,3}\right]\sin m\theta\right. \\
&\quad \left.+\left[\alpha'_{m,k}F^{r\theta}_{m,k,1}+\beta'_{m,k}F^{r\theta}_{m,k,2}+\gamma'_{m,k}F^{r\theta}_{m,k,3}\right]\cos m\theta\right\} .
\end{aligned}
\right\} \qquad (6)
$$

* Note that $\mu = E/[2(1+\nu)]$, where E is Young's modulus and ν is Poisson's ratio.

It may be noted that several indeterminacies may arise in the Equations (5) for points along the axis where $\rho = 0$, namely in the ratios $U_{m,k,i}/\rho$ and $V_{m,k,i}/\rho$. These indeterminacies can be resolved readily by l'Hospital's rule, using the relation,

$$\frac{\partial}{\partial \rho} I^{n'}_{M,N} = \frac{1}{2}\left[I^{n'+1}_{M-1,N} - I^{n'+1}_{M+1,N}\right] \tag{7}$$

which follows from a recursion formula for Bessel functions. In particular, one finds that

$$\lim_{\rho \to 0}\left[\frac{m+1}{\rho} U_{m,k,i}\right] = 0 \qquad \text{for } i = 1,2,3, \text{ if } m \neq 0\ , \tag{8a}$$

but if $m = 0$ then

$$\lim_{\rho \to 0}\left[\frac{m+1}{\rho} U_{m,k,1}\right] = -\frac{1}{4}\left[(1-2\nu) I^{1}_{0,2k+1}(0,\zeta) - |\zeta| I^{2}_{0,2k+1}(0,\zeta)\right]\ ,$$

$$\lim_{\rho \to 0}\left[\frac{m+1}{\rho} U_{m,k,2}\right] = \frac{\epsilon}{4}\left[(2-\nu) I^{1}_{0,2k+2}(0,\zeta) - \frac{|\zeta|}{2} I^{2}_{0,2k+2}(0,\zeta)\right]\ , \tag{8b}$$

$$\lim_{\rho \to 0}\left[\frac{m+1}{\rho} U_{m,k,3}\right] = \begin{cases} -\dfrac{\zeta}{4(2-\nu)} I^{2}_{0,0}(0,\zeta) & \text{for } k = 0 \\ -\dfrac{\epsilon}{4}\left[\nu I^{1}_{0,2k}(0,\zeta) + \dfrac{|\zeta|}{2} I^{2}_{0,2k}(0,\zeta)\right] & \text{for } k \geq 1 \end{cases}\ .$$

Again, one finds that

$$\lim_{\rho \to 0}\left[\frac{m-1}{\rho} V_{m,k,i}\right] = 0 \qquad \text{for } i = 1,2,3 \qquad \text{if } m \neq 0 \text{ or } 2\ , \tag{9a}$$

but if $m = 0$ or 2, then

$$\lim_{\rho\to 0}\left[\frac{m-1}{\rho}\, V_{m,k,1}\right] = -\frac{1}{4}\left[(1-2\nu) I^1_{0,m+2k+1}(0,\zeta) - |\zeta| I^2_{0,m+2k+1}(0,\zeta)\right],$$

$$\lim_{\rho\to 0}\left[\frac{m-1}{\rho}\, V_{m,k,2}\right] = -\frac{\varepsilon}{4}\left[\nu I^1_{0,m+2k+2}(0,\zeta) + \frac{|\zeta|}{2}\, I^2_{0,m+2k+2}(0,\zeta)\right], \tag{9b}$$

$$\lim_{\rho\to 0}\left[\frac{m-1}{\rho}\, V_{m,k,3}\right] = \begin{cases} \dfrac{\varepsilon}{2(2-\nu)}\left[2(1-\nu) I^1_{0,m}(0,\zeta) - \dfrac{|\zeta|}{2}\, I^2_{0,m}(0,\zeta)\right] & \text{for } k = 0 \\ \dfrac{\varepsilon}{4}\left[(2-\nu) I^1_{0,m+2k}(0,\zeta) - \dfrac{|\zeta|}{2}\, I^2_{0,m+2k}(0,\zeta)\right] & \text{for } k \geq 1 \end{cases}.$$

These expressions can replace the indeterminate expressions in the Equations (5) for $\rho = 0$.

In the Equations (6), the coefficients $\alpha'_{m,k}$, $\beta'_{m,k}$, $\gamma'_{m,k}$, $\hat{\alpha}'_{m,k}$, $\hat{\beta}'_{m,k}$, and $\hat{\gamma}'_{m,k}$ are weighted sums of earlier constants first introduced as coefficients of Fourier-Bessel expansions for the load distributions on the crack. Those earlier constants (called $\alpha_{m,n}$, $\beta_{m,n}$, and so forth) were arbitrary since they were introduced to describe arbitrary load distributions, so the newer constants ($\alpha'_{m,k}$, $\beta'_{m,k}$, and so forth) are also almost all arbitrary. An exception to arbitrariness for them is a mathematical requirement to take $\gamma'_{0,k} = \hat{\gamma}'_{0,k} = 0$ for all k, these being constants that arise as fictions undetermined by the loads on the crack. The remaining newer constants can be evaluated in various ways, and in particular it is proper to seek them by assigning values to stresses or displacements on chosen points anywhere in the body and then solving equations such as those in Equations (6) for the desired constants. This is essentially what will be done in the hybrid stress analysis except that there contributions from more than one loading system will be considered simultaneously. A special point to observe is that all the functions multiplying $\hat{\alpha}'_{0,k}$ in the Equations (6) vanish identically for all values of k, so that these constants cannot be found from specified stresses or displacements. The reason for this is that these constants, $\hat{\alpha}'_{0,k}$, are also mathematical fictions, undetermined by loads on the crack. Apart from the $\gamma'_{0,k}$, $\hat{\alpha}'_{0,k}$, and $\hat{\gamma}'_{0,k}$, all the coefficients $\alpha'_{m,k}$, $\beta'_{m,k}$, ---, $\hat{\gamma}'_{m,k}$ are physically meaningful and may be used in analyses of stresses of bodies having circular or part-circular cracks.

Knowledge of the coefficients $\alpha'_{m,k}$, $\beta'_{m,k}$, ---, $\hat{\gamma}'_{m,k}$ can lead at once to an evaluation of the stress intensity factors of all three modes. In particular, if the stress intensity factor of the first mode is defined to be

$$k_1 = \lim_{r\to a} \sqrt{2(r-a)}\ \sigma_z(r,\theta,0) \quad , \tag{10}$$

then (as was shown in [1] and [4])

$$k_1 = \mu\sqrt{a} \sum_{m=0}^{\infty} (\alpha''_m \cos m\theta - \hat{\alpha}''_m \sin m\theta) \quad , \tag{11}$$

where

$$\alpha''_m = \sqrt{\frac{2}{\pi}} \sum_{k=0}^{\infty} (-1)^k \alpha'_{m,k} \quad , \qquad \hat{\alpha}''_m = \sqrt{\frac{2}{\pi}} \sum_{k=0}^{\infty} (-1)^k \hat{\alpha}'_{m,k} \quad . \tag{12}$$

The stress intensity factors of the second and third modes are defined to be

$$\begin{aligned} k_2 &= \lim_{r\to a+} \sqrt{2(r-a)}\ \tau_{zr}\ (r,\theta,0) \quad , \\ k_3 &= \lim_{r\to a+} \sqrt{2(r-a)}\ \tau_{\theta z}\ (r,\theta,0) \quad , \end{aligned} \tag{13}$$

and for them it was found that

$$\begin{aligned} k_2 &= \mu\sqrt{a} \sum_{m=0}^{\infty} \left[\left(\beta''_m - \gamma''_m\right) \cos m\theta - \left(\hat{\beta}''_m - \hat{\gamma}''_m\right) \sin m\theta \right] \quad , \\ k_3 &= \mu\sqrt{a} \sum_{m=0}^{\infty} \left[\left(\beta''_m + \gamma''_m\right) \sin m\theta + \left(\hat{\beta}''_m + \hat{\gamma}''_m\right) \cos m\theta \right] \quad , \end{aligned} \tag{14}$$

where

$$\beta''_m = \frac{1}{\sqrt{2\pi}} \sum_{k=0}^{\infty} (-1)^k \beta'_{m,k} - \frac{\nu\gamma'_{m,0}}{\sqrt{2\pi}(2-\nu)} \quad , \qquad \gamma''_m = \frac{1}{\sqrt{2\pi}} \sum_{k=0}^{\infty} (-1)^k \gamma'_{m,k} \quad , \tag{15}$$

with correponding definitions for $\hat{\beta}''_m$ and $\hat{\gamma}''_m$ starting from $\beta'_{m,k}$ and $\gamma'_{m,k}$. Knowing the coefficients in Equations (11) and (14) allows calculation of stress intensity factors for as many values of θ as the analyst desires. Reference 4 provides interpretation for individual coefficients of those kinds.

Although the major calculations contemplated here involved simultaneous use of several or many load constants, it is helpful to know the effects associated with some particular constants that correspond to particular simple crack loads. Among these are $\alpha'_{0,0}$ ($\sim$ uniform normal load), $\alpha'_{1,0}$ ($\sim$ tilted normal load), $\gamma'_{1,0}$ ($\sim$ uniform, unidirectional shear) and $\beta'_{0\,0}$ ($\sim$ uniform twist). These cases are discussed in Reference 3.

Reformulation of the Crack-Function Integrals

Although the series in the Equations (6) may not always be long, there are nevertheless many of the integrals $I^{n'}_{M,N}(\rho,\zeta)$ required since many combinations of the indices n', M, and N appear there. Moreover, one should not be unduly limited in how large m and k may be or in how many ρ's and θ's may be used. Thus, the workability of this analysis depends on how readily the integrals $I^{n'}_{M,N}(\rho,\zeta)$ can be evaluated. It is possible with modern computers to perform the needed integration directly, but the time to do this becomes prohibitive because of the number of integrals needed. To overcome this problem, reformulations of the integrals into more readily computable forms will be given.

Some help for reducing the number of integrations needed can be had from two recursion formulas which follow directly from familiar recursion properties of Bessel functions. These recursion formulas are

$$I^{n'}_{M+2,N}(\rho,\zeta) = \frac{2(M+1)}{\rho} I^{n'-1}_{M+1,N}(\rho,\zeta) - I^{n'}_{M,N}(\rho,\zeta) \quad , \tag{16}$$

$$I^{n'}_{M,N+2}(\rho,\zeta) = (2N+3) I^{n'-1}_{M,N+1}(\rho,\zeta) - I^{n'}_{M,N}(\rho,\zeta) \quad . \tag{17}$$

Use of these formulas makes it easy to compute a large set of functionals for a given ρ and ζ if only a suitable base set is computed first, such as all those with M = 0 or 1 and with N up to some suitable value. For N > 1 it is possible also to omit the integrals for n' = 1 or 2, since those integrals too can be found by recursion.

Values Where $\zeta > 0$. To get efficient means for computing the base set of integrals for a given ρ and ζ, the integrals were recast through use of integral representations for the Bessel functions $J_M(\rho\xi)$ and $J_{N+1/2}(\xi)$ in Equation (1). After considerable manipulation (Reference [1]), it was found that if $\zeta > 0$, the integrals for n' = 0 and M = 0 or 1 can be rewritten as

$$I^0_{0,N}(\rho,\zeta) = \frac{(-1)^{\left[\frac{N}{2}\right]}[1+(-1)^N]}{4\sqrt{\pi}\,\rho}\int_{-1}^{1} R(x,\rho,\zeta)\cdot\frac{1}{\sqrt{(x+\rho)^2+\zeta^2}}\cdot P_N(x)dx + \\ - \frac{(-1)^{\left[\frac{N}{2}\right]}[1-(-1)^N]}{4\sqrt{\pi}\,\rho\zeta}\int_{-1}^{1} R(x,\rho,\zeta)\cdot\frac{x+\rho}{\sqrt{(x+\rho)^2+\zeta^2}}\cdot P_N(x)dx\,, \tag{18}$$

$$I^0_{1,N}(\rho,\zeta) = \frac{(-1)^{\left[\frac{N}{2}\right]}[1+(-1)^N]}{4\sqrt{\pi}\,\rho^2\zeta}\int_{-1}^{1}\left\{\sqrt{2}\,\rho\zeta - R(x,\rho,\zeta)\cdot\frac{\zeta^2+x(x+\rho)}{\sqrt{(x+\rho)^2+\zeta^2}}\right\}\cdot P_N(x)dx + \\ + \frac{(-1)^{\left[\frac{N}{2}\right]}[1-(-1)^N]}{4\sqrt{\pi}\,\rho}\int_{-1}^{1} R(x,\rho,\zeta)\cdot\frac{1}{\sqrt{(x+\rho)^2+\zeta^2}}\cdot P_N(x)dx\,, \tag{19}$$

where

$$R(x,\rho,\zeta) = \sqrt{-\left(x^2-\rho^2+\zeta^2\right)+\sqrt{\left(x^2-\rho^2+\zeta^2\right)^2+4\rho^2\zeta^2}}\,, \tag{20}$$

$P_N(x)$ is a Legendre polynomial of the form

$$P_N(x) = \frac{1}{2^N N!}\frac{d^N}{dx^N}\left[\left(x^2-1\right)^N\right] = \sum_{r=0}^{N}\binom{N}{r}^2\left(\frac{x+1}{2}\right)^{N-r}\left(\frac{x-1}{2}\right)^r\,, \tag{21}$$

and

$$\left[\frac{N}{2}\right] = \begin{cases} \frac{N}{2} & \text{if N is even} \\ \frac{N+1}{2} & \text{if N is odd} \end{cases} . \qquad (22)$$

These formulas are well suited for computation since their sensitive features are controllable. Thus, though many significant digits may be lost by subtraction in computing the polynomials $P_N(x)$, those functions are free of ρ and ζ so they can be precomputed carefully without repetitious expense. The fluctuations of the $P_N(x)$ also waste significant digits during the integration, but the polynomial nature of the fluctuations provides compensation by making them conform well to the approximations of the integrand used in the standard Gauss integration if its order is high enough. To complete the base set of integrals for $\zeta > 0$, one may use the following integrated forms for the needed cases having $n' = 1$ or 2.

$$I^1_{0,0}(\rho,\zeta) = \frac{a_1}{\sqrt{2\pi}\,\rho\zeta c_1^2}\left[(1+\rho) + (1-\rho)c_1^2\right] , \qquad (23a)$$

$$I^1_{0,1}(\rho,\zeta) = I^0_{0,0}(\rho,\zeta) - \frac{a_1}{\sqrt{2\pi}\,\rho c_1^2}\left(1+c_1^2\right) , \qquad (23b)$$

$$I^1_{1,0}(\rho,\zeta) = -\frac{a_1}{\sqrt{2\pi}\,\rho c_1^2}\left(1-c_1^2\right) , \qquad (23c)$$

$$I^1_{1,1}(\rho,\zeta) = I^0_{1,0}(\rho,\zeta) - \frac{2}{\sqrt{2\pi}\,\rho} + \frac{a_1}{\sqrt{2\pi}\,\rho^2\zeta c_1^2}\left[\left(\zeta^2+1+\rho\right) + \left(\zeta^2+1-\rho\right)c_1^2\right] , \qquad (23d)$$

$$I^2_{0,0}(\rho,\zeta) = \frac{a_1^2}{4\sqrt{2\pi}\,\rho^2\zeta b_1 c_1^6}\left\{c_1^2\left(1+c_1^2\right)^2\left[(1+\rho)+(1-\rho)c_1^2\right] + 4b_1^2\left[(1+\rho)+(1-\rho)c_1^6\right]\right\} , \qquad (23e)$$

$$I^2_{0,1}(\rho,\zeta) = -\frac{a_1^2}{4\sqrt{2\pi}\,\rho^2 b_1 c_1^6}\left[c_1^2\left(1+c_1^2\right)^3 + 4b_1^2\left(1+c_1^6\right)\right] + \frac{a_1}{\sqrt{2\pi}\,\rho\zeta c_1^2}\left[(2+\rho) + (2-\rho)c_1^2\right] , \qquad (23f)$$

$$I^2_{1,0}(\rho,\zeta) = -\frac{a_1^2}{4\sqrt{2\pi}\,\rho^2 b_1 c_1^6}\left[c_1^2\left(1+c_1^2\right)\left(1-c_1^4\right) + 4b_1^2\left(1-c_1^6\right)\right] + \frac{a_1}{\sqrt{2\pi}\,\rho\zeta c_1^2}\left(1-c_1^2\right) , \qquad (23g)$$

$$I^2_{1,1}(\rho,\zeta) = -\frac{a_1^2}{4\sqrt{2\pi}\,\rho^2\zeta b_1 c_1^6}\left\{c_1^2\left(1-c_1^4\right)\left[(1+\rho)+(1-\rho)c_1^2\right] + 4b_1^2\left[(1+\rho)-(1-\rho)c_1^6\right]\right\} + \tag{23h}$$

$$-\frac{a_1}{\sqrt{2\pi}\,\rho c_1^2}\left(1-c_1^2\right) \quad .$$

Here

$$a_1 = \sqrt{\frac{-\left(1-\rho^2+\zeta^2\right) + \sqrt{\left(1-\rho^2+\zeta^2\right)^2 + 4\rho^2\zeta^2}}{2\left[(1-\rho)^2+\zeta^2\right]}} \quad , \tag{24a}$$

$$b_1 = \sqrt{\frac{\left(1-\rho^2+\zeta^2\right) + \sqrt{\left(1-\rho^2+\zeta^2\right)^2 + 4\rho^2\zeta^2}}{2\left[(1-\rho)^2+\zeta^2\right]}} \quad , \tag{24b}$$

$$c_1 = \sqrt{a_1^2 + b_1^2} \tag{24c}$$

The formulas (18) through (24c) provide a suitable base for computing the needed integrals for $\zeta > 0$ (that is off the plane of the crack), and use of the recursion formulas (16) and (17) can complete their computation. The integrals needed at places where $\zeta < 0$ are to be computed in the same way since ζ appears inside the integral only as $|\zeta|$.

The evaluation method for the crack function integrals as described above is limited not only in requiring $\zeta > 0$, it also fails if $\rho = 0$ since several of its expressions are then indeterminate, and in Equation (16) it involves an explosive recursion if ρ is sufficiently small. Cases with $\zeta > 0$ and $\rho = 0$ are tractable, however. Thus one may note first that the original integral for $I^n_{M,N}(\rho,\zeta)$ vanishes for $\rho = 0$ if $M > 0$. If $M = 0$, then evaluating the limit $R(x,\rho,\zeta)/\rho$ as $\rho \to 0$ in Equation (18) shows

$$I^{0}_{0,N}(0,\zeta) = \frac{(-1)^{\left[\frac{N}{2}\right]}[1+(-1)^{N}]\zeta}{2\sqrt{2\pi}} \int_{-1}^{1} \frac{P_N(x)}{x^2+\zeta^2}\,dx - \frac{(-1)^{\left[\frac{N}{2}\right]}[1-(-1)^{N}]}{2\sqrt{2\pi}} \int_{-1}^{1} \frac{xP_N(x)}{x^2+\zeta^2}\,dx \ , \qquad (25)$$

and values computed from this relation provide the familiar basis for recursion to get all the required values of $I^{n'}_{0,N}(0,\zeta)$ provided one includes the following additional limiting values for $\rho \to 0$.

$$I^{1}_{0,0}(0,\zeta) = \frac{\sqrt{2/\pi}}{1+\zeta^2} \ , \qquad (26a)$$

$$I^{1}_{0,1}(0,\zeta) = \sqrt{\frac{2}{\pi}}\left(\arctan\frac{1}{|\zeta|} - \frac{|\zeta|}{1+\zeta^2}\right) \ , \qquad (26b)$$

$$I^{2}_{0,0}(0,\zeta) = \frac{2|\zeta|\sqrt{2/\pi}}{(1+\zeta^2)^2} \ , \qquad (26c)$$

$$I^{2}_{0,1}(0,\zeta) = \frac{2\sqrt{2/\pi}}{(1+\zeta^2)^2} \ . \qquad (26d)$$

If $\zeta > 0$ and ρ is not zero but small, then it seems natural to seek evaluations made by modifying those for $\rho = 0$, and indeed such evaluations are possible. Thus one can show that

$$I^{n'}_{M,N}(\rho,\zeta) = \sum_{s=0}^{\infty} \frac{(-1)^s}{(M+2s)!}\left(\frac{\rho}{2}\right)^{M+2s} {}_{M+2s}C_s \; I^{n'+M+2s}_{0,N}(0,\zeta) \ .$$

Use of such a ρ-series involves evaluation of integrals with $\rho = 0$ and n' increasingly large. Integrals with large n' have potential difficulties with convergence, but those difficulties can be resolved so that series of this form are useful. The forthcoming paper on evalution of the integrals*, treats these matters in detail, and the methodology described there has been included as an alternate procedure in FRAC3D so that integrals with small positive ρ and $\zeta > 0$ can be computed efficiently. The reader is referred to the forthcoming paper for details.

---

* J. C. Bell, "Evaluation of Integrals Involving Products of Bessel Functions Having Application to Crack Stress Analysis".

Values Where $\zeta = 0$ or is Small. For points on the plane of the crack (for which $\zeta = 0$), special formulas are needed, and their forms depend on whether the point is on the crack (with $\rho < 1$) or beyond it (with $\rho > 1$). One simplification available is that all the integrals with $n' = 2$ are multiplied by ζ in the formulas (5) and (6) for the stresses and displacements, so that they can be shown to need no immediate consideration. With this in view, a suitable base of integrals for starting the recursion for $\zeta = 0$ and $\rho > 1$ can be shown [1] to be

$$I^0_{0,N}(\rho,0) \quad (\rho > 1) = \begin{cases} \dfrac{2}{\sqrt{2\pi}} \arcsin \dfrac{1}{\rho} & \text{for } N = 0 , \\ 0 & \text{for } N \text{ odd} , \\ \dfrac{(-1)^{\frac{N}{2}}[1\cdot 3\cdot 5\cdot \cdots \cdot (N-1)]}{\sqrt{2\pi}\, 2^{N/2}\left(\frac{N}{2}\right)!\, \rho^{N+1}} \displaystyle\int_0^1 t^{\frac{N-1}{2}} (1-t)^{\frac{N}{2}} \left(1-t\rho^{-2}\right)^{-\frac{N+1}{2}} dt & \text{for } N \text{ even and} \geq 2 , \end{cases} \tag{27}$$

$$I^0_{1,N}(\rho,0) \quad (\rho > 1) = \begin{cases} \dfrac{2}{\sqrt{2\pi}\,\rho} & \text{for } N = 0 , \\ \dfrac{1}{\sqrt{2\pi}} \left[\rho \arcsin \dfrac{1}{\rho} - \dfrac{\sqrt{\rho^2-1}}{\rho}\right] & \text{for } N = 1 , \\ 0 & \text{for } N \text{ even and} \geq 2 , \\ \dfrac{(-1)^{\frac{N-1}{2}}(1\cdot 3\cdot 5\cdot \ldots \cdot N)}{\sqrt{2\pi}\, 2^{(N+1)/2}\left(\frac{N+1}{2}\right)!\, \rho^{N+1}} \displaystyle\int_0^1 t^{\frac{N-2}{2}} (1-t)^{\frac{N+1}{2}} \left(1-t\rho^{-2}\right)^{-\frac{N+2}{2}} dt & \text{for } N \text{ odd and} \geq 3 , \end{cases} \tag{28}$$

using also these four special cases with n' = 1,

$$I^1_{0,0}(\rho,0) = 0 \ , \qquad (\rho > 1) \tag{29a}$$

$$I^1_{0,1}(\rho,0) = \frac{2}{\sqrt{2\pi}}\left[\arcsin\frac{1}{\rho} - \frac{1}{\sqrt{\rho^2-1}}\right] , \qquad (\rho > 1) \tag{29b}$$

$$I^1_{1,0}(\rho,0) = \frac{2}{\sqrt{2\pi}\,\rho\,\sqrt{\rho^2-1}} \ , \qquad (\rho > 1) \tag{29c}$$

$$I^1_{1,1}(\rho,0) = 0 \quad . \qquad (\rho > 1) \tag{29d}$$

For points on the crack surface itself (with $\zeta = 0$ and $\rho < 1$), most of the crack functionals become either polynomials in ρ or polynomials multiplied by $\sqrt{1-\rho^2}$. In order to express coefficients of the polynomials, it is helpful to use the Pochhammer notation $(\alpha)_n$:

$$(\alpha)_n = \alpha(\alpha+1)(\alpha+2)\cdot\ldots\cdot(\alpha+n-1) \ , \qquad (\alpha)_0 = 1 \quad . \tag{30}$$

For $\zeta = 0$ and $\rho < 1$, a suitable base set of functionals for starting the recursion can then be derived [1] to be

$$I^0_{0,N}(\rho,0) \quad (\rho<1) = \begin{cases} \dfrac{[1\cdot3\cdot5\cdot\text{----}\cdot(N+1)]\pi}{\sqrt{2\pi}(N+1)2^{N/2}\left(\frac{N}{2}\right)!} \displaystyle\sum_{n=0}^{\frac{N}{2}} \frac{\left(\frac{N+1}{2}\right)_n \left(-\frac{N}{2}\right)_n \rho^{2n}}{(1)_n n!} & \text{for N even ,} \\ \dfrac{2^{(N+1)/2}\left(\frac{N-1}{2}\right)!\,\sqrt{1-\rho^2}}{\sqrt{2\pi}\ (1\cdot3\cdot5\cdot\text{----}\cdot N)} \displaystyle\sum_{n=0}^{\frac{N-1}{2}} \frac{\left(\frac{1-N}{2}\right)_n \left(\frac{N+2}{2}\right)_n \rho^{2n}}{(1)_n\, n!} & \text{for N odd ,} \end{cases} \tag{31}$$

$$I^{0}_{1,N}(\rho,0) \quad (\rho < 1) = \begin{cases} \frac{2}{\sqrt{2\pi}\,\rho}\left[1 - \sqrt{1-\rho^2}\right] & \text{for } N = 0 \ , \\ \frac{2^{\frac{N}{2}}\left(\frac{N}{2}\right)!\ \rho\sqrt{1-\rho^2}}{\sqrt{2\pi}\,[1\cdot3\cdot5\cdot\cdots\cdot(N-1)]} \sum_{n=0}^{\frac{N-2}{2}} \frac{\left(\frac{2-N}{2}\right)_n \left(\frac{N+3}{2}\right)_n \rho^{2n}}{(2)_n n!} & \text{for } N = 2,4,6,\cdots \ , \\ \frac{(1\cdot3\cdot5\cdot\cdots\cdot N)\ \pi\rho}{\sqrt{2\pi}\ 2^{(N+1)/2}\left(\frac{N-1}{2}\right)!} \sum_{n=0}^{\frac{N-1}{2}} \frac{\left(\frac{N+2}{2}\right)_n \left(\frac{1-N}{2}\right)_n \rho^{2n}}{(2)_n n!} & \text{for } N \text{ odd} \ , \end{cases} \tag{32}$$

using also these four special cases with $n' = 1$,

$$I^{1}_{0,0}(\rho,0) = \frac{2}{\sqrt{2\pi(1-\rho^2)}} \quad , \qquad (\rho < 1) \tag{33a}$$

$$I^{1}_{0,1}(\rho,0) = \sqrt{\frac{\pi}{2}} \quad , \qquad (\rho < 1) \tag{33b}$$

$$I^{1}_{1,0}(\rho,0) = 0 \quad , \qquad (\rho < 1) \tag{33c}$$

$$I^{1}_{1,1}(\rho,0) = \frac{2\rho}{\sqrt{2\pi(1-\rho^2)}} \quad . \qquad (\rho < 1) \tag{33d}$$

A small region which still remains troublesome with the above formulas and procedures is that for which ζ is small and ρ is little less than unity. In this region, as is shown in the forthcoming paper on evaluation of the integrals, it is possible to employ a series of the form

$$I^{n'}_{M,N}(\rho,\zeta) = \sum_{s=0}^{\infty} \frac{(-1)^s}{s!}\,\zeta^s\, I^{n'+s}_{M,N}(\rho,0) \quad .$$

The coefficient integrals of this ζ-series surprisingly are evaluable though with a little more manipulation than is needed for those of the ρ-series, so this ζ-series too has has been included as an alternate evaluation procedure in FRAC3D. The reader is referred to the forthcoming paper for details.

Computations of Crack Stresses in an Infinite Body

The present analysis for crack stresses in an infinite body began by finding expressions for all the stress components and displacements in terms of a single kind of integral, denoted as $I^{n'}_{M,N}(\rho,\zeta)$, so evaluating integrals of that form is the key to stress computations. The most general plan for evaluating them is to seek them as entire sets for a given ρ and ζ, beginning with a base set for a few combinations of indices, and then building the rest by recursion. The formulas for integrals of the base set vary somewhat according to the choice of ρ and ζ so several alternative calculations must be prepared, but even before this some preparations must be made for the numerical quadratures. Thus, several stages of computing are involved in evaluating the integrals.

Gaussian quadrature was chosen for the integrals actually integrated numerically. This was advantageous not only as being a well-developed method of quadrature but also as providing very efficient approximations for the most variable factors in the integrands, that is the Legendre polynomials in Equations (18), (19), and (25). To implement this method of quadrature, values of the polynomials $P_N(x)$ were found for all values of N up to a given maximum and for the Gaussian abscissae x for three finenesses of quadrature. In order to allow m and k in the Equations (6) to become as large as 10 or up to $m + 2k = 16$ and also to allow for truncation of N as M increases in the recursion, values of N as high as 50 were chosen; and, in order to compute Legendre polynomials of such high order, double precision arithmetic was used here, carrying 30 significant digits in order to counteract the loss of up to 15 digits in adding terms of the polynomials. Thus, this most exacting part of the calculation was done in advance, before any ρ or ζ was assigned, and does not need to be repeated unless the fineness of the quadrature were to be changed - which seems quite unnecessary. The finenesses that were selected used 32 or 64 or 96 points over the range of integration. After testing showed that even the 96-point quadrature ran acceptably fast, it was taken as standard for FRAC3D, but results based on other finenesses were employed for accuracy checks. The evaluations of $P_N(x)$ were multiplied by the customary Gauss weights for for the same abscissae so now these products can be used as revised weights in the integration and no further evaluations of the $P_N(x)$ are needed.

With this background, subroutines were prepared to evaluate the alternative bases of integrals to begin the recursion. These subroutines are as follows.

Subroutine	Range of ρ and ζ	Equations Employed
EVAL	$\zeta > 0$, $\rho > 0$	(18) to (24c)
RHOEQ0	$\zeta > 0$, $\rho = 0$	(25) to (26d)
RHOGT1	$\zeta = 0$, $\rho > 1$	(27) to (29d)
RHOLT1	$\zeta = 0$, $\rho < 1$	(30) to (33d)

These subroutines were employed in building another subroutine, called RECUR, which uses recursion based on Equations (16) and (17) and builds an entire set of integrals for a given ρ and ζ for indices $n' = 0,1,2$, and $M = 0,1,2,\ldots,17$, and $N = 0,1,2,\ldots,42$ for $M = 0$, or $N = M-1$ to $43-M$ for $M > 0$. RECUR includes programming to determine which further subroutine should be called for constructing the base set of integrals prior to recursion, including also provision for two exceptional regions where EVAL might yield poor results. One exceptional region is where $0 < \rho < 0.7$ in which the ρ-series is to be used as a substitute procedure, and the other is where $0.7 \leq \rho < 1$ and $0 < \zeta < (1-\rho)/5$ in which the ζ-series is to be used. Programming for both the ρ-series and the ζ-series is included in RECUR.

The success of this approach to the evaluation of the integrals $I^{n'}_{M,N}(\rho,\zeta)$ can be seen in that even with the 96-point quadrature for the bases, entire sets of 1000^+ integrals for a given ρ and ζ are computable on a CDC Cyber 73 in little over one second and with good accuracy. By contrast, direct integration by the same machine using the original form (1) for the integral typically took 40 to 50 seconds per integral and provided less accuracy. Thus, the streamlined procedure using RECUR seems to speed the integration by a factor up to 10^4 or more and brings the rate into an acceptable range.

Stresses Due to Normal and Tangential Loads on a Half Space

Formulation of Effects of Surface Loads

In the crack stress analysis being undertaken, one or more analyses for surface-loaded half spaces are to be combined with an analysis for a crack in an infinite body in order to represent a lesser body with a crack. To make a half-space analysis adaptable for this use, it is important that the surface load pattern should be quite flexible. Therefore, an analysis is chosen here in which three components of load may be specified arbitrarily at many points on the surface of a half space, and it is assumed that surface loads at intermediate points can be approximated satisfactorily by linear interpolation in either of two perpendicular directions. This representation of loads makes them continuous, and this is beneficial in that it avoids the artifical singularities of stress that discontinuous loads would imply.

The points where the load components are specifiable are taken as corners of a grid which is rectangular but does not need to be uniform and may be incomplete (that is, some boundaries may cross only part of the pattern). The loads can be assigned arbitrarily, of course, only at points where four rectangles meet since the linear interpolability denies arbitrariness elsewhere, but this is not a serious limitation. Within this general plan, patterns can be drawn which should have ample flexibility to fit a wide variety of load distributions. To keep the loads continuous over the entire plane, they should of course decrease to zero before they terminate.

Initially, the elemental load pattern was taken to be the distribution of a single component (whether normal or shear) over a rectangle, as determined by four arbitrary corner values. This pattern produces stress singularities which should be cancelled by singularities caused by combining effects of matching loads on adjacent rectangles, but it would be tedious to account for this in treating loads on many rectangles. Therefore, an alternative kind of elemental load pattern was chosen. This load pattern can be related to the earlier load pattern in two stages: first by splitting patterns of the earlier kind into four parts of the same general form but

with only one non-zero corner value, and second by combining such parts from the four rectangles sharing one corner, as illustrated in Figure A1. Elemental loads of this kind can be added together to give essentially the same overall patterns as would be representable by the earlier rectangular elemental loads, but with the newer elements the stress discontinuities are eliminated. These new elements are tentatively being called pyramidal since this roughly describes their shape, although the faces really are hyperboloidal.

To formulate stresses induced by the rectangular or pyramidal patterns, rectangular coordinates (x,y,z) are introduced with z = 0 being the surface of the half space, and auxiliary variables α and β are used to represent x- and y-distances from a point where stress is to be evaluated to where load is applied. In particular, if $(x_c, y_c, 0)$ is a corner point of an elemental load pattern generating stresses at (x,y,z), then the corresponding corner values of α and β are

$$\alpha_c = x_c - x \ , \qquad \beta_c = y_c - y \qquad . \tag{34}$$

In the analysis, certain functions of α, β, and z appear repeatedly, needing evaluation for corner values of α and β, and a certain combination of corner values associated with any pyramidal load also appears repeatedly, The functions associated with stresses are here denoted as $H_i^j(\alpha,\beta,z)$ with i identifying the load component and j the stress component. In particular j = 1 (or xx) $\sim \sigma_x$, 2 (or yy) $\sim \sigma_y$, 3 (or zz) $\sim \sigma_z$, 4 (or yz) $\sim \tau_{yz}$, 5 (or zx) $\sim \tau_{zx}$, 6 (or xy) $\sim \tau_{xy}$. The load component identified by i = 1 is a normal load p $\sim -\sigma_z$, that for i = 2 is shear load s $\sim \tau_{zx}$, and that for i = 3 is another shear load t $\sim \tau_{yz}$. (Note that the order of the shear loads differs from that for shear stresses, this being an inheritance from earlier reference material.) The functions associated with displacements are denoted as $\mathcal{H}_i^j(\alpha,\beta,z)$, with i used as before, and with j = 1 for u, 2 for v, and 3 for w. The functions $H_i^j(\alpha,\beta,z)$ and $\mathcal{H}_i^j(\alpha,\beta,z)$, to be listed later, were derived as shown in Reference 1. The combination of corner evaluations which appears repeatedly for any one of these functions H_i^j (or $\mathcal{H}_i^j$) is the following.

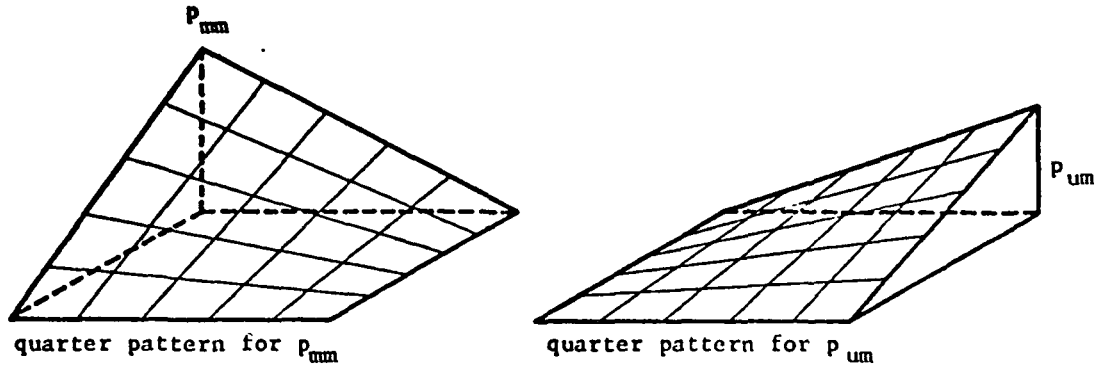

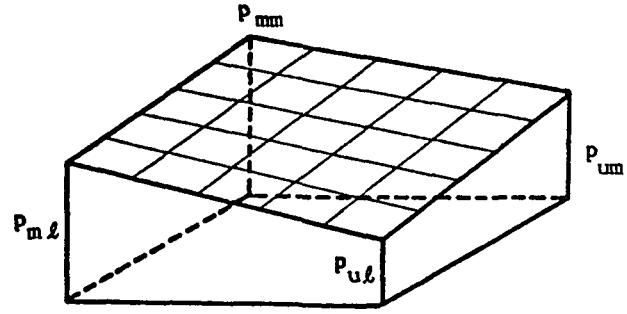

sum of four surrounding quarter patterns

a. Breakdown of rectilinear load pattern into quarter patterns determined by the corner values

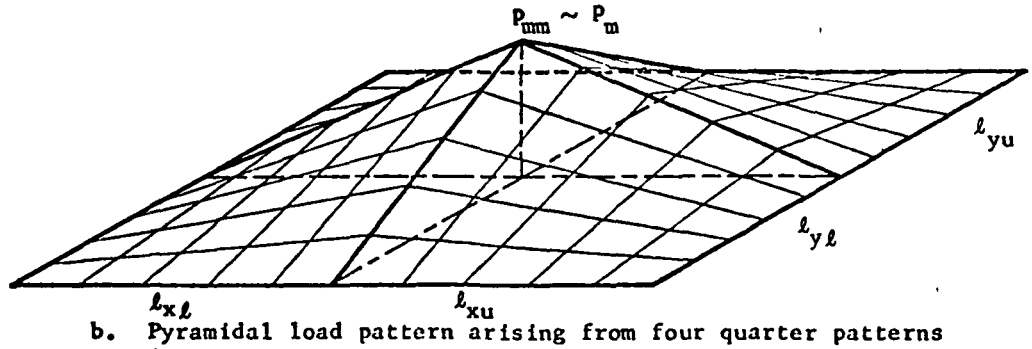

b. Pyramidal load pattern arising from four quarter patterns determined by the same corner value

FIGURE A1. PYRAMIDAL LOAD PATTERNS PROVIDING LOAD REPRESENTATION EQUIVALENT TO THAT PROVIDED BY RECTILINEAR PATTERNS

$$\left[H_i\right]^* = \frac{1}{\ell_{x\ell}\ell_{yu}} H_{i,\ell u} - \left(\frac{1}{\ell_{x\ell}}+\frac{1}{\ell_{xu}}\right)\frac{1}{\ell_{yu}} H_{i,mu} + \frac{1}{\ell_{xu}\ell_{yu}} H_{i,uu} +$$

$$- \frac{1}{\ell_{x\ell}}\left(\frac{1}{\ell_{y\ell}}+\frac{1}{\ell_{yu}}\right)H_{i,\ell m} + \left(\frac{1}{\ell_{x\ell}}+\frac{1}{\ell_{xu}}\right)\left(\frac{1}{\ell_{y\ell}}+\frac{1}{\ell_{yu}}\right)H_{i,mm} - \frac{1}{\ell_{xu}}\left(\frac{1}{\ell_{y\ell}}+\frac{1}{\ell_{yu}}\right)H_{i,um} + \quad (35)$$

$$+ \frac{1}{\ell_{x\ell}\ell_{y\ell}} H_{i,\ell\ell} - \left(\frac{1}{\ell_{x\ell}}+\frac{1}{\ell_{xu}}\right)\frac{1}{\ell_{y\ell}} H_{i,m\ell} + \frac{1}{\ell_{xu}\ell_{y\ell}} H_{i,u\ell} \quad ,$$

Here $\ell_{x\ell}$, ℓ_{xu}, $\ell_{y\ell}$, and ℓ_{yu} are x- or y-lengths of the lower (ℓ) or upper (u) rectangles beneath the pyramidal load, and extra subscripts ℓ, m, u applied to H_i^j (or $\mathcal{H}_i^j$) call for evaluation using lower, middle, or upper corner values of α and β. The contribution that a pyramidal load with peak value p_m, s_m, or t_m [that is, $-\sigma(x_m,y_m,0)$, $\tau_{zx}(x_m,y_m,0)$, or $\tau_{yz}(x_m,y_m,0)$] makes to stress or displacement components at any point (x,y,z) is readily expressible in terms of these combinations of corner evaluations. Indeed, if influence functions $K_i^j(x,y,z)$ [or $\mathcal{K}_i^j(x,y,z)$] are defined to be

$$K_i^j(x,y,z) = -\frac{1}{2\pi}\left[H_i^j(\alpha,\beta,z)\right]^* , \qquad \mathcal{K}_i^j(x,y,z) = -\frac{1}{2\pi}\left[\mathcal{H}_i^j(\alpha,\beta,z)\right]^* , \quad (36)$$

then the three elemental pyramidal load patterns on the four-rectangular area around $(x_m,y_m,0)$ produce these stresses and displacements at (x,y,z):

$$\sigma^j(x,y,z) = p_m K_1^j(x,y,z) + s_m K_2^j(x,y,z) + t_m K_3^j(x,y,z) \quad ,$$

$$2\mu u^j = \frac{E u^j(x,y,z)}{(1+\nu)} = p_m \mathcal{K}_1^j(x,y,z) + s_m \mathcal{K}_2^j(x,y,z) + t_m \mathcal{K}_3^j(x,y,z) \quad , \quad (37)$$

where the new superscripts by definition imply

$$\sigma^1 = \sigma_x, \quad \sigma^2 = \sigma_y, \quad \sigma^3 = \sigma_z, \quad \sigma^4 = \tau_{yz}, \quad \sigma^5 = \tau_{zx}, \quad \sigma^6 = \tau_{xy},$$

$$u^1 = u, \quad u^2 = v, \quad u^3 = w \quad .$$

To calculate the total stresses and displacements caused at (x,y,z) by the three kinds of overall load patterns on the surface of the half space, it is necessary only to sum the contributions from all the pyramidal loads.

In addition to the quantities α and β, each of which is the difference of a corner value (such as x_c or y_c) and a stress location coordinate (x or y), the H_i^j and $\mathcal{H}_i^j$ involve also the quantities

$$\begin{aligned} \rho &= \sqrt{\alpha^2+\beta^2+z^2} \quad , \\ \theta_1 &= \arctan\frac{\beta}{\alpha} - \arctan\frac{\beta z}{\alpha\rho} \quad , \\ \theta_2 &= \arctan\frac{\alpha}{\beta} - \arctan\frac{\alpha z}{\beta\rho} \quad , \\ \theta_3 &= \arctan\frac{\alpha\beta}{z\rho} \quad , \end{aligned} \tag{38}$$

and the logarithms $\ln(\rho+\alpha)$, $\ln(\rho+\beta)$ and $\ln(\rho+z)$. Examination of the functions H_i^j and $\mathcal{H}_i^j$ shows that wherever the argument of one of these logarithms would vanish that logarithm is itself multiplied by another vanishing quantity so that the product too would vanish. This disposes of all the singularities that would have arisen if the elemental load had not been made to vary continuously.

It remains to list the functions H_i^j and $\mathcal{H}_i^j$. They are:

$$H_1^{xx} = -2z\rho + \alpha z\ln(\alpha+\rho) + 2\beta z\ln(\beta+\rho) + \alpha\beta\theta_3 + (1-2\nu)\left\{\frac{z\rho}{2} - \alpha z\ln(\alpha+\rho) + \right.$$
$$\left. - \frac{\alpha^2-\beta^2}{2}\ln(z+\rho) - \alpha\beta\theta_2\right\}$$

$$H_2^{xx} = \frac{1}{2}\alpha\rho - \frac{3(\beta^2-z^2)}{2}\ln(\alpha+\rho) - 2\alpha\beta\ln(\beta+\rho) + 3\beta z\theta_3 + (1-2\nu)\left\{\frac{\alpha\rho}{2} + \right. \tag{39a}$$
$$\left. + \frac{\beta^2-z^2}{2}\ln(\alpha+\rho) - \alpha z\ln(z+\rho) - \beta z\theta_2\right\}$$

$$H_3^{xx} = \beta\rho - \alpha\beta\ln(\alpha+\rho) + z^2\ln(\beta+\rho) + \alpha z\theta_3 + (1-2\nu)\left\{-\beta\rho + \alpha\beta\ln(\alpha+\rho) + \right.$$
$$\left. + \beta z\ln(z+\rho) - \alpha z\theta_2\right\}$$

$$H_1^{yy} = -2z\rho + 2\alpha z\ln(\alpha+\rho) + \beta z\ln(\beta+\rho) + \alpha\beta\theta_3 + (1-2\nu)\left\{\frac{z\rho}{2} - \beta z\ln(\beta+\rho) + \right.$$
$$\left. + \frac{\alpha^2-\beta^2}{2}\ln(z+\rho) - \alpha\beta\theta_1\right\}$$

$$H_2^{yy} = \alpha\rho + z^2\ln(\alpha+\rho) - \alpha\beta\ln(\beta+\rho) + \beta z\theta_3 + (1-2\nu)\left\{-\alpha\rho + \alpha\beta\ln(\beta+\rho) + \right. \quad (39b)$$
$$\left. + \alpha z\ln(z+\rho) - \beta z\theta_1\right\}$$

$$H_3^{yy} = \frac{1}{2}\beta\rho - 2\alpha\beta\ln(\alpha+\rho) - \frac{3(\alpha^2-z^2)}{2}\ln(\beta+\rho) + 3\alpha z\theta_3 + (1-2\nu)\left\{\frac{\beta\rho}{2} + \frac{\alpha^2-z^2}{2}\ln(\beta+\rho) + \right.$$
$$\left. - \beta z\ln(z+\rho) - \alpha z\theta_1\right\}$$

$$H_1^{zz} = z\rho + \alpha\beta\theta_3$$

$$H_2^{zz} = -z^2\ln(\alpha+\rho) - \beta z\theta_3 \quad (39c)$$

$$H_3^{zz} = -z^2\ln(\beta+\rho) - \alpha z\theta_3$$

$$H_1^{xy} = \beta z\ln(\alpha+\rho) + \alpha z\ln(\beta+\rho) - z^2\theta_3 + (1-2\nu)\left\{\frac{\alpha\beta}{2} + \beta z\ln(\alpha+\rho) + \alpha z\ln(\beta+\rho) + \right.$$
$$\left. + \alpha\beta\ln(z+\rho) + \frac{1}{2}\alpha^2\theta_1 + \frac{1}{2}\beta^2\theta_2 - \frac{z^2}{2}\theta_3\right\}$$

$$H_2^{xy} = \beta\rho - \alpha\beta\ln(\alpha+\rho) + z^2\ln(\beta+\rho) + \alpha z\theta_3 + (1-2\nu)\left\{-\frac{\beta\rho}{2} - \frac{\alpha^2-z^2}{2}\ln(\beta+\rho) + \right. \quad (39d)$$
$$\left. + \beta z\ln(z+\rho) + \alpha z\theta_1\right\}$$

$$H_3^{xy} = \alpha\rho + z^2\ln(\alpha+\rho) - \alpha\beta\ln(\beta+\rho) + \beta z\theta_3 + (1-2\nu)\left\{-\frac{\alpha\rho}{2} - \frac{\beta^2-z^2}{2}\ln(\alpha+\rho) + \right.$$
$$\left. + \alpha z\ln(z+\rho) + \beta z\theta_2\right\}$$

$$H_1^{yz} = z^2\ln(\beta+\rho) + \alpha z\theta_3$$

$$H_2^{yz} = -\beta z\ln(\alpha+\rho) - \alpha z\ln(\beta+\rho) + z^2\theta_3 \quad (39e)$$

$$H_3^{yz} = 2z\rho - 2\alpha z\ln(\alpha+\rho) - \beta z\ln(\beta+\rho) - \alpha\beta\theta_3$$

$$H_1^{zx} = z^2 \ln(\alpha+\rho) + \beta z \theta_3$$

$$H_2^{zx} = 2z\rho - \alpha z \ln(\alpha+\rho) - 2\beta z \ln(\beta+\rho) - \alpha\beta\theta_3 \qquad (39f)$$

$$H_3^{zx} = -\beta z \ln(\alpha+\rho) - \alpha z \ln(\beta+\rho) + z^2\theta_3$$

$$\mathcal{H}_1^u = \frac{\alpha z \rho}{2} - \frac{z(\beta^2-z^2)}{2}\ln(\alpha+\rho) - \alpha\beta z \ln(\beta+\rho) + \beta z^2\theta_3 + (1-2\nu)\left\{\frac{\alpha\beta^2}{6} + \frac{\alpha z\rho}{3} + \right.$$
$$- \frac{z(3\beta^2-z^2)}{6}\ln(\alpha+\rho) - \alpha\beta z\ln(\beta+\rho) + \frac{\alpha(\alpha^2-3\beta^2)}{6}\ln(z+\rho) - \frac{\alpha^2\beta\theta_1}{2} +$$
$$\left. - \frac{\beta^3\theta_2}{6} + \frac{\beta z^2\theta_3}{2}\right\} \qquad (40a)$$

$$\mathcal{H}_2^u = -\frac{(\beta^2-2z^2)\rho}{2} + \alpha\left(\beta^2-z^2\right)\ln(\alpha+\rho) + \frac{\beta(\alpha^2-3z^2)}{2}\ln(\beta+\rho) - 2\alpha\beta z\theta_3 + (1-2\nu)\left\{-\frac{\alpha^2\rho}{2} + \right.$$
$$\left. + \frac{\rho^3}{6} + \frac{\beta(\alpha^2-z^2)}{2}\ln(\beta+\rho) + \frac{z(\alpha^2-\beta^2)}{2}\ln(z+\rho) - \alpha\beta z\theta_1\right\}$$

$$\mathcal{H}_3^u = -\frac{\alpha\beta\rho}{3} - \frac{\beta(\beta^2+3z^2)}{6}\ln(\alpha+\rho) - \frac{\alpha(\alpha^2+3z^2)}{6}\ln(\beta+\rho) + \frac{z^3}{3}\theta_3 + (1-2\nu)\left\{-\frac{\alpha\beta z}{2} + \right.$$
$$+ \frac{\alpha\beta\rho}{3} + \frac{\beta(\beta^2-3z^2)}{6}\ln(\alpha+\rho) + \frac{\alpha(\alpha^2-3z^2)}{6}\ln(\beta+\rho) - \alpha\beta z\ln(z+\rho) - \frac{\alpha^2 z\theta_1}{2} +$$
$$\left. - \frac{\beta^2 z\theta_2}{2} + \frac{z^3\theta_3}{6}\right\}$$

$$\mathcal{H}_1^v = \frac{\beta z\rho}{2} - \alpha\beta z\ln(\alpha+\rho) - \frac{z(\alpha^2-z^2)}{2}\ln(\beta+\rho) + \alpha z^2\theta_3 + (1-2\nu)\left\{\frac{\alpha^2\beta}{6} + \frac{\beta z\rho}{3} - \alpha\beta z\ln(\alpha+\rho) + \right.$$
$$\left. - \frac{z(3\alpha^2-z^2)}{6}\ln(\beta+\rho) - \frac{\beta(3\alpha^2-\beta^2)}{6}\ln(z+\rho) - \frac{\alpha^3\theta_1}{6} - \frac{\alpha\beta^2\theta_2}{2} + \frac{\alpha z^2\theta_3}{2}\right\}$$

$$\mathcal{H}_2^v = -\frac{\alpha\beta\rho}{3} - \frac{\beta(\beta^2+3z^2)}{6}\ln(\alpha+\rho) - \frac{\alpha(\alpha^2+3z^2)}{6}\ln(\beta+\rho) + \frac{z^3}{3}\theta_3 + (1-2\nu)\left\{-\frac{\alpha\beta z}{2} + \frac{\alpha\beta\rho}{3} + \right.$$
$$\left. + \frac{\beta(\beta^2-3z^2)}{6}\ln(\alpha+\rho) + \frac{\alpha(\alpha^2-3z^2)}{6}\ln(\beta+\rho) - \alpha\beta z\ln(z+\rho) - \frac{\alpha^2 z\theta_1}{2} - \frac{\beta^2 z\theta_2}{2} + \frac{z^3\theta_3}{6}\right.$$

$$\mathcal{H}_3^v = -\frac{(\alpha^2-2z^2)\rho}{2} + \frac{\alpha(\beta^2-3z^2)}{2}\ln(\alpha+\rho) + \beta(\alpha^2-z^2)\ln(\beta+\rho) - 2\alpha\beta z\theta_3 + (1-2\nu)\left\{-\frac{\beta^2\rho}{2} + \right.$$
$$\left. + \frac{\rho^3}{6} + \frac{\alpha(\beta^2-z^2)}{2}\ln(\alpha+\rho) - \frac{z(\alpha^2-\beta^2)}{2}\ln(z+\rho) - \alpha\beta z\theta_2\right\}$$

$$\mathcal{H}_1^w = \frac{\rho^3}{6} + \frac{z^2\rho}{2} - \frac{\alpha(\beta^2+z^2)}{2}\ln(\alpha+\rho) - \frac{\beta(\alpha^2+z^2)}{2}\ln(\beta+\rho) + (1-2\nu)\left\{\frac{\rho^3}{6} - \frac{z^2\rho}{2} + \right.$$
$$\left. - \frac{\alpha(\beta^2-z^2)}{2}\ln(\alpha+\rho) - \frac{\beta(\alpha^2-z^2)}{2}\ln(\beta+\rho) + \alpha\beta z\theta_3\right\}$$

$$\mathcal{H}_2^w = -\frac{\alpha z\rho}{2} + \frac{z(\beta^2-z^2)}{2}\ln(\alpha+\rho) + \alpha\beta z\ln(\beta+\rho) - \beta z^2\theta_3 + (1-2\nu)\left\{\frac{\alpha\beta^2}{6} + \frac{\alpha z\rho}{3} + \right. \quad (40c)$$
$$- \frac{z(3\beta^2-z^2)}{6}\ln(\alpha+\rho) - \alpha\beta z\ln(\beta+\rho) + \frac{\alpha(\alpha^2-3\beta^2)}{6}\ln(z+\rho) - \frac{\alpha^2\beta\theta_1}{2} +$$
$$\left. - \frac{\beta^3\theta_2}{6} + \frac{\beta z^2\theta_3}{2}\right\}$$

$$\mathcal{H}_3^w = -\frac{\beta z\rho}{2} + \alpha\beta z\ln(\alpha+\rho) + \frac{z(\alpha^2-z^2)}{2}\ln(\beta+\rho) - \alpha z^2\theta_3 + (1-2\nu)\left\{\frac{\alpha^2\beta}{6} + \frac{\beta z\rho}{3} - \alpha\beta z\ln(\alpha+\rho) + \right.$$
$$\left. - \frac{z(3\alpha^2-z^2)}{6}\ln(\beta+\rho) - \frac{\beta(3\alpha^2-\beta^2)}{6}\ln(z+\rho) - \frac{\alpha^3\theta_1}{6} - \frac{\alpha\beta^2\theta_2}{2} + \frac{\alpha z^2\theta_3}{2}\right\}$$

Remarks on Calculation of Stresses Due to Surface Loads

Calculations of stresses due to surface loads involve the same quantities ρ, θ_1, θ_2, θ_3, $\ln(\rho+\alpha)$, $\ln(\rho+\beta)$ and $\ln(\rho+z)$ many times, so precalculating them shortens the work. In addition, several other groupings of term occur repeatedly in the functions H_i^j and $\mathcal{H}_i^j$, so in the subroutine used for calculating surface load effects (SURFAC) these further groupings too are precalculated, but more importantly it is recognized that a corner evaluation of an H_i^j or $\mathcal{H}_i^j$ made for one pyramidal load may be reused for several other pyramidal loads sharing that corner. Therefore, before any influence functions K_i^j or $\mathcal{K}_i^j$ are calculated by SURFAC for given stress point, (x,y,z), the functions $H_i^j(\alpha,\beta,z)$ and $\mathcal{H}_i^j(\alpha,\beta,z)$ are precalculated for all the anticipated corner values of α and β (that is for all $\alpha_c = x_c - x$ and $\beta_c = y_c - y$ where $(x_c, y_c, 0)$ ranges over all points where rectangles of the surface lattice have corners). In order to employ the correct corner evaluations for each pyramidal load, the user assigns index numbers to all the corner positions in the plane and then specifies as computing input both the position of the pyramidal peak and the indices of the nine corners associated with it. The order of specification moves from low x to high x, then from high y to low y. By convention, all the pyramidal peak positions are numbered first, then the remaining lattice points are numbered. (Since it is tedious to assign these index numbers, a computer program LATTICE

was prepared to do it.) When the computer receives these specifications for the pyramids plus coordinates for the remaining lattice points, the subroutine SURFAC finds the required evaluations of H_i^j and $\mathcal{H}_i^j$ for the given stress point and combines them to find the influence functions K_i^j and $\mathcal{K}_i^j$. In another mode of operation, if all the peak loads p_m, s_m and t_m are specified, the program can compute the stress and displacement components.

Coordination of Contributing Stress Analyses

Stress analyses have been formulated for a semi-infinite body with an arbitrary set of quasi-pyramidal loads (both normal and shearing) acting on its surface, and for an infinite body with a circular crack subject to normal and shearing loads expressed by series with arbitrary coefficients. Now as an example it will be considered how one may combine three such analyses (two surface analyses and one crack analysis) in order to determine stresses in a uniformly thick slab with a circular (or part circular) crack, with preassigned load (or displacement) distributions on the two faces and the crack. A first step in doing this is to determine how coordinates, displacements, and stresses expressed in the coordinates for any one of these contributing analyses can be reexpressed in terms used in either of the other analyses. Then it becomes possible to establish overall boundary conditions which imply what hypothetical surface loads should be attributed to each of the three loading systems. Evaluation of these hypothetical loads (that is evaluation of surface and crack load constants) makes complete stress evaluation for the slab possible, including stress intensity factors at the crack front.

Coordinate Relationships

The geometric relationships between the three coordinates systems used for the contributing analyses are shown in Figure A2. The rectangular system (x,y,z) associated the front face has its axes parallel to those of the back-face system (x',y',z') with the z- and z'-axes colinear but oppositely oriented. The x- and x'-axes are oriented alike, but the y- and y'-

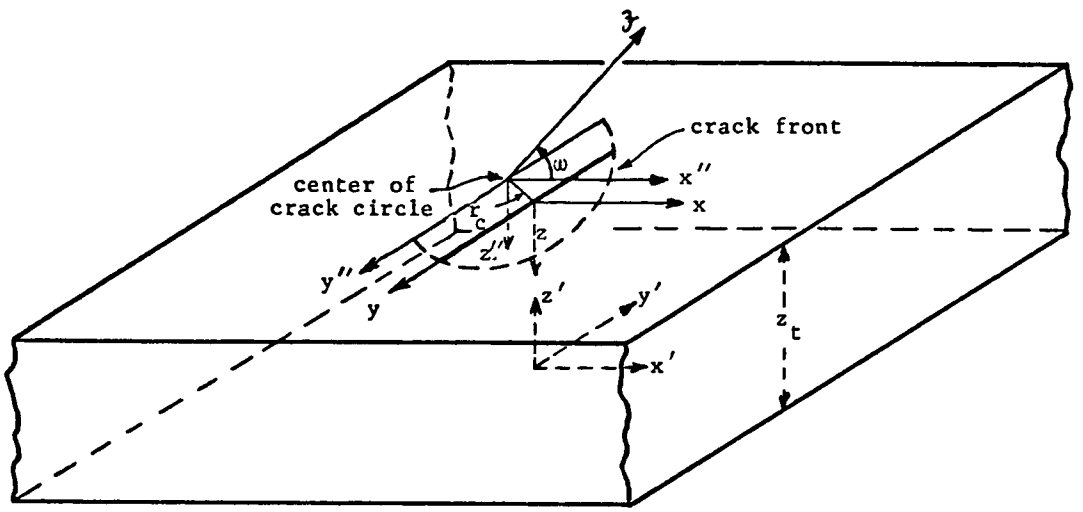

FIGURE A2. COORDINATE SYSTEMS FOR CONTRIBUTING STRESS ANALYSES FOR A PLATE

axes are not so that both systems can be right-handed. The cylindrical coordinates (r,θ,ζ) associated with the crack have the plane where $\theta = 0$ coinciding with the xz-plane and the ζ-axis is directed outward at an inclination ω from the positive direction of the x-axis. The crack front has $r = a$ and $\zeta = 0$, and the radial offset of its center from the front face of the slab is called r_c, this being positive if that center is outside the slab, negative is it is inside. The thickness of the slab is called z_t or T.

The expressions for back-face coordinates in terms of front-face coordinates are

$$\left.\begin{aligned} x' &= x \quad , \\ y' &= -y \quad , \\ z' &= z_t - z \quad , \end{aligned}\right\} \tag{41}$$

and the inverse expressions are

$$\left.\begin{aligned} x &= x' \quad , \\ y &= -y' \quad , \\ z &= z_t - z' \quad , \end{aligned}\right\} \tag{41'}$$

The front-face coordinates in terms of the cylindrical coordinates can be shown to be

$$\left.\begin{aligned} x &= r\cos\theta\sin\omega + \zeta\cos\omega - r_c\sin\omega \quad , \\ y &= -r\sin\theta \quad , \\ z &= r\cos\theta\cos\omega - \zeta\sin\omega - r_c\cos\omega \quad . \end{aligned}\right\} \tag{42}$$

The expression for the inverse of this relation is chosen to make $-\pi < \theta \leq \pi$, and with this provision becomes

$$\left.\begin{aligned} r &= \left[(x\sin\omega + z\cos\omega + r_c)^2 + y^2\right]^{1/2} \quad , \\ \theta &= \arctan\frac{-y}{x\sin\omega + z\cos\omega + r_c} - \frac{\pi}{2}(1-E_1)E_2 \quad , \\ \zeta &= x\cos\omega - z\sin\omega \quad , \end{aligned}\right\} \tag{42'}$$

where

$$E_1 = \text{sgn}\ (x \sin\omega + z \cos\omega + r_c)$$

$$E_2 = -\text{sgn}(-y)$$

$$\text{sgn}\ X = \begin{cases} X/|X| & \text{if} \quad X \neq 0 \\ 1 & \text{if} \quad X = 0 \end{cases} \quad ,$$

and the arctangent takes its principal value (between $-\pi/2$ and $\pi/2$). If the denominator of its argument vanishes, the arctangent is put equal to $\pi/2$ sgn(numerator). The relationship between the coordinates for the back face and those for the cylindrical system is evidently

$$\left.\begin{aligned} x' &= r \cos\theta \sin\omega + \zeta \cos\omega - r_c \sin\omega \ , \\ y' &= r \sin\theta \ , \\ z' &= -r \cos\theta \cos\omega + \zeta \sin\omega + r_c \cos\omega + z_t \ , \end{aligned}\right\} \quad (43)$$

or the inverse form,

$$\left.\begin{aligned} r &= \left[(x' \sin\omega - z' \cos\omega + z_t \cos\omega + r_c)^2 + y'^2 \right]^{1/2} \ , \\ \theta &= \arctan \frac{y'}{x' \sin\omega - z' \cos\omega + z_t \cos\omega + r_c} - \frac{\pi}{2} (1 - E_1') E_2' \ , \\ \zeta &= x' \cos\omega + z' \sin\omega - z_t \sin\omega \ , \end{aligned}\right\} \quad (43')$$

where

$$E_1' = \text{sgn}\ (x' \sin\omega - z' \cos\omega + z_t \cos\omega + r_c) \ ,$$

$$E_2' = -\ \text{sgn}\ y' \ ,$$

with the definition of sgn X as before and with the same principal-value choice for the arctangent. If $x' \sin\omega - z' \cos\omega + z_t \cos\omega + r_c = y' = 0$, then θ is again indeterminate but immaterial since $r = 0$.

Stress and displacement components defined in any one system also need to be expressed in either of the other systems, so notation is needed which identifies the coordinate system as well as the component. Other entities often needing identification include the point where the stress is

evaluated (the "stress point"), the face where the responsible load element is applied, the kind of load component applied, and the load position. To provide these identifications for both stresses (σ) and displacements (u), superscripts are used to identify in order the stress coordinate systems, the stress component, and the stress point, and subscripts are used to identify in order the loaded face, the load component, and the load position, but unneeded or undetermined indices may be dropped. Entities associated with the front face, the back face, or the crack face will be identified respectively by a, b, or c, and matrix notation will be used to denote sets of components. Thus, the values of stress components expressed respectively in the front-face, back-face, or crack-face systems are denoted as

$$\left[\sigma^{a}\right] = \begin{bmatrix} \sigma^{a,1} \\ \sigma^{a,2} \\ \sigma^{a,3} \\ \sigma^{a,4} \\ \sigma^{a,5} \\ \sigma^{a,6} \end{bmatrix} = \begin{bmatrix} \sigma_{xx} \\ \sigma_{yy} \\ \sigma_{zz} \\ \tau_{yz} \\ \tau_{zx} \\ \tau_{xy} \end{bmatrix}, \quad \left[\sigma^{b}\right] = \begin{bmatrix} \sigma^{b,1} \\ \sigma^{b,2} \\ \sigma^{b,3} \\ \sigma^{b,4} \\ \sigma^{b,5} \\ \sigma^{b,6} \end{bmatrix} = \begin{bmatrix} \sigma_{x'x'} \\ \sigma_{y'y'} \\ \sigma_{z'z'} \\ \sigma_{y'z'} \\ \sigma_{z'x'} \\ \sigma_{x'z'} \end{bmatrix}, \quad \left[\sigma^{c}\right] = \begin{bmatrix} \sigma^{c,1} \\ \sigma^{c,2} \\ \sigma^{c,3} \\ \sigma^{c,4} \\ \sigma^{c,5} \\ \sigma^{c,6} \end{bmatrix} = \begin{bmatrix} \sigma_{rr} \\ \sigma_{\theta\theta} \\ \sigma_{zz} \\ \tau_{\theta z} \\ \tau_{zr} \\ \tau_{r\theta} \end{bmatrix}, \tag{44}$$

and the values of the displacement components are denoted as

$$\left[u^{a}\right] = \begin{bmatrix} u^{a,1} \\ u^{a,2} \\ u^{a,3} \end{bmatrix} = \begin{bmatrix} u_x \\ u_y \\ u_z \end{bmatrix}, \quad \left[u^{b}\right] = \begin{bmatrix} u^{b,1} \\ u^{b,2} \\ u^{b,3} \end{bmatrix} = \begin{bmatrix} u_{x'} \\ u_{y'} \\ u_{z'} \end{bmatrix}, \quad \left[u^{c}\right] = \begin{bmatrix} u^{c,1} \\ u^{c,2} \\ u^{c,3} \end{bmatrix} = \begin{bmatrix} u_r \\ u_\theta \\ u_z \end{bmatrix}. \tag{45}$$

(Here u_x, u_y, u_z are the same as the components u, v, w in the front-face system; u'_x, u'_y, u'_z are the same as u, v, w in the back-face system; and u_r, u_θ, u_z are the same as u, v, w in the crack system.) Evaluation of $\sigma^{a,j}$ for example at a particular stress point, say the n^{th}, will be designated by a third superscript, making it $\sigma^{a,j,n}$. In similar fashion, a first subscript (a, b, c) identifies which face is loaded to produce the stress (provided the loading is on a single face). A second subscript shows which kind of load is acting. (For loads on rectangular faces, this is 1 for normal loads

$p \sim -\sigma_z$ or $-\sigma_{z'}$, 2 for shearing loads $s \sim \tau_{zx}$ or $\tau_{z'x'}$, 3 for shearing loads $t \sim \tau_{yz}$ or $\tau_{y'z'}$. For loads on the crack face it is 1,2,...,6 for loads associated with the coefficients α', β', γ', $\hat{\alpha}'$, $\hat{\beta}'$, $\hat{\gamma}'$, respectively.) A third subscript may be used to show which one of a set of load positions (on a plane face) or load coefficients (on the crack face) is being used. A "load position" on a rectangular face is understood to imply both the peak position and the four base lengths used in defining the pyramidal load element. The load coefficient designation for the crack accounts for the values of both the summation indices m and k.

Using this new notation, the relationship between stresses and displacements in the front-face and back-face systems becomes in matrix notation:

$$\begin{aligned} \left[\sigma^b\right] &= M_{b,a}\left[\sigma^a\right] \quad \text{and} \quad \left[u^b\right] = \mathcal{M}_{b,a}\left[u^a\right] \quad , \quad \text{or} \\ \left[\sigma^a\right] &= M_{a,b}\left[\sigma^b\right] \quad \text{and} \quad \left[u^a\right] = \mathcal{M}_{a,b}\left[u^b\right] \quad , \end{aligned} \tag{46}$$

where

$$M_{b,a} = \begin{bmatrix} 1 & 0 & 0 & 0 & 0 & 0 \\ 0 & 1 & 0 & 0 & 0 & 0 \\ 0 & 0 & 1 & 0 & 0 & 0 \\ 0 & 0 & 0 & 1 & 0 & 0 \\ 0 & 0 & 0 & 0 & -1 & 0 \\ 0 & 0 & 0 & 0 & 0 & -1 \end{bmatrix} \quad , \quad \text{so that } M_{a,b} = M_{b,a}^{-1} = M_{b,a} \quad , \tag{47}$$

and

$$\mathcal{M}_{b,a} = \begin{bmatrix} 1 & 0 & 0 \\ 0 & -1 & 0 \\ 0 & 0 & -1 \end{bmatrix} \quad , \quad \text{so that } \mathcal{M}_{a,b} = \mathcal{M}_{b,a}^{-1} = \mathcal{M}_{b,a} \quad . \tag{48}$$

The relationship between the components in the cylindrical system and those in the front-face system can be shown to be as follows.

$$\left[\sigma^c\right] = M_{c,a}\left[\sigma^a\right] \quad \text{and} \quad \left[u^c\right] = \mathcal{M}_{c,a}\left[u^a\right] \quad , \tag{49}$$

where

$$M_{c,a} = \begin{bmatrix} \cos^2\theta\sin^2\omega & \sin^2\theta & \cos^2\theta\cos^2\omega & -\sin2\theta\cos\omega & \cos^2\theta\sin2\omega & -\sin2\theta\sin\omega \\ \sin^2\theta\sin^2\omega & \cos^2\theta & \sin^2\theta\cos^2\omega & \sin2\theta\cos\omega & \sin^2\theta\sin2\omega & \sin2\theta\sin\omega \\ \cos^2\omega & 0 & \sin^2\omega & 0 & -\sin2\omega & 0 \\ -\frac{1}{2}\sin\theta\sin2\omega & 0 & \frac{1}{2}\sin\theta\sin2\omega & \cos\theta\sin\omega & -\sin\theta\cos2\omega & -\cos\theta\cos\omega \\ \frac{1}{2}\cos\theta\sin2\omega & 0 & -\frac{1}{2}\cos\theta\sin2\omega & \sin\theta\sin\omega & \cos\theta\cos2\omega & -\sin\theta\cos\omega \\ -\frac{1}{2}\sin2\theta\sin^2\omega & \frac{1}{2}\sin2\theta & -\frac{1}{2}\sin2\theta\cos^2\omega & -\cos2\theta\cos\omega & -\frac{1}{2}\sin2\theta\sin2\omega & -\cos2\theta\sin\omega \end{bmatrix}, \quad (50)$$

and

$$\mathcal{M}_{c,a} = \begin{bmatrix} \cos\theta\sin\omega & -\sin\theta & \cos\theta\cos\omega \\ -\sin\theta\sin\omega & -\cos\theta & -\sin\theta\cos\omega \\ \cos\omega & 0 & -\sin\omega \end{bmatrix} . \quad (51)$$

Inverting these relationships shows

$$\left[\sigma^a\right] = M_{a,c}\left[\sigma^c\right] \quad \text{and} \quad \left[u^a\right] = \mathcal{M}_{a,c}\left[u^c\right] , \quad (49')$$

where

$$M_{a,c} = M_{c,a}^{-1} = \begin{bmatrix} \cos^2\theta\sin^2\omega & \sin^2\theta\sin^2\omega & \cos^2\omega & -\sin\theta\sin2\omega & \cos\theta\sin2\omega & -\sin2\theta\sin^2\omega \\ \sin^2\theta & \cos^2\theta & 0 & 0 & 0 & \sin2\theta \\ \cos^2\theta\cos^2\omega & \sin^2\theta\cos^2\omega & \sin^2\omega & \sin\theta\sin2\omega & -\cos\theta\sin2\omega & -\sin2\theta\cos^2\omega \\ -\frac{1}{2}\sin2\theta\cos\omega & \frac{1}{2}\sin2\theta\cos\omega & 0 & \cos\theta\sin\omega & \sin\theta\sin\omega & -\cos2\theta\cos\omega \\ \frac{1}{2}\cos^2\theta\sin2\omega & \frac{1}{2}\sin^2\theta\sin2\omega & -\frac{1}{2}\sin2\omega & -\sin\theta\cos2\omega & \cos\theta\cos2\omega & -\frac{1}{2}\sin2\theta\sin2\omega \\ -\frac{1}{2}\sin2\theta\sin\omega & \frac{1}{2}\sin2\theta\sin\omega & 0 & -\cos\theta\cos\omega & -\sin\theta\cos\omega & -\cos2\theta\sin\omega \end{bmatrix} \quad (50')$$

and

$$\mathcal{M}_{a,c} = \mathcal{M}_{c,a}^{-1} = \begin{bmatrix} \cos\theta\sin\omega & -\sin\theta\sin\omega & \cos\omega \\ -\sin\theta & -\cos\theta & 0 \\ \cos\theta\cos\omega & -\sin\theta\cos\omega & -\sin\omega \end{bmatrix} . \quad (51')$$

It follows that the relationship between components in the cylindrical system and those in the back-face system are

$$\left[\sigma^c\right] = M_{c,b}\left[\sigma^b\right] \quad \text{and} \quad \left[u^c\right] = \mathcal{M}_{c,b}\left[u^b\right] \ , \quad \text{or}$$
$$\left[\sigma^b\right] = M_{b,c}\left[\sigma^c\right] \quad \text{and} \quad \left[u^b\right] = \mathcal{M}_{b,c}\left[u^c\right] \ , \tag{52}$$

where

$$M_{c,b} = M_{c,a}M_{a,b} \ , \qquad \mathcal{M}_{c,b} = \mathcal{M}_{c,a}\mathcal{M}_{a,b} \ ,$$
$$M_{b,c} = M_{c,b}^{-1} = M_{b,a}M_{a,c} \ , \qquad \mathcal{M}_{b,c} = \mathcal{M}_{c,b}^{-1} = \mathcal{M}_{b,a}\mathcal{M}_{a,c} \ . \tag{53}$$

Statement of Boundary Conditions

In order to fit the three contributing stress analyses together into a single analysis for a slab with a crack, load coefficients are sought for the three analyses so that taken together they yield a least-squares fit to boundary conditions prescribed at many points on all three surfaces. To state these boundary conditions, it is necessary first to determine the influence functions for each of the desired coefficients at all the points where the boundary conditions are to be applied. Formulas for the influence functions $K_i^j(x,y,z)$ and $\mathcal{K}_i^j(x,y,z)$ for the surface load constants for a single load position have been stated already [see Equations (36) to (40)]. The same kinds of functions apply, of course, for front and back surface loads. Using the revised notation, those influence functions for the front face loads will now be denoted as $K_{a,i}^{a,j}$ and $\mathcal{K}_{a,i}^{a,j}$, since they also express the effects in front-face coordinates; and if the load is at the ℓ^{th} position and the effects are evaluated at the n^{th} stress (or boundary) point, then they will be called $K_{a,i,\ell}^{a,j,n}$ or $\mathcal{K}_{a,i,\ell}^{a,j,n}$. The influence functions for the back-face load constants for the ℓ'^{th} position, acting on the n^{th} stress point and expressed in back-face coordinates, are given by the same equations but are here denoted as $K_{b,i,\ell'}^{b,j,n}$ or $\mathcal{K}_{b,i,\ell'}^{b,j,n}$. Influence functions for crack load constants are readily derived in the crack coordinates from the Equations (6), being products of an F and cos mθ or sin mθ with appropriate sign. Here the

influence on the j^{th} stress component at the n^{th} point due to the i^{th} kind of load coefficient (with i = 1 for $\alpha'_{n,k}$,...,6 for $\hat{\gamma}_{m,k}$) is denoted as $K^{c,j,n}_{c,i,\ell''}$, with $\ell'' = mn_k + k + 1$ where n_k is the number of k's used. The influence functions $K^{c,j,n}_{c,i,\ell''}$ for the displacements are also evident from the Equations (6). (Note that $\gamma'_{0,k}$, $\hat{\alpha}'_{0,k}$ and $\hat{\gamma}'_{0,k}$ will eventually be dropped.)

The load constants p_m, s_m, t_m for the ℓ^{th} position on the front face are now called $c_{1,\ell}$, $c_{2,\ell}$, and $c_{3,\ell}$ respectively, while those for the ℓ'^{th} position on the back face are called $c'_{1,\ell'}$, $c'_{2,\ell'}$, and $c'_{3,\ell'}$. The constants $\mu\alpha'_{m,k}$, $\mu\beta'_{m,k}$,...,$\mu\hat{\gamma}'_{m,k}$ for the crack are now called $c''_{i,\ell''}$, with i = 1,2,...,6 respectively and with $\ell'' = mn_k + k + 1$, where n_k is the total number of k's being used. Adding the effects of all front-face loads (which include three kinds for each ℓ = 1,2,...,L), Equation (37) implies that the overall components of stress and displacement at the n^{th} stress point are

$$\sigma_a^{a,j,n} = \sum_{\ell=1}^{L} \sum_{i=1}^{3} K^{a,j,n}_{a,i,\ell}\, c_{i,\ell} \quad , \qquad j = 1,2,\ldots,6 \quad , \tag{54}$$

$$u_a^{a,j,n} = \frac{1}{2\mu} \sum_{\ell=1}^{L} \sum_{i=1}^{3} K^{a,j,n}_{a,i,\ell}\, c_{i,\ell} \quad , \qquad j = 1,2,3 \quad . \tag{55}$$

Using matrix notation, Equation (54) may be written as

$$\left[\sigma_a^a\right]^n = \left[K_a^a\right]^n [c] \quad , \tag{56}$$

where

$$\left[\sigma_a^a\right]^n = \begin{Bmatrix} \sigma_a^{a,1,n} \\ \sigma_a^{a,2,n} \\ \sigma_a^{a,3,n} \\ \sigma_a^{a,4,n} \\ \sigma_a^{a,5,n} \\ \sigma_a^{a,6,n} \end{Bmatrix} \quad , \qquad [c] = \begin{Bmatrix} c_{1,1} \\ c_{2,1} \\ c_{3,1} \\ c_{1,2} \\ \vdots \\ c_{3,L} \end{Bmatrix} \quad , \tag{57}$$

and

$$\left[K_a^a\right]^n = \begin{Bmatrix} K_{a,1,1}^{a,1,n} & K_{a,2,1}^{a,1,n} & K_{a,3,1}^{a,1,n} & K_{a,1,2}^{a,1,n} & K_{a,2,2}^{a,1,n} & - - - & K_{a,3,L}^{a,1,n} \\ K_{a,1,1}^{a,2,n} & K_{a,2,1}^{a,2,n} & K_{a,3,1}^{a,2,n} & K_{a,1,2}^{a,2,n} & K_{a,2,2}^{a,2,n} & - - - & K_{a,3,L}^{a,2,n} \\ - - - & - - - & - - - & - - - & - - - & - - - & - - - \\ K_{a,1,1}^{a,6,n} & K_{a,2,1}^{a,6,n} & K_{a,3,1}^{a,6,n} & K_{a,1,2}^{a,6,n} & K_{a,2,2}^{a,6,n} & - - - & K_{a,3,L}^{a,6,n} \end{Bmatrix} . \quad (58)$$

Equation (55) for the displacements can be written as

$$\left[u_a^a\right]^n = \frac{1}{2\mu}\left[\kappa_a^a\right]^n [c] \quad , \quad (59)$$

where

$$\left[u_a^a\right]^n = \begin{Bmatrix} u_a^{a,1,n} \\ u_a^{a,2,n} \\ u_a^{a,3,n} \end{Bmatrix} \quad (60)$$

and

$$\left[\kappa_a^a\right]^n = \begin{Bmatrix} \kappa_{a,1,1}^{a,1,n} & \kappa_{a,2,1}^{a,1,n} & \kappa_{a,3,1}^{a,1,n} & \kappa_{a,1,2}^{a,1,n} & \kappa_{a,2,2}^{a,1,n} & - - - & \kappa_{a,3,L}^{a,1,n} \\ \kappa_{a,1,1}^{a,2,n} & \kappa_{a,2,1}^{a,2,n} & \kappa_{a,3,1}^{a,2,n} & \kappa_{a,1,2}^{a,2,n} & \kappa_{a,2,2}^{a,2,n} & - - - & \kappa_{a,3,L}^{a,2,n} \\ \kappa_{a,1,1}^{a,3,n} & \kappa_{a,2,1}^{a,3,n} & \kappa_{a,3,1}^{a,3,n} & \kappa_{a,1,2}^{a,3,n} & \kappa_{a,2,2}^{a,3,n} & - - - & \kappa_{a,3,L}^{a,3,n} \end{Bmatrix} \quad (61)$$

In like manner, the overall stresses and displacements caused at the n^{th} stress point by all the back-face loads (including three for each $\ell = 1,2,\ldots,$ L') are, if expressed in the back-face coordinates,

$$\left[\sigma_b^b\right]^n = \left[K_b^b\right]^n [c'] \quad ,$$

$$\left[u_b^b\right]^n = \frac{1}{2\mu}\left[\mathcal{K}_b^b\right]^n [c'] \quad , \tag{62}$$

where $\left[K_b^b\right]^n$ is like the matrix in Equation (58) and $\left[\mathcal{K}_b^b\right]^n$ is like that in Equation (61) except that b's replace all the a's and there are 3L' constants $c'_{i,\ell'}$ instead of 3L constants $c_{i,\ell}$. Again, the overall stresses and displacements caused at the n^{th} stress point by all the crack loads* (including six for each $\ell'' = 1,2,\ldots,L''$) are, if expressed in the crack coordinates,

$$\left[\sigma_c^c\right]^n = \left[K_c^c\right]^n [c''] \quad ,$$

$$\left[u_c^c\right]^n = \frac{a}{\mu}\left[\mathcal{K}_c^c\right]^n [c''] \quad , \tag{63}$$

where $\left[K_c^c\right]$ is like the matrix in Equation (58) and $\left[\mathcal{K}_c^c\right]^n$ is like that in Equation (61) except that c's replace all the a's and there are 3L" columns instead of 3L. Also [c"] is like [c] except that it contains 6L" constants $c'_{i,\ell''}$ instead of 3L constants $c_{i,\ell}$. Of course, the coordinates of the n^{th} stress point must be evaluated in the system being used, and the Equations (41) through (43') make this possible.

Before the stresses and displacements expressed in different systems can be combined, they must be reexpressed into a single system. This can be arranged using Equations (46) through (53), but the matrices $M_{c,a}$, $\mathcal{M}_{c,a}$, and so forth must be evaluated at the chosen stress point, so that they are denoted as $\left[M_{c,a}\right]^n$, $\left[\mathcal{M}_{c,a}\right]^n$, and so forth for the n^{th} stress point. Thus, the overall stresses from back-face loads expressed in the front-face system at the n^{th} stress point are**

---

* If n_m is the number of m's and n_k is the number of k's used for each m there are 6L" crack constants, where $L'' = n_m n_k$, but $3n_k$ of these are to be dropped.

**Of course $\left[M_{a,b}\right]^n = M_{a,b}$, but that kind of simplification does not hold for matrices involving the crack coordinates.

$$\left[\sigma_b^a\right]^n = \left[M_{a,b}\right]^n \left[\sigma_b^b\right]^n = \left[M_{a,b}\right]^n \left[K_b^b\right]^n [c'] \quad ,$$

so that

$$\left[\sigma_b^a\right]^n = \left[K_b^a\right]^n [c'] \quad , \qquad \text{where} \quad \left[K_b^a\right]^n = \left[M_{a,b}\right]^n \left[K_b^b\right]^n \quad . \tag{64}$$

The overall stresses from crack loads expressed in the front-face system similarly are

$$\left[\sigma_c^a\right]^n = \left[K_c^a\right]^n [c''] \quad , \qquad \text{where} \quad \left[K_c^a\right]^n = \left[M_{a,c}\right]^n \left[K_c^c\right]^n \quad . \tag{65}$$

Thus, the overall stresses at the n^{th} stress point, being expressed in the front-face system are

$$\left[\sigma^a\right]^n = \left[K_a^a\right]^n [c] + \left[K_b^a\right]^n [c'] + \left[K_c^a\right]^n [c''] \quad . \tag{66}$$

If these stresses are expressed in the back-face system, they become

$$\left[\sigma^b\right]^n = \left[K_a^b\right]^n [c] + \left[K_b^b\right]^n [c'] + \left[K_c^b\right]^n [c''] \quad , \tag{67}$$

where

$$\left[K_a^b\right]^n = \left[M_{b,a}\right]^n \left[K_a^a\right]^n \quad , \qquad \left[K_c^b\right]^n = \left[M_{b,c}\right]^n \left[K_c^c\right]^n \quad .$$

In the crack-face system, they become

$$\left[\sigma^c\right]^n = \left[K_a^c\right]^n [c] + \left[K_b^c\right]^n [c'] + \left[K_c^c\right]^n [c''] \quad , \tag{68}$$

where

$$\left[K_a^c\right]^n = \left[M_{c,a}\right]^n \left[K_a^a\right]^n \quad , \qquad \left[K_b^c\right]^n = \left[M_{c,b}\right]^n \left[K_b^b\right]^n \quad .$$

In like manner, the displacements at the n^{th} stress point, being expressed alternatively in the three coordinate systems are

$$\begin{aligned}
\left[u^a\right]^n &= \frac{1}{2\mu}\left[K_a^a\right]^n[c] + \frac{1}{2\mu}\left[K_b^a\right]^n[c'] + \frac{a}{\mu}\left[K_c^a\right]^n[c''] \quad , \\
\left[u^b\right]^n &= \frac{1}{2\mu}\left[K_a^c\right]^n[c] + \frac{1}{2\mu}\left[K_b^b\right]^n[c'] + \frac{a}{\mu}\left[K_c^b\right]^n[c''] \quad , \\
\left[u^c\right]^n &= \frac{1}{2\mu}\left[K_a^c\right]^n[c] + \frac{1}{2\mu}\left[K_b^c\right]^n[c'] + \frac{a}{\mu}\left[K_c^c\right]^n[c''] \quad ,
\end{aligned} \tag{69}$$

where

$$\begin{aligned}
\left[K_b^a\right]^n &= \left[M_{a,b}\right]^n\left[K_b^b\right]^n \quad , \qquad \left[K_c^a\right]^n = \left[M_{a,c}\right]^n\left[K_c^c\right]^n \quad , \\
\left[K_a^b\right]^n &= \left[M_{b,a}\right]^n\left[K_a^a\right]^n \quad , \qquad \left[K_c^b\right]^n = \left[M_{b,c}\right]^n\left[K_c^c\right]^n \quad , \\
\left[K_a^c\right]^n &= \left[M_{c,a}\right]^n\left[K_a^a\right]^n \quad , \qquad \left[K_b^c\right]^n = \left[M_{c,b}\right]^n\left[K_b^b\right]^n \quad .
\end{aligned}$$

Equations (66) through (69), together with (58) and (61) and the associated definitions of $\left[K_b^a\right]^n$, $\left[K_b^a\right]^n$, and so forth, provide formulas for computing the overall stress and displacement components if the constants $c_{i,\ell}$, $c'_{i,\ell'}$, and $c''_{i,\ell''}$ are known. If the constants are not known but values of the boundary forces are specified, at least in a least squares sense, at a sufficient number of boundary points, then the portions of these equations referring to transmissible boundary forces provide means for evaluating those constants. It has been arranged that the boundary forces transmissible across any face correspond to stress components with j = 3,4,5, when the stresses are expressed in the coordinates for that face. (Thus across the front face the transmissible forces correspond to $\sigma^{a,3} \sim \sigma_z$, $\sigma^{a,4} \sim \tau_{yz}$, $\sigma^{a,5} \sim \tau_{zx}$.) If one assembles the influence functions for all front-face loads in producing stresses transmissible across that face at all the specified stress points on that face (say for n = 1,2,...,N), he has

$$\left\{K^{a,j,n}_{a,i,\ell}\right\} \equiv \begin{bmatrix} K^{a,3,1}_{a,1,1} & K^{a,3,1}_{a,2,1} & K^{a,3,1}_{a,3,1} & K^{a,3,1}_{a,1,2} & K^{a,3,1}_{a,2,2} & K^{a,3,1}_{a,3,2} & - - - & K^{a,3,1}_{a,3,L} \\ K^{a,4,1}_{a,1,1} & K^{a,4,1}_{a,2,1} & K^{a,4,1}_{a,3,1} & K^{a,4,1}_{a,1,2} & K^{a,4,1}_{a,2,2} & K^{a,4,1}_{a,3,2} & - - - & K^{a,4,1}_{a,3,L} \\ K^{a,5,1}_{a,1,1} & K^{a,5,1}_{a,2,1} & K^{a,5,1}_{a,3,1} & K^{a,5,1}_{a,1,2} & K^{a,5,1}_{a,2,2} & K^{a,5,1}_{a,3,2} & - - - & K^{a,5,1}_{a,3,L} \\ K^{a,3,2}_{a,1,1} & K^{a,3,2}_{a,2,1} & K^{a,3,2}_{a,3,1} & K^{a,3,2}_{a,1,2} & K^{a,3,2}_{a,2,2} & K^{a,3,2}_{a,3,2} & - - - & K^{a,3,2}_{a,3,L} \\ K^{a,4,2}_{a,1,1} & K^{a,4,2}_{a,2,1} & K^{a,4,2}_{a,3,1} & K^{a,4,2}_{a,1,2} & K^{a,4,2}_{a,2,2} & K^{a,4,2}_{a,3,2} & - - - & K^{a,4,2}_{a,3,L} \\ K^{a,5,2}_{a,1,1} & K^{a,5,2}_{a,2,1} & K^{a,5,2}_{a,3,1} & K^{a,5,2}_{a,1,2} & K^{a,5,2}_{a,2,2} & K^{a,5,2}_{a,3,2} & - - - & K^{a,5,2}_{a,3,L} \\ \cdot\cdot & \cdot\cdot & \cdot\cdot & \cdot\cdot & \cdot\cdot & \cdot\cdot & \cdot\cdot & \cdot\cdot \\ \cdot\cdot & \cdot\cdot & \cdot\cdot & \cdot\cdot & \cdot\cdot & \cdot\cdot & \cdot\cdot & \cdot\cdot \\ \cdot\cdot & \cdot\cdot & \cdot\cdot & \cdot\cdot & \cdot\cdot & \cdot\cdot & \cdot\cdot & \cdot\cdot \\ K^{a,5,N}_{a,1,1} & K^{a,5,N}_{a,2,1} & K^{a,5,N}_{a,3,1} & K^{a,5,N}_{a,1,2} & K^{a,5,N}_{a,2,2} & K^{a,5,N}_{a,3,2} & - - - & K^{a,5,N}_{a,3,L} \end{bmatrix} \tag{70}$$

Similar matrices can be assembled for the influence functions for back-face loads acting produce forces transmissible across the front face, that is $\left\{K^{a,j,n}_{b,i,\ell'}\right\}$ and for the remaining combinations of load face and transmission face. Let the stress points on the back face be numbered $n' = 1,2,\ldots,N'$, while those on the crack face are numbered $n'' = 1,2,\ldots,N''$. Then the entire collection of boundary conditions to be satisfied in the least squares sense is

$$\begin{bmatrix} \left\{K^{a,j,n}_{a,i,\ell}\right\} & \left\{K^{a,j,n}_{b,i,\ell'}\right\} & \left\{K^{a,j,n}_{c,i,\ell''}\right\} \\ \left\{K^{b,j,n'}_{a,i,\ell}\right\} & \left\{K^{b,j,n'}_{b,i,\ell'}\right\} & \left\{K^{b,j,n'}_{c,i,\ell''}\right\} \\ \left\{K^{c,j,n''}_{a,i,\ell}\right\} & \left\{K^{c,j,n''}_{b,i,\ell'}\right\} & \left\{K^{c,j,n''}_{c,i,\ell''}\right\} \end{bmatrix} \begin{bmatrix} [c] \\ [c'] \\ [c''] \end{bmatrix} \approx \begin{bmatrix} \left\{\sigma^{a,j,n}\right\} \\ \left\{\sigma^{b,j,n'}\right\} \\ \left\{\sigma^{c,j,n'}\right\} \end{bmatrix} \tag{71}$$

where the specified boundary forces on the three faces are

$$\left\{\sigma^{a,j,n}\right\} = \begin{Bmatrix} \sigma^{a,3,1} \\ \sigma^{a,4,1} \\ \sigma^{a,5,1} \\ \sigma^{a,3,2} \\ \sigma^{a,4,2} \\ \sigma^{a,5,2} \\ - - - \\ - - - \\ \sigma^{a,5,N} \end{Bmatrix}, \quad \left\{\sigma^{b,j,n'}\right\} = \begin{Bmatrix} \sigma^{b,3,1} \\ \sigma^{b,4,1} \\ \sigma^{b,5,1} \\ \sigma^{b,3,2} \\ \sigma^{b,4,2} \\ \sigma^{b,5,2} \\ - - - \\ - - - \\ \sigma^{b,5,N'} \end{Bmatrix}, \quad \left\{\sigma^{c,j,n''}\right\} = \begin{Bmatrix} \sigma^{c,3,1} \\ \sigma^{c,4,1} \\ \sigma^{c,5,1} \\ \sigma^{c,3,2} \\ \sigma^{c,4,2} \\ \sigma^{c,5,2} \\ - - - \\ - - - \\ \sigma^{c,5,N''} \end{Bmatrix} \tag{72}$$

It is understood here that the indices in each submatrix run through their complete range as required, namely three values for j, N for n, N' for n', N" for n", 3 or 6 for i, L for ℓ, L' for ℓ', and $n_m n_k$ for ℓ''. (Here n_m is the number of m's used in Equations (6) and n_k is the number of k's.) Thus, the number of equations implied by Equation (71) is 3N + 3N' +3N", and the number of constants to be found is 3L + 3L' + $6n_m n_k$ but $3n_k$ of these will be dropped.

Solving the Equations (71) in the least-squares sense provides the constants $c_{i,\ell}$, $c'_{i,\ell'}$, $c''_{i,\ell''}$ needed to determine stresses and/or displacements anywhere in the body using the Equations (66) through (69) or to compute crack stress intensity factors using the Equations (11) through (15).

Computational Procedures

To implement the above plan for analyzing stresses in a slab with a crack, the computing program called FRAC3D has been prepared. What it does, briefly, is to accept input data describing the geometry of a slab with a crack, together with front-face and back-face lattices, and to call the subroutines SURFAC and CRACK for the influence functions related to all the assignable load parameters for all the points at which boundary conditions are to be imposed. In doing this, FRAC3D calls the subroutine TRANSF to find the needed coordinate transformations using Equations (41) through (43'), and it calls the subroutine CONVRT to find the needed stress transformations by using Equations (46) through (53). It coordinates the additive

stresses as in Equations (67) through (70) so that contributions from all three loading systems are expressed in the coordinate system to which the particular boundary conditions refer. Then it assembles all the results into a matrix of the form displayed in Equations (70) through (72), readying them for solution for the loading constants using a previously available program called MATSOL.

The program FRAC3D is capable of treating geometries and loadings having wide generality, and in particular, having little or no symmetry. If, however, the crack is perpendicular to the faces of the slab and the loading has symmetry around both the xz- and yz-planes, then the matrix is unduly large. For such cases, a subroutine AXYZ has been included which combines columns of the matrix which relate to unknown constants which must be equal or merely of opposite sign on account of the symmetry. As a result of this reduction of columns, the rows of the matrix for stress points symmetrically situated with respect to the coordinate axes on each face become identical. Therefore, boundary conditions for front and back faces are assigned for only one quadrant (including its edges), and those for the crack only for $\theta \geq 0$. The program weights each row according to the number of boundary conditions it represents, the weights being $1, \sqrt{2}$ or 2 according to whether there are 1, 2 or 4 represented. This yields a much reduced system of equations to submit to MATSOL, but the computed results are the same as if the matrix has not been reduced. This capacity of AXYZ actually extends to allowing for several kinds of symmetry and to treating symmetry when the body includes as many as six sides of a rectangular parallelopiped.

The program MATSOL performs a least-square solution for the loading constants for both flat faces and the crack. Once these have been found, in particular once the crack constants $\alpha'_{m,k}$, $\beta'_{m,k}$,..., are determined, it is straightforward to find the variation of stress intensity factors, along the crack, using Equations (11) through (15) or to get half the crack opening displacement, using the surface displacement w as computed by CRACK from one of the Equations (6). The program also computes residuals at the points where boundary conditions are fitted and provides constants which could be applied in the Equations (6), (39), and (40) to find stresses or displacements anywhere in the slab. The program MATSOL has an option also of using several exact equations in conjunction with those being solved in

the least squares sense. Such an exact equation can be used to impose an equilibrium equation among the applied loads, and that is usually done as a matter of propriety. An expanded version of MATSOL has editing capability by which blocks of equations may be weighted differently and selected load constants can be removed from being used. (It is not necessary to use MATSOL to remove the spurious crack constants $\gamma_{0,k}$, $\hat{\alpha}'_{0,k}$ and $\hat{\gamma}'_{0,k}$, however, since FRAC3D does that automatically.)

Use of the program FRAC3D requires choosing of surface lattices, choosing the structure of crack function series, and assignment of boundary conditions. Such matters are discussed in the body of this report and also in the report to which this manual is a supplement [2]. It may be noted here that some structuring of the crack function series can be accomplished by using some simple, available inserts for the subroutine AXYZ which can remove terms for odd m's and then also terms for which $m+2k > 2n_k$, if that is desired and if the only constants are $\alpha'_{m,k}$. The early structuring is handled through the assignment of the n_m and n_k to be applied for each of the six kinds of crack load constants.

APPENDIX B

COMPONENTS OF FRAC3D

The program FRAC3D has many subroutines which are employed according to the location of the points and kinds of stresses being considered at any stage of the calculation. A brief description of the various parts follows.

Program FRAC3D

This is the part of the program which reads input and starts a course of action depending on the mode, on the face where a boundary condition is assigned, and on the system in which the load under consideration acts. Detailed calculations are referred to appropriate subroutines but returned to FRAC3D for reporting as output.

In the SOLVE mode, the intent of FRAC3D is to construct a matrix of the form shown in Equation (71) of Appendix A. The notation in that equation, and discussion of how its parts are formed are provided in the subsection of Appendix A containing that equation. In the RESULT mode, similar matrix rows are formed for each stress evaluation point, with all stress components being retained and all displacement components being included. The elements of each row are multiplied by the corresponding load constants and summed to determine the stresses and displacements.

Brief descriptions of the subroutines follow:

SURFAC - This calculates influence functions and other entities related to or arising from loads on the plane surfaces. Equations used by this subroutine are shown as Equations (35) through (40) in Appendix A. It is presumed the input specifies lattice points and pyramidal base indices as provided by the program LATTICE.

CRACK - This directs calculations for influence functions and other entities related to or arising from loads on the crack. In its assembly work it employs Equations (3) through (9) of Appendix A. In doing this, it refers evaluation of the many needed integrals to other subroutines via the subroutine RECUR.

AUXEQ - This assembles the auxiliary equations relating to overall equilibrium. These equations are employed in the SOLVE mode, but are kept apart from the regular boundary conditions. After formation of normal equations from the boundary-condition equations by MATSOL, these equilibrium equations are attached to the system by a bordering process. Thereafter, they are simply members of the system which MATSOL solves to find the load constants.

CONVRT - This performs conversions of stress components from one coordinate system to another. Equations for the conversions are given by Equations (44) to (53) of Appendix A.

TRANSF - This performs transformations of coordinates between cylindrical and rectangular coordinate systems. The equations used for this purpose are provided by Equations (41) to (43') of Appendix A.

AXYZ - This constructs the symmetry chain which is described on Pages 14 to 16 and illustrated by Pages 50 to 52. This routine on a logical, step-by-step process with many branches.

RECUR - This is the controlling subroutine for evaluation of the integrals used by the crack functions. Usually it assigns some other subroutine the task of evaluating a base set of the integrals, as described in Appendix A, and on their return it applies recursion processes to enlarge the set of integrals greatly. The recursion is two dimensional, being based on Equations (16) and (17) of Appendix A. Two special classes of integrals are treated almost entirely within RECUR itself, namely those for integrals with $\rho < 0.7$ (treated by the ρ-series) or with both $0.7 \leqslant \rho < 1$ and $0 < \zeta < (1-\rho)/5$ (treated by the ζ-series). These special series are only sketched in Appendix A, but they derived and discussed rather fully in the forthcoming paper mentioned in connection with those series in Appendix A. The use of recursion following efficient evaluation of base sets of integrals explains the great speed of evaluation of the crack integrals, but recursion can magnify numerical errors rapidly. As the forthcoming paper explains, accuracy as well as speed was studied until a good procedure was found for RECUR to select for any combination (ρ,ζ).

EVAL - This computes the most frequently used type of base integrals by a modified Gaussian quadrature of integrals greatly transformed by analytic processes. It employs mainly the Equations (18) to (24) of Appendix A. The quadrature is greatly speeded by precalculations of many Legendre polynomials multiplied by Gauss weights, with the results being recorded in the subroutine BLKDAT.

RHOEQ0 - This computes base sets of crack integrals for cases with $\rho = 0$. It employs Equations (25) and (26) of Appendix **A.**

RHOGT1 - This computes sets of crack integrals for cases with $\zeta = 0$ and $\rho > 1$. It uses Gaussian quadrature applied to Equations (27) to (29) of Appendix A.

RHOLT1 - This computes base sets of crack integrals for cases with $\zeta = 0$ and $\rho < 1$ transformed into polynomials as shown by Equations (30) to (33) of Appendix A.

LOGF1 - This is a tool used by SURFAC to eliminate indeterminacies in the surface load functions.

TH1F - This computes a special function arising in SURFAC, denoted as θ_1 in the Equations (38) of Appendix A.

TH3F - This computes a special function arising in SURFAC, denoted as θ_3 in the Equations (38) of Appendix A.

BLKDAT - This contains data for the Gaussian quadrature performed by RHOGT1 and for the modified Gaussian quadrature performed by EVAL with Gauss weights multiplied by Legendre polynomials.